Establishment of recombinant cell lines and characterization of primary cells for stem cell technology applications

Von der Naturwissenschaftlichen Fakultät

der Gottfried Wilhelm Leibniz Universität Hannover

zur Erlangung des Grades

Doktor der Naturwissenschaften

Dr. rer. nat.

genehmigte Dissertation

von

M.Sc. Pierre Moretti

geboren am 27.03.1981 in Algrange (Frankreich)

2010

Erklärung

Ich versichere, dass ich diese Dissertation selbstständig und nur unter Verwendung der angegebenen Hilfsmittel und Quellen durchgeführt habe. Diese Arbeit wurde nicht als Diplomarbeit oder ähnliche Prüfungsarbeit verwendet.

Hannover, im Mai 2010

„A cœur vaillant…“

Jacques Cœur

Acknowledgements

I am grateful to my supervisor Prof. Dr. Thomas Scheper for giving me the chance to perform my thesis on a highly interesting topic in his group at the Institute of Technical Chemistry, for his guidance and critical advices. Also, I am very thankful for the opportunity of two exciting scientific internships at the Technion University of Israel.

I thank PD Dr. Cornelia Kasper for being the co-advisor of this thesis, for her constant support and suggestions, as well as for the interesting scientific projects she allowed me to work on during my thesis at the TCI.

I am thankful to Prof. Dr. Martijn van Griensven for accepting to be a member of the final examination committee.

My colleagues Stefani Boehm, Antonina Lavrentieva and Tim Hatlapatka: it was really great to work with you! I thank Dr. Ingrida Majore for the numerous scientific discussions we shared on the topic of stem cells and Dr. Dr. Axel Schambach for his contribution to this work and for the very interesting conversation on the topic of retroviral vectors. I am very grateful to Martina Weiss for the HPLC analysis and to Martin Pähler for his assistance for the transcriptional analysis and to all the colleagues, who also contributed to make the TCI such a nice place to work!

I am grateful to the students Sanketha Kenthirapalan and Nina Bahnemann for the fruitful Bachelor and Master thesis. I also thank the students Alexandra Heilkenbrinker, Lena Völlger, Bilyana Suvandzhieva, Maren Drewitz, Karina Oberheide, Franziska Steffen and Paul Moretti for the nice works they performed during their practical courses or thesis at the TCI.

Tack så mycket Anna for the careful reading and correction of this work!

Илияна, мила моя „DrumBeach sister", много ти благодаря за ентусиазираните коректури и твоята невероятна положителна енергия. Ти си просто прекрасна.

Mes chères parents pour leur soutien durant mon parcourt universitaire.

Moja piękna Madziu! Bez Ciebie wszystko było by nie możliwe. Dziękuję Ci za Twoje nieustanne wsparcie i miłość. Gdy jesteś przy mnie, wszystko jest piękniejsze…

Kurzfassung

<u>Schlagworte</u>: Stammzellen, Zytokine, mesenchymale Stromazellen, Nabelschnurgewebe.

Eine Herausforderung der regenerativen Medizin ist die Wiederherstellung defekter Gewebe des menschlichen Körpers durch den Einsatz von Stammzellen. Zu diesem Zweck werden Stammzellen *ex vivo* prozessiert, wobei die Vermehrung und die Ausdifferenzierung der Zellen zielgerichtet kontrolliert werden müssen. In diesem Zusammenhang spielen Zytokine eine entscheidende Rolle. Darüber hinaus stellt die Quelle der prozessierten Zellen einen wichtigen Aspekt für die Etablierung eines reproduzierbaren und technisch vertretbaren Bioprozesses dar.

Im Rahmen dieser Arbeit wurden rekombinante CHO Zelllinien zur Produktion der Stammzell-relevanten Zytokine *Angiopoietin-like protein* 1 und 2 (Angptl1 und Angptl2), sowie *Leukemia Inhibitory Factor* (LIF) etabliert. Während Angptl1 und Angptl2 intrazellulär exprimiert wurden, konnten jedoch die Proteine extrazellulär nicht nachgewiesen werden. Dagegen konnte das LIF Protein von der etablierten Zelllinie erfolgreich sekretiert werden. Die Bioaktivität des aufgereinigten LIF wurde daraufhin anhand von Suspensionskulturen muriner ES-Zellen demonstriert. Mittels durchflusszytometrischer Zellsortierung wurden schließlich klonale CHO Zelllinien generiert, die eine Optimierung des LIF Produktionsprozesses erlauben könnten.

Ferner erfolgte eine Charakterisierung mesenchymaler Stromazellen (MSC) aus dem Nabelschnurgewebe. Im Hinblick auf therapeutische Anwendungen wurden xeno-freie Isolierungs- und Expansionsprozesse durchgeführt. So zeigten die isolierten MSCs ein hohes Proliferationspotential und wiesen einen stabilen Phänotyp auf, was für die Etablierung biotechnologischer Prozesse hoch interessant ist. Eine große Anzahl an undifferenzierte hoch qualitativer Zellen für die Bereitstellung therapeutischer Dosen könnte somit in kurzer Zeit erhalten werden. Schließlich wurde das osteogene Differenzierungspotential der Zellen untersucht. Hierbei konnte kein funktioneller osteogener Phänotyp induziert werden. Allerdings wurde gezeigt, dass die Zellen dennoch auf einen osteogenen Stimulus reagierten, was unter anderem durch die Herunterregulierung des Oberflächenmarkers CD90 zu erkennen war. Zukünftige Arbeiten sollten untersuchen, ob die isolierten MSCs über alternative Differenzierungsmethoden effizienter osteogen induziert werden können. Darüber hinaus bleibt die Frage offen, ob die Zellen ein höheres Potential für weitere mesodermale Differenzierungswege aufweisen.

Abstract

<u>Keywords</u>: stem cells, cytokine, Mesenchymal Stromal Cells, umbilical cord tissue

The engineering of stem cells to restore defect functions in human tissues is an ambitious aim in the field of regenerative medicine. The establishment of stem cell-based bioprocesses is challenging, as it requires the control of the cellular fate *ex vivo*. In this context, bioactive cytokines are key elements of the process. Moreover, the implementation of reliable and reproducible bioprocesses would be facilitated by the use of non-controversial and easily accessible stem cells in the human body.

In the present work, recombinant CHO cell lines were established for the production of the cytokines Angiopoietin-like proteins 1 and 2 (Angptl1 and Angptl2) and Leukaemia Inhibitory Factor (LIF), which are of high interest for stem cell technology applications. While the intracellular expression of Angptl1 and Angptl2 was demonstrated, the cytokines could not be detected in the cuture supernatants. In contrast, the CHO cell line established for the production of LIF secreted the recombinant protein. The bioactivity of the purified LIF was demonstrated using suspension cultures of ES cells. Given the bioactivity of the expressed cytokine, clonal CHO cell lines were eventually generated for the optimization of the LIF production process.

The second part of this work focused on the characterization of MSCs derived from human umbilical cord tissue. In the perspective of clinical applications, xeno-free isolation and expansion procedures were proposed. A large number of MSCs could be isolated from the tissue in a reproducible manner. The isolated cells exhibited a high proliferation potential and were found to display a stable MSC phenotype during long-term expansion. These features are particularly interesting in terms of cell engineering. Compared to MSCs derived from other sources, clinical doses could be obtained more rapidly from UC-MSCs. Finally, with regard to tissue engineering applications, the osteogenic differentiation potential of the cells was evaluated. The isolated cells could not be induced to a functional osteogenic phenotype, but responded to osteogenic stimulation, as illustrated by a down-regulation of the surface antigen CD90. Further investigations should be conducted to achieve a more efficient osteogenic differentiation and elucidate if the isolated cells may be more committed to other mesodermal lineages.

List of abbreviations

αMEM	Minimum essential medium alpha
Angptl	Angiopoietin-like protein
AP	Alkaline phosphatase
bFGF	Basic fibroblast growth factor
BSL	Biosafety level
bp	Base pair
BP	Bandpass filter
BM	Bone marrow
BrdU	5-bromo-2-deoxyuridine
CC	Coiled-coil domain
CCE	Counterflow centrifugal elutration
CD	Cluster of differentiation
cDNA	Complementary Deoxyribonucleic Acid
CFU-F	Colony forming unit-fibroblast
CHO	Chinese hamster ovary
CMV	Cytomegalievirus
Col I	Collagen type I
DAPI	4',6-diamidino-2-phenylindole
DEAE	Diethylaminoethyl
DHFR	Dihydrofolate reductase
ELISA	Enzyme-linked immunosorbent assay
ES cell	Embryonic stem cell
env	Gene coding for the retroviral envelope proteins
gag	Gene coding for he retroviral matrix and core proteins
GFP	Green fluorescent protein
GMP	Good manufacturing practice
GvHD	Graft-versus-host disease
FACS	Fluorescence-activated cell sorting
FCS	Fetal calf serum
FD	Fibrinogen-like domain
FGF	Fibroblast growth factor
FSC	Forward scatter
FITC	Fluorescein isothiocyanate
Glc	Glucose
Gln	Glutamine
GS	Glutamine synthetase
HA	Hyaluronic acid
HEK	Human embryonic kidney
HGF	Hepatocyte growth factor
HIV	Human immunodeficiency virus
HLA	Human leukocyte antigen
hLIF	Human leukemia inhibitory factor
HUCPVC	Human umbilical cord perivascular cell
HS	Human serum
HSC	Hematopoietic stem cell

List of abbreviations

Ig	Immunoglobulin
IgG:	Immunoglobulin G
IgM	Immunoglobulin M
IMAC	Immobilized metal affinity chromatography
ISCT	International Society for Cellular Therapy
kDa	Kilo dalton
Lac	Lactate
LIF	Leukemia inhibitory factor
LTR	Long terminal repeat
MHC	Major histocompatibility complex
MSC	Mesenchymal stromal cell
MSX	Methionine sulphoximine
MTX	Methotrexate
NLSs	Nuclear localization signals
OCN	Osteocalcin
OPN	Osteopontin
ORI	Origin of replication
PAGE	Polyacrylamidgelelectrophoresis
PAMAM	Polyamidoamine
PCR	Polymerase chain reaction
PE	Phycoerythrin
PEI	Polyethylenimine
PBMC	Peripheral blood mononuclear cell
PBS	Phosphate buffered saline
Pi	Propidium iodide
PLL	Peptide poly-L-lysine
Pol	Gene coding for the retroviral enzyme
PPT	polypurine tract
PRE	post-transcriptional regulatory element
RNAse	Ribonuclease A
RRE	Rev response element
RSV	Rous-sarkoma virus
RT	Reverse transcriptase
SDF-1	Stromal-derived factor 1
SDS	Sodium dodecyl sulfate
SFFV	Spleen focus forming virus
SIN	Self inactivating
SSC	Side scatter
TCA	Trichloride acetic acid
TEMED	Tetramethylethylenediamine
TGF	Transforming growth factor
UC	Umbilical cord
UCB	Umbilical cord blood
VEGF	Vascular endothelial growth factor
VSV-G	Protein G from Vesicular Stomatitis Virus
WJ	Wharton's jelly
WJC	Wharton's jelly cell

Contents

Contents

1 Introduction

The engineering of stem cells to restore defect functions in human tissues is an exciting challenge in the field of regenerative medicine. The aim of this fast emerging interdisciplinary area is the isolation of stem cells from niches of the human body and the use of their biological potential for clinical and tissue engineering applications. Stem cell based therapies exist since the first successful bone-marrow transplantations in 1968[1, 2]. Ever since, the procedure has been routinely used to treat hematopoietic disorders. In this context, minimal *ex vivo* manipulations have been required as hematopoietic stem cells have been transplanted following tissue isolation mostly as an heterogeneous population.

Many advances achieved over the last decades enlarged the perspectives for clinical applications of stem cells. The establishment of human embryonic stem (ES) cell lines opened possibilities for the use of pluripotent stem cells[3]. Adult stem cell niches were identified in various tissues of the body, exhibiting the potential to give rise to specific cell types. It was soon observed that these cells may be much less lineage restricted than previously thought, showing a so-called "stem cell plasticity" [4]. Expanded knowledge was gained for the isolation, the cultivation and the directed differentiation of the cells, so that *ex vivo* engineering of stem cell is now conceivable.

The development of bioprocesses for the delivery of highly qualitative cells to a patient is challenging, as each process step may influence the safety and the efficiency of the final cell product. A schematic view of the approach is given in Fig. 1.1 highlighting some questions that must be addressed for each step of the process.
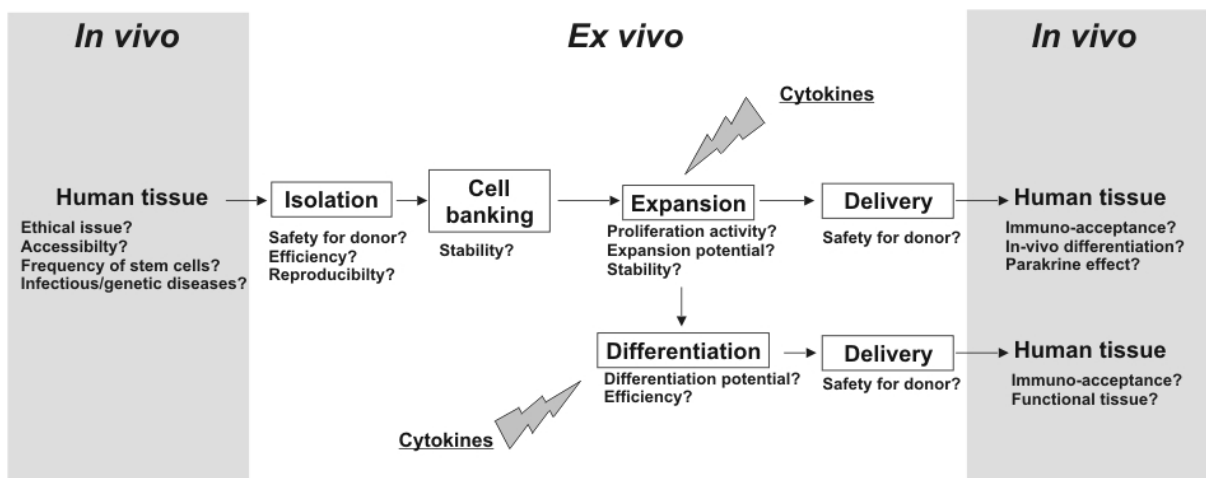
Fig. 1.1: Schematic overview of a stem cell-based bioprocess for clinical or tissue engineering applications.

In some cases, stem cells will be isolated and subsequently expanded to deliver a sufficient number of cells to support the regeneration of damaged tissues *in vivo*. For other applications, it will be desirable to differentiate stem cells *in vitro*, for instance for tissue reconstruction before delivery into the human body.

The cellular fate of stem cells is directed by bioactive proteins called cytokines, which are provided *in vivo* to the cells by their cellular environment. An important challenge of the *ex vivo* procedures is to determine cultivation conditions allowing the preservation of stem cell characteristics or the efficient differentiation into a specific lineage. In this context, the identification of cytokines and their production is crucial for the development of stem cell-based bioprocesses. For some cell populations, such as hematopoietic stem cells, *ex vivo* expansion remains difficult because appropriate culture conditions are still lacking. Newly described cytokines may help solving this problem[5]. In the case of embryonic stem cells, several factors have been identified making their *ex vivo* expansion possible[6-9]. The identification of these factors has been a breakthrough in this field, allowing in some cases the elimination of serum[8, 10] and the use of adherent co-cultures involving feeder cells[10-12], so that perspectives have been opened for the scale-up of the expansion processes. To date, cytokines represent an important part of the cultivation costs and their availability constitutes a bottleneck during the development of a stem cell-based bioprocess, in particular if large scale approaches are intended.

Stem cell availability is an essential point for the implementation of reliable and reproducible bioprocesses. In addition, the question of the public and political acceptance of the technologies plays an important role, especially for biotechnological companies, which still consider stem cell technology financially and technologically risky[13]. In this context, the source for the derivation of stem cells is crucial and should be carefully chosen according to the potential and the application field of the isolated cells, but also according to the related ethical issues.

Embryonic stem (ES) cells have a great potential in regenerative medicine due to their pluripotency, but their use may be limited by serious ethical considerations. Recent findings evidencing the reprogramming of somatic cells to pluripotent stem cells, termed as iPS cells[14], open ethically acceptable perspectives. Pluripotent stem cells may represent the most efficient approach for the generation of large amount of cardiac tissue[15, 16]. Even so, the concern

remains that undifferentiated iPS cells as well as ES cells may form teratomas after transplantation in the body. As a consequence, their clinical application would introduce additional challenges.

Adult Mesenchymal Stem or Stromal Cells (MSCs) are considered a valuable alternative to pluripotent stem cells. Since their discovery in bone marrow (BM) by Friedenstein et al. [17], BM-MSCs have been extensively investigated and their use in animal studies as well as in clinical trials showed encouraging results [18]. Today BM-MSCs are still considered as the "gold standard" for the use of adult MSCs. However, BM as a source for MSCs presents several disadvantages. Besides the invasive and painful collecting procedure, MSCs are present at very low frequency (approx. 0.001-0.01 % [19]) in BM-aspirates and their quality varies with the age of the donor. The low frequency implies that an extensive *ex vivo* expansion of the cells will be required to deliver clinical doses to a patient, which enhances the risk of epigenetic damages as well as viral and bacterial contaminations. The donor dependent quality is problematic for the establishment of a reproducible bioprocess. For these reasons, alternative sources of MSCs should be considered.

In this context, non-controversial and accessible sources of MSCs such as human adipose tissue or the umbilical cord have gained more and more attention in recent years. The human umbilical cord in particular, which used to be a waste product at birth, is a non-controversial and accessible source of autologous cells. It has been demonstrated that MSCs are present in the blood (UCB)[20] but also in the tissues of the umbilical cord. UCB-derived MSCs may have a limited technological potential because their frequency is even lower than in BM (ranging from 0.001–0.000001%) [21] and their isolation is hardly reproducible [22, 23]. In contrast, the frequency of MSCs in UC-tissues is believed to be much higher and the first generation of studies strongly suggests that these multipotent primitive cells may have a high potential for clinical and tissue engineering applications.

Aims of the work

Given the challenges of the development of stem cell-based bioprocesses and the recent findings in the field of MSCs, two objectives are defined for this work.

In the first part, stable recombinant CHO cell lines are established for the production of cytokines of high interest in stem cell technology. Among them, the production of two

Angiopoietin-like proteins (Angptl), which have been recently proposed to support the *ex vivo* expansion of hematopoietic stem cells, is intended. In addition, a CHO cell line is established for the production of human Leukaemia Inhibitory Factor (hLIF), a key cytokine for ES cell cultures. To allow the rapid establishment of stable CHO cell lines, lentiviral gene transfer is used and the efficiency of this technique is evaluated.

The second part of this work focuses on the characterization of MSCs derived from human umbilical cord tissue. In the perspective of a clinically relevant bioprocess, xeno-free isolation and expansion procedures are proposed. The primary cells isolated in these conditions are characterized and their potential is evaluated for the establishment of a reliable process to provide cells for therapeutic applications.

2 Theoretical background

2.1 Gene transfer techniques for the establishment of recombinant cell lines

The establishment of recombinant animal cell lines for the expression of heterologous proteins requires the transfer of foreign DNA into the host cell. The expression of a recombinant protein can be transient, i.e. the transgene is not integrated into the genome and will be lost at cell division. Transient gene expression is useful for the rapid production of protein, e.g. for initial screening of bioactivity[24]. For the establishment of a reliable process, stable cell lines which permanently express the transgene are necessary. Stable protein expression usually requires the integration of the expression construct into the host cell genome, although long-term episomal gene expression was also reported [25].

Several barriers have to be overcome for the delivery of expression vectors into the cell nucleus. Thus, DNA plasmids must be first condensed using cationic reagents or be packaged in a transfer vehicle to facilitate cell entry. After internalization, the DNA has to escape degradation in the cytoplasm and finally reach the nucleus. Once inside the nucleus, the delivered expression construct has to integrate into the genome of the host cell. Every step may limit the efficiency of the procedure.

Many approaches have been used for the transfer of expression vectors into mammalian cells. The methods can be roughly divided into non-viral transfer, denominated as "transfection", and viral transfer, termed as "transduction". An overview of current methods is given in Table 2.1. The methods are briefly discussed subsequently.

Table 2.1: Overview of transfection and transduction methods for mammalian cells.

DNA delivery methods	Chosen Ref.
Physical methods	
Electroporation	[26]
Microinjection	[27]
Particle bombardment	[28]
Sonoporation	[29]
Chemical methods	
Calcium phosphate	[30]
DEAE-dextran	[31]
Lipid-mediated	[32]
Peptid-mediated	[33]
Cationic dendrimers	[34]
Cationic polymers	[35]
Viral methods	
Adenoviruses	[36]
Adeno-associated viruses	[37]
Alphaviruses	[38]
Baculovirus	[39]
Herpes Simplex viruses	[40]
Retroviruses	[41]

2.1.1 Non-viral gene transfer

Physical methods

Physical methods such as microinjection, electroporation, sonoporation and particle bombardment are available techniques for DNA transfer into cells. Microinjection is efficient, as in this case foreign DNA can be directly introduced into the nucleus. However, the technique can be applied only for a limited number of cells and is used for specific applications, such as the manipulation of embryos [42]. Particle bombardment implicates the use of DNA-coated microparticles that are accelerated through the cell membrane. This technique has mostly found applications for the *in vivo* administration of DNA to animal tissues [43] or to plant cells [44]. Electroporation is a widely used technique and is applicable to many cell types. The cells are exposed to a high voltage electrical field inducing the formation of pores in the cell membrane and allowing exogenous DNA to pass into the cytoplasm. The procedure is rapid, but a high mortality of the cells is caused by the exposure to the electrical field and optimizations are required for every cell type. Similar limitations are observed for sonoporation, where ultrasound is used to transiently induce cell membrane poration [45].

Chemical methods

DNA transfer methods using chemical reagents have mostly been used for the establishment of recombinant mammalian cell lines.The general principle of chemical methods relies on the interaction of negatively charged DNA with positively charged reagents to form a complex, which is then internalized, presumably via endocytosis. DEAE-dextran transfection or calcium phosphate (CaPO$_4$) precipitation belong to the earliest chemical methods and have been widely used for the transfection of mammalian cells. However, DEAE is not appropriate for a stable transfection[31] and the efficiency of CaPO$_4$ transfection is strongly dependent on the presence of serum[46], which may be a major limitation for the establishment of industrial cell lines. Many reagents were developed for lipid-mediated DNA delivery. In this approach, cationic lipids are added to the DNA to form a complex called "lipoplex". The complex interacts with the hydrophobic and positively charged cell membrane and passes via endocytosis into the cytosol. The principle of the uptake is presented in Fig. 2.1.
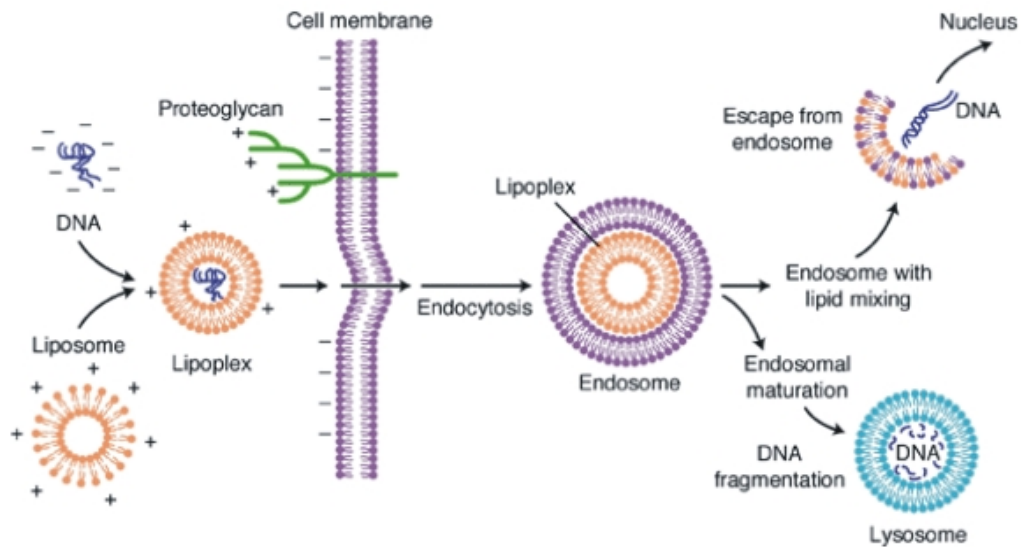
Fig. 2.1: Lipid-mediated-gene delivery[47]

Other approaches involving peptide-based delivery methods have been used. For instance, the cationic peptide poly-L-lysine (PLL) can be used to condensate DNA for efficient intracellular uptake[48]. Also many cationic polymers have been developed, such as polyamidoamine (PAMAM) dendrimers [49] or polyethylenimine polymer (PEI)[50] and its derivates such as mannose-PEI [51] or transferrin-PEI [52]. PEI has been shown to be one of the most effective reagent for the transfection of mammalian cells [53, 54]. The highly branched polycationic molecule (Fig. 2.2.A) forms a dense complex with the DNA, which can be efficiently internalized by the cells (Fig. 2.2.B).

Many of the transfer methods mentioned above are highly effective for DNA delivery into the cytoplasm. CaPO$_4$, cationic lipids or polymers are able to mediate a DNA uptake into almost every treated cell. However, subsequent barriers limit the efficiency of the transfection. Many delivered transfection particles remain sequestered in the endocytic vesicles and are degraded among the endosomal pathway (see Fig. 2.1). The high efficiency of the PEI transfection methods has been explained by its ability to destabilize endosomes after DNA uptake. This phenomenon, illustrated in Fig. 2.2.B, is most likely due to the buffer effect of the polymers, which leads to an increased osmotic pressure during endosomal acidification (driven by proton pumps) and

Fig. 2.2: PEI-mediated DNA uptake.
In A: structure of branched PEI. In B: internalization of the PEI/DNA complex (1), release from the endosome, (2) and nuclear targeting (3), adapted from [54]

eventually to lysis. Additionally, the PEI/DNA complex seems to protect the plasmid from cytoplasmic nucleases after release from the endosome [55].

Besides the intracellular degradation process, the targeting into the nucleus plays also a limiting factor. In most cases, only a small fraction of the delivered DNA eventually reaches the nucleus. For instance, Holmes *et al.* measured that only 0.3 % of delivered DNA reached the nucleus 24h after transfection by cationic lipids[56]. In contrast, high nuclear trafficking may be possible when PEI/DNA complexes are used[57]. In order to optimize nucleus targeting, several strategies have been developed, as for instance the use of viral nuclear localization signals (NLSs) and nuclear-targeting peptides [58, 59].

Finally, the efficiency of non-viral methods is limited by the integration of DNA into the host genome. This process is inefficient and needs to be accompanied by the simultaneous introduction of a marker in the genome in order to select transfected cells. The selection marker can be imported on the same vector as the gene of interest or on a separate plasmid[60]. Commonly used selection systems involve the expression of the enzyme dihydrofolate

reductase (DHFR), which is essential for the *de novo* synthesis of nucleotide, and glutamine synthetase (GS). Cells that contained the expression vectors episomally may first survive, but will then be eliminated over the next cell generations. The selective pressure can be subsequently increased using for instance inhibitor such as methotrexate (MTX) for the enzyme DHFR or methionine sulphoximine (MSX) for the enzyme GS. As a response, the transgene copy number is increased in the genome, which leads to a higher recombinant protein expression [24].

It should be mentioned that integration in the genome alone does not guarantee a stable protein expression. The site of integration has also been found to be of tremendous importance. The random integration of the transgene in a transcriptional inactive area of the chromosomes, e.g. in heterochromatin, and/or silencing phenomenon such as DNA methylation and histone hypoacetylation, leads in many cases to the inactivation of the recombinant protein expression [61]. Many scientific efforts have been made to allow a site specific integration in transcriptional active area of the genome[62-64]. The topic is outside the scope of this overview, but has been the subject of previous reviews [24, 65].

The establishment of stable cell lines using physical and chemical methods is challenging, as many cellular barriers and mechanisms have to be overcome for the integration of a transgene into the host cell genome. In contrast, biological vectors such as viruses are able to efficiently integrate DNA into the host genome. This natural ability has been employed to design viral vectors for foreign DNA delivery. In the following section, retroviral DNA delivery is discussed shortly and the lentiviral vector preparation used in this work is presented in more detail.

2.1.2 Viral gene transfer: retroviral vectors

Many viruses have been used for the delivery of expression constructs into mammalian cells (see Table 2.1). Retroviruses present unique features that make them particularly interesting in this regard. During their life cycle, these RNA viruses can stably integrate their genomes into the chromosmes of infected cells for a subsequent high expression level of viral proteins. The following part briefly presents the mechanisms involved.

Retrovirus life cycle

Fig. 2.3.A presents the 3D structure of a retrovirus. The viral capsid contains the RNA genome (two identical copies) as well as the viral enzymes (protease, reverse transcriptase/RNAse, integrase) necessary for the replication of the viruses. Envelop proteins are embedded in the lipid bilayer membrane (in red, Fig. 2.3.A). Surface glycoproteins are involved in the specific recognition of the host target cells. The genes *gag*, *pol*, *env* coding for the structural protein or viral enzymes are indicated.
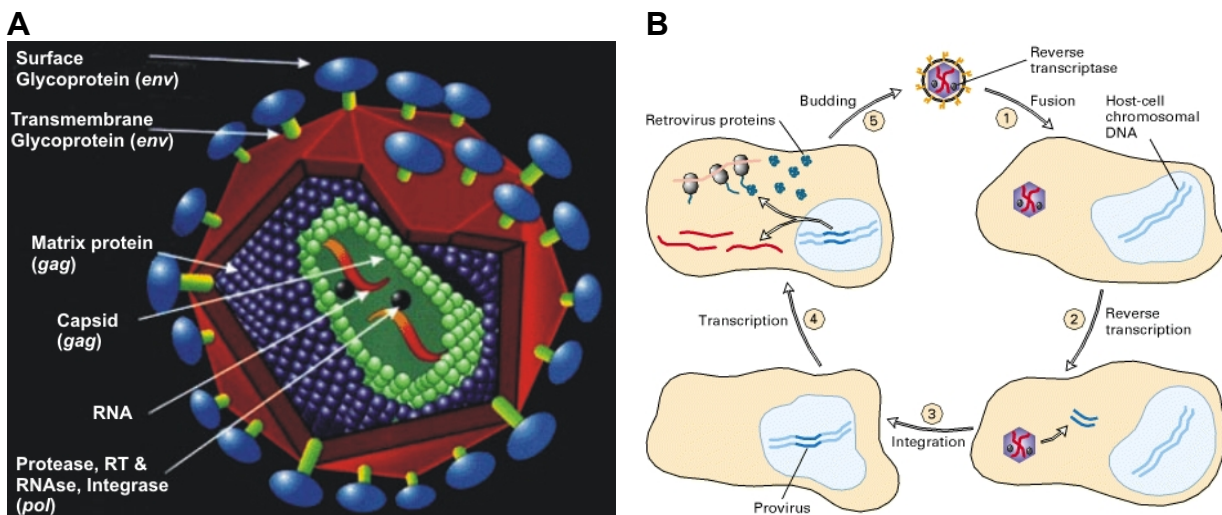
Fig. 2.3: 3D structure of a retrovirus (in A, adapted from http://www.stanford.edu/group/nolan) and retrovirus life cycle (in B, adapted from [66]**)**

The life cycle of retroviruses begins with the infection of the host cell (Fig. 2.3.B). The viral surface glycoproteins bind to receptors of the targeted host cells and initiate the internalization. Following internalization, the RNA genome is reverse transcribed into DNA (2) and integrated into the host genome by viral integrases. Once in the genome, the transcription of the viral gene is promoted by the retroviral promotor (4). The protein synthesis machinerie of the host cell is then used for the translation of new viral proteins, which finally assemble for the formation and the budding of new viruses out of the cells (5).

By modification of the retroviral genome and the use of packaging cells for virus production, retrovirus-based delivery systems have been developed for the insertion of a transgene into a host cell genome. A crucial aspect of this approach has been the inactivation of retroviral replication, so that after genome integration, a new generation of retroviruses can not arise from the infected cells. Many retroviruses only integrate into dividing cells, thus limiting the delivery to a subset of cells within the treated population. Lentiviruses, a sub-class of

retrovirus, have been found to have the ability to transduce dividing and non-dividing cells[67], so that very high transduction efficiency can be attained using this delivery system.

Retroviral gene delivery using lentiviral vectors

Lentiviral vectors have been widely used for the transfer of transgenes to mammalian cells in the perspective of gene therapy [68, 69]. Lentiviral vectors can integrate long DNA sequences (up to 10 kb) and most importantly allow a long-term expression of a transgene, because they incorporate preferentially within active transcription areas of the host genome[70]. The biosafety of the vector systems, in particular if the vectors are based on viruses infectious for human (e.g. HIV-1), has been a source of concerns. Several modifications of the virus genome have been made to guarantee the biosafety of the transfer methods [69, 71]. First, as mentioned above, non-replication competent viruses are used, i.e. the viruses are able to infect host cells, but will not form new viruses. Also, the vector transferred to the host cell is "self inactivating" (SIN), which means that after integration into the genome, the transcription of viral sequences is not possible.

In this work, replication incompetent viruses transferring a SIN lentiviral vector designed by Schambach *et al.* [71, 72] was used for the transduction of CHO cells. The vector preparation is based on the Human Immunodeficiency Virus (HIV-I). The approach is presented here in short.

The production of lentiviruses for the transduction of the CHO cells take place in so called packaging cells. HEK 293T cells are frequently used for this purpose. These cells are transiently transfected with several plasmids providing all genetic elements necessary for the production of the lentiviruses. Thus, the production of replication incompetent viruses is achieved by segregating the key coding and regulatory sequences of the HIV-I genome on four separated plasmids. Only the vector containing the gene of interest exhibits the packaging signal ψ (SIN vector in Fig. 2.4.B), i.e. only this vector is packaged into the viruses for delivery. This point is illustrated in Fig. 2.4.B. In comparison, a schematic representation of the HIV-I genome is given (in A).

A

B
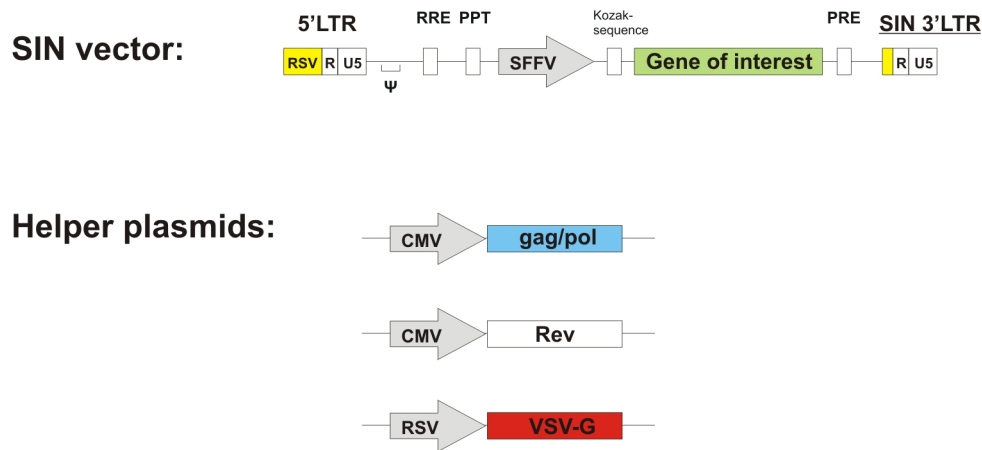
Fig. 2.4: Schematic representation of the HIV-I genome (in A), a part of the genome (gene Nef, Vpr, Vpu, Vif and Tat) has been omitted. Schematic representation of the SIN vector and helper plasmids used for the production of lentiviruses. LTR: long terminal repeats; ψ: packaging signal; RRE: Rev response element; PPT: polypurine tract; SFFV: Spleen focus forming Virus promotor; PRE: post-transcriptional regulatory element; SIN: self inactivating; CMV: Cytomegalievirus promoter; RSV: Rous-Sarkoma Virus promoter.

The sequences coding for the viral proteins are delivered by the so-called helper plasmids. Thus, the gene *gag*, coding for the matrix and core proteins, and the gene *pol* coding for the viral enzymes (reverse transcriptase, integrase, RNAse, see Fig. 2.3) are delivered with one plasmid. A second plasmid brings the gene coding for the Rev protein, an essential viral protein for the transport of the viral RNA into the cytoplasm of the packaging cells. The third plasmid contains the gene coding for the surface proteins of the lentiviruses. For the infection of CHO cells, the HIV-I surface glycoprotein ENV (see Fig. 2.4.A), which specifically interacts with the surface receptor CD4 of human T lymphocytes, was replaced by the protein G of Vesicular Stomatitis Virus (VSV-G in Fig. 2.4.B), which recognizes a broad range of mammalian cells [73].

The lentiviral vector contains the gene of interest flanked with a strong promoter SFFV (Fig. 2.4.B), which allows a high expression of the transgene in the CHO cells once transduction has occurred. The lentiviral vector also harbors the regulatory sequences necessary for the transcription of the plasmid DNA into viral RNA in the packaging cells. These regulatory

promoter and enhancer sequences are contained in the so called long terminal repeat (5'LTR and 3'LTR). In the vector used, the promoter sequence of HIV-I (U3 in the 5'LTR, Fig. 2.4.A) has been replaced by a strong RSV promoter (see 5'LTR in Fig. 2.4.B) to allow a higher virus production in the HEK 293 T cells. The sequence interacting with the REV protein (RRE, Rev response element) for the nuclear export of the RNA is also present. Additional regulatory sequences such as the post-transcriptional regulatory element (PRE) and the polypurine tract (PPT) are also present on the vector and promote a high expression of the transgene after transduction[74].

Once integrated by the lentiviruses into the CHO genome, it is important that the viral transcriptional activity conferred by the LTRs is inactivated. This is the main feature of self inactivating "SIN" vectors. The transcriptional activity in the HIV genome is conferred by the U3 region of the 3'LTR (yellow sequence in Fig. 2.4.A). Thus, in the SIN vector used in this work, the portion of the 3'LTR exhibiting the transcriptional activity is deleted (yellow sequence in Fig. 2.4.B), so that the vector finally integrated in the CHO genome is a promoter-lacking sequence. In this context, non lentiviral transcription activity can be triggered in the CHO genome.

2.2 The human umbilical cord: a source of multipotent primitive cells with potential for clinical and tissue engineering applications.

The human umbilical cord harbors several primitive cell populations of biotechnological interest. For instance, human umbilical vein endothelial cells (HUVEC), which can be isolated by well established procedures, may be used for tissue engineering applications, in particular for the generation of blood vessels *in vitro* [75-77]. The umbilical cord blood (UCB) has been the focus of many studies in the context of hematopoietic stem cells. Sub-populations of hematopoietic progenitors such as $CD34^+$ and $CD133^+$ cells can be isolated from the UCB [78]. Clinical transplantations of cord blood hematopoietic cells have been proposed for more than 20 years [19] for the reconstitution of the blood system.

During the last decade, the human umbilical cord (UC) gained more and more attention as a source of MSCs (see Fig. 2.5). The acronym "MSC" has been used in the literature to denominate Mesenchymal Stromal Cells as well as Mesenchymal Stem Cells. In this work, "MSC" will be used for mesenchymal stromal cell (see 2.2.3). It has been demonstrated that MSCs are present both in the blood [20] and in the tissues of the umbilical cord. However,
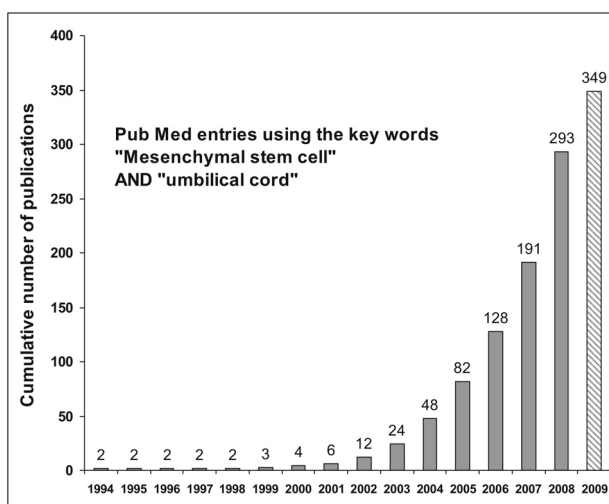
Fig. 2.5: Cumulative number of publications over the last 15 years dealing with UC-derived MSCs (entries by PubMed using the terms "mesenchymal stem cells" AND "umbilical cord" until July 2009).

MSC represent a rare cell population in the UCB with a frequency ranging from 0.001–0.000001% [21] and their isolation is hardly reproducible [22, 23]. In contrast, the frequency of MSCs in UC-tissues is believed to be much higher. In the following sections, an overview of the isolation, the characteristics, the differentiation potential, as well as the reported applications of UC-MSCs is given.

2.2.1 The human umbilical cord: a source of MSCs

The human umbilical cord (UC) consist of two arteries and a vein, which are surrounded by connective tissue, the so-called Wharton's jelly (WJ), enclosed by the amniotic epithelium (Fig. 2.6.A). In recent years, several studies described at least four separate regions of the umbilical cord containing MSCs (Fig. 2.6.B). Mesenchymal stromal cells could successfully be isolated from umbilical cord blood[79], the umbilical vein subendothelium[80], from the Wharton's jelly[81, 82], and from the perivascular region[83]. The present overview will focus on MSCs derived from UC tissue.
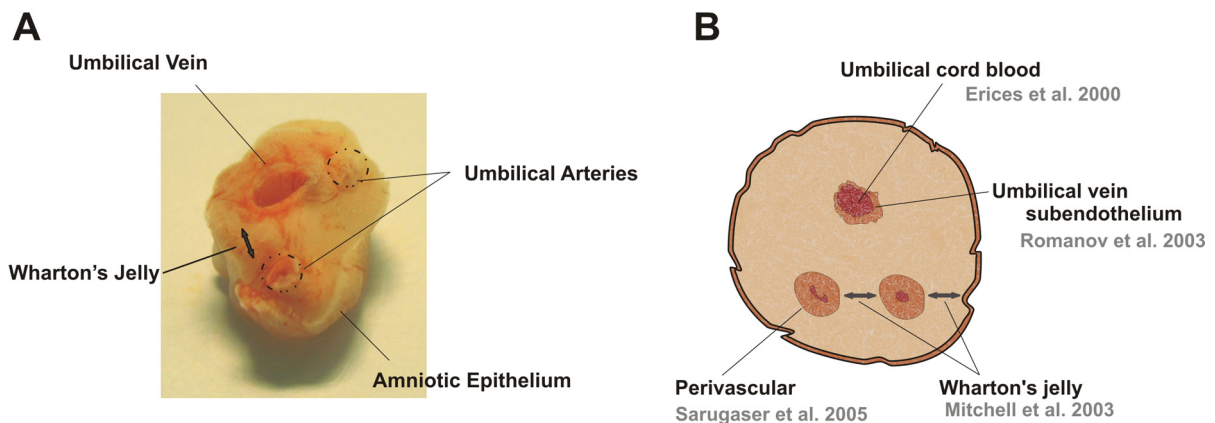
Fig. 2.6: Localization of MSCs within the tissues of the human umbilical cord.

2.2.2 Isolation of MSCs from the umbilical cord

Several protocols were published for the isolation of MSCs from the umbilical cord tissue. Depending on which compartment of the cord the cells are isolated from, different approaches have been adopted, combining mechanical and/or enzymatic treatment of the tissue. A schematic overview of the applied isolation approaches is given in Fig. 2.7. Basically, the isolation procedure starts with the removal of umbilical vessels. The cord is then cut in smaller segments or chopped into small pieces which are subsequently enzymatically digested [81, 84, 85]. Alternative isolation methods without removal of vessels [86, 87] and without enzymatic digestions [82, 86] or explant cultures [88, 89] have also been described. More specifically, further methods have been established in order to isolate cells from the perivascular tissue or the subendothelium of the umbilical vein [80, 83, 90-92]. For instance, Romanov *et al.* isolated a culture of endothelial cells by enzymatic digestion of the vein subendothelium, which was subsequently overgrown by MSCs within one week[80]. Sarugaser *et al.* first isolated the blood

vessels with the surrounding connective tissue. The perivascular tissue was then digested using collagenase and blood cell depletion (CD45^{+} cells) was performed subsequently using magnetic activated cell separation (MACS) [83].

To date, it still remains to be investigated whether cells isolated from different compartments or derived by different isolation procedures share the same cell characteristics, e.g. proliferation and differentiation potential and immunologic properties.
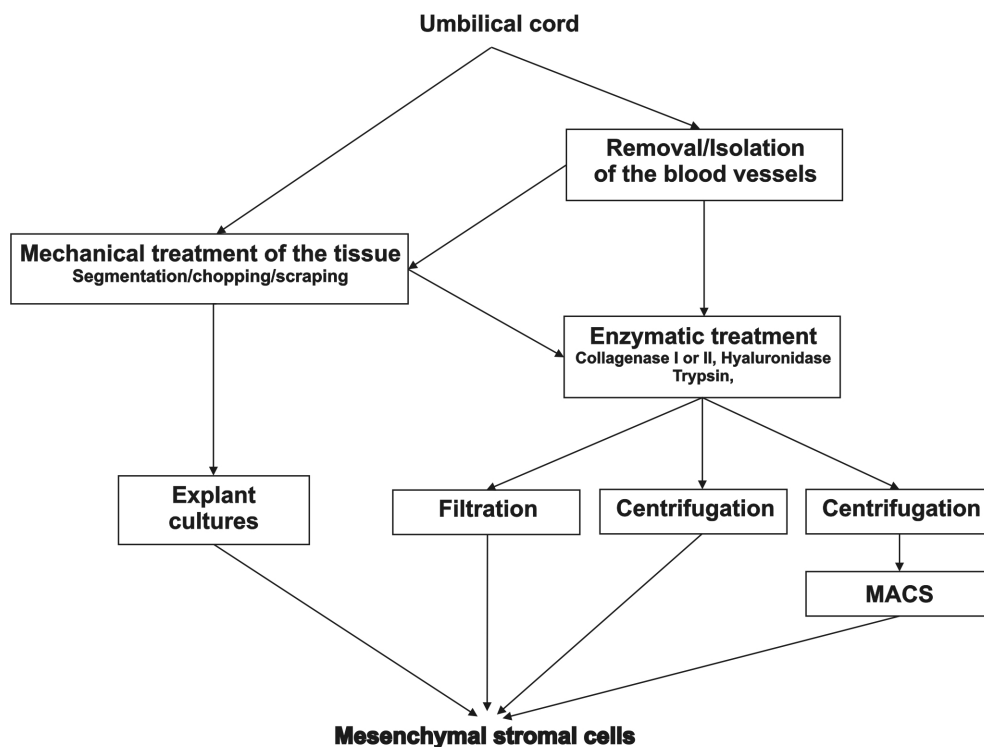
Fig. 2.7: Schematic overview of applied protocols for the isolation of UC-MSCs

2.2.3 Characterization of UC-derived MSCs

The acronym "MSC" has been widely used in the literature for "Mesenchymal Stromal Cell" as well as for "Mesenchymal Stem Cell" to denominate plastic-adherent fibroblast-like cultures isolated from different adult or extra-embryonic tissues. Because there is currently no consensus set of markers allowing the identification of MSCs and considering the fact that the definition criteria for stem cell are not unanimously accepted [47], it appeared unwise to apply the term "stem cell" for mesenchymal cell populations. In view of this, the International Society for Cellular Therapy (ISCT) proposed to define plastic-adherent fibroblast cultures as

"Multipotent Mesenchymal Stromal Cells" (MSC) [93] and published the minimal criteria defining these cells [94] in 2006.

UC-derived stromal cells meet the basic criteria defined by the ISCT, namely the adherence to plastic, the expression of a set of specific surface antigens (see below) and a multipotent differentiation potential (discussed in 2.2.4).

Histologically, cells freshly isolated from the UC are mainly fibroblastic in appearance (see Fig. 2.8). An additional feature of MSCs is their clonogenicity. A single cell is able to rise to a fibroblastic colony in a so-called colony forming unit fibroblast (CFU-F) assay. Historically, this characterization parameter is linked to the pioneer work of Friedenstein et al., who first isolated stromal cells from bone
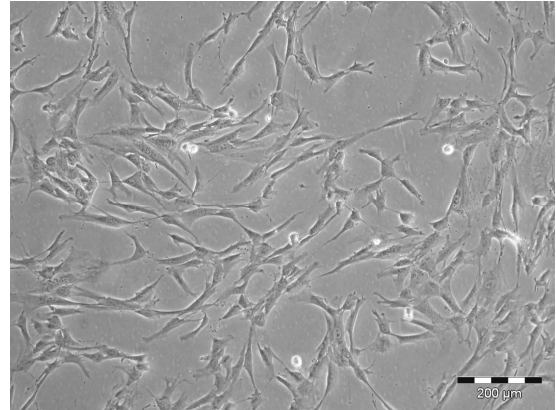
Fig. 2.8: Fibroblastic morphology of UC-derived MSCs

marrow according to their capability to form fibroblastic colonies and demonstrated their osteogenic potential *in vitro* [17]. The CFU-F assay gives the frequency of fibroblast-like cells within a population capable of extensive proliferation and thus, able to give rise to a colony (see Fig. 2.9).
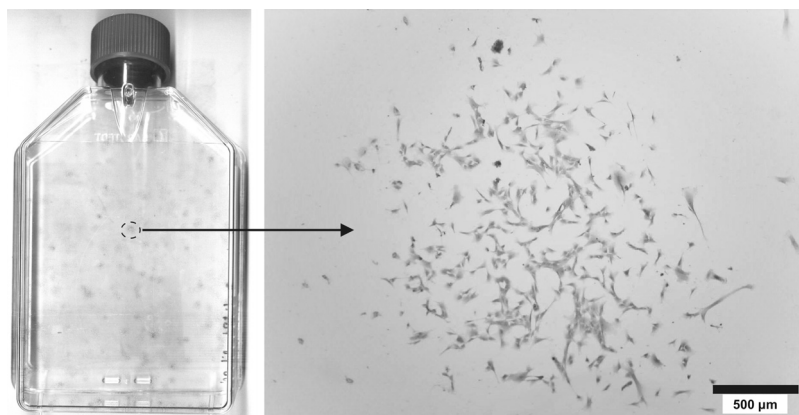
Fig. 2.9: CFU-F assay of UC-derived stromal cells.

This assay is commonly used to enumerate MSCs in a particular tissue [19]. For instance Lu et al. recently evaluated the frequency at 1 CFU-F per 1609 mononuclear cells (MNCs) in whole umbilical cord tissues [87]. More specifically, 1 CFU-F per 333 MNCs was reported in cells isolated from perivascular tissues of the umbilical cord vein [83]. In comparison, the isolation frequency of CFU-F from bone marrow was estimated to be in a range of 1-10 CFU-F per 10^5

MNCs [19] and only 1 CFU-F per 10^8 MNCs [22] to 1-3 CFU-F per 10^6 MNCs were reported in umbilical cord blood [95, 96]. According to these data, the human umbilical cord is considered to harbour a higher number of MSCs than those found in bone marrow or the umbilical cord blood. The results of the CFU-F assay, however, depend on different parameters such as the isolation method, culture conditions, as well as the cell seeding density. This leads to a high degree of variability in the results and makes the comparison of the published data difficult. The analysis of specific molecules expression at the single cell level via flow cytometry is strongly advisable in order to identify MSCs within a mixed cell population.

In contrast to other progenitor cell populations as for instance hematopoeitic stem cells, there is currently no specific marker available defining human MSCs. The expression of a set of markers combined with the demonstration of *in vitro* multi-lineage differentiation potential is necessary to identify MSCs in UC-derived cell populations. Table 2.2 summarizes extracellular and intracellular molecules expressed by UC-MSCs reported in the literature until July 2009. The surface antigen SH2 (CD105), SH3 (CD73) and Thy-1 (CD90) are widely used for the identification of UC-derived stromal cells (see Table 2.2), as these markers are proposed by the ISCT as positive markers for human MSCs [94]. The cells are not from haematopoietic or endothelial origin and thus lack the expression of the surface markers CD45, CD34 (common leukocytes and heamatopoeitic progenitor antigens, respectively) or CD31 (endothelial marker). Additionally, like MSCs isolated from other tissues, UC-derived stromal cells do not express the human leukocyte antigen HLA-DR, but express HLA-I. However, Sarugaser *et al.* reported that the expression of the latter marker may be manipulated *in vitro*, which may be very promising in term of allogenic transplantations [83].

UC-derived stromal cells were found positive for pluripotency markers usually expressed by embryonic stem cells such as Oct-3/4, Nanog, Sox-2 or SSEA-4 (see Table 2.2), which underlines their primitive nature. The primitive character of the UC-derived cells is also illustrated by their high proliferation and expansion capacity. UC-derived stromal cells have shorter doubling times compared to adult BM-MSCs [87, 90, 97, 98], exhibit telomerase activity [82, 84, 99] and could be expanded *in vitro* to a number of population doublings ranging from 20 to 80 without evidence of senescence or abnormal karyotype [82, 85, 86, 100].

Table 2.2: Reported intra- and extra-cellular markers of UC-derived MSCs till July 2009.

Marker	Expression	References
CD10	+	85, 101
CD13	+	85, 87, 101-108
CD14	–	84, 85, 87, 101, 103, 109, 110
CD29 (integrin β1)	+	85, 87, 106, 107, 109-116
CD31 (PECAM)	–	85, 87, 90, 106, 107, 112, 113
CD33	–	85, 117
CD34	–	83-85, 87, 89, 90, 100, 101, 103, 104, 106-110, 112-117
CD38	–	100, 107, 115
CD44	+	83-85, 87, 89, 101, 104, 106-108, 110, 112, 113, 115-117
CD45	–	83-85, 87, 89, 90, 100, 101, 104, 106-108, 110, 112, 113, 116, 117
CD49b (integrin α2)	+	85, 104
CD49c (integrin α4)	+	85
CD49d (integrin α3)	+	85
CD49e	+	85, 90
CD51 (integrin α5)	+	85, 116, 118
CD54 (ICAM-1)	-/+ *	100, 104, 113
CD56	–	85
CD71	-/+	110, 115
CD73 (SH3)	+	83, 84, 87, 89, 99, 101, 108-114, 116, 118
CD90 (Thy-1)	+	83, 85, 87, 89, 90, 99-101, 104, 106, 108, 110-112, 114, 117
CD105 (endoglin, SH2)	+	83-85, 87, 89, 99-101, 103, 104, 107, 109, 112, 113, 116-118
CD106 (VCAM-1)	-/+ *	83, 87, 104, 106, 119, 120
CD117 (c-kit)	-/+ *	82, 83, 90, 99, 101, 104, 106, 110, 111, 117
CD123 (IL-3 receptor)	–	83
CD133	–	85
CD146	+	90, 119, 121
CD166 (ALCAM)	+	87, 99, 108, 109, 111, 113, 122
CD235a (glycophorin A)	–	83
CD271	n.d.	
Bmi-1	+	115, 123
Esrrb	–	123
GD2	+	124
HLA-1	+	85, 100, 115, 125
HLA-DR (MHC class II)	–	83, 85, 87, 88, 101, 104, 106-108, 111, 112, 114, 115, 120
HLA-DP (MHC class II)	–	83, 101, 107, 110
HLA-DQ (MHC class II)	–	83, 101, 110
HLA-A, B, C (MHC class I)	+	83, 87, 101, 104, 106, 108-111
HLA-G (MHC class I)	-/+*	83, 86, 126
Hoxb-4	–	123
MSCA-1	n.d.	
Nanog	+	85, 99, 123-125, 127
Nucleostemin	+	115, 123, 127
Oct-3/4	-/+*	86, 99, 123-125, 127, 128
Rex-1	+	99
Sox-2	+	85, 99, 124, 127
SSEA-3	-/+*	99, 123
SSEA-4	-/+*	83, 99, 112, 123, 124
STRO-1	-/+*	83, 90, 125
Tbx-3	–	123
TCL-1	–	123
Tra-1-60	-/+*	99, 123
Tra-1-81	-/+*	99, 123
ZFX	+	123
Zic-3	–	123

*discrepancy among the published results

19

It was first unclear whether UC-derived stromal cells were homogenous regarding their primitiveness or if UC-derived stromal populations rather harbour a subset of primitive MSCs [129]. For instance population doubling times estimated between 60 to 85 hours for freshly isolated UC-cells rapidly decreased within 2-3 passages to approx. 25 hours [83, 84], which may indicate the presence of a fast growing sub-population of more primitive cells overgrowing the initial population. This hypothesis was further strengthened in recent works demonstrating via flow cytometry the existence of a subset of cells expressing pluripotency markers [124, 125]. Zhang *et al.* for instance reported that approx. 20 % of stromal cells isolated from perivascular tissues of the umbilical arteria express Oct-3/4 and Nanog [125].

With a growing number of data showing that MSC-like cell population isolated from UC tissues are rather heterogeneous, at least in regard to primitive marker expression, the identification of a universal marker defining primitive human MSCs remains challenging. Several cell surface molecules were recently proposed for the identification and isolation of MSCs in bone marrow aspirates such as CD271 [130, 131], MSCA-1 [131], SSEA-4 [132] and the neural ganglioside GD2 [75, 133]. To our knowledge CD271 and MSCA-1 expressions have not been reported yet in UC-derived stromal cell populations. Xu *et al.* recently isolated a subset of GD2$^+$ cells exhibiting a high clonogenicity as well as proliferation capacity but also a significantly stronger multi-differentiation potential than GD2$^-$ cells. According to their results, GD2 may be a useful marker to isolate multipotent MSCs from UC-tissues, but further studies are needed to verify these findings.

The most convincing biological property for the identification of MSCs remains the capability to differentiate into mesodermal lineages. In the next section, the *in vitro* differentiation potential of UC-derived stromal cells is presented.

2.2.4 In vitro differentiation potential

The differentiation repertoire of stromal cells derived from UC tissue reported in the literature till July 2009 is summarized in Table 2.3. The potential of UC stromal cells to differentiate into adipocytes, chondrocytes and osteocytes has been widely investigated and well established by several groups. According to the minimal definition criteria proposed by the ISCT, UC-derived stromal cells are considered multipotent MSCs [94].

Table 2.3: Differentiation potential of stromal cells derived from human umbilical cord tissue reported in the literature till July 2009.

	Cell type	References
Mesodermal lineage	Adipocyte	84, 86, 87, 90-92, 97, 99, 100, 106, 109, 110, 113-117, 119-121, 125, 134-137
	Chondrocyte	84, 90, 92, 97, 99, 109, 110, 114, 116, 117, 119, 121, 125, 134-136, 138
	Osteocyte *	80, 83, 84, 86, 87, 89-92, 97, 99, 100, 106, 109, 110, 112-117, 119-121, 125, 134-137, 139, 140
	Cardiomyocyte *	113, 116, 119, 141
	Skeletal myocyte	100
	Endothelial cells	97, 106, 114
Ectodermal lineage	Neuronal cells	81, 82, 84, 87, 117, 118, 142-144
Endodermal lineage	Islet-like cells	98, 145
	Unmature hepatocytes	146

*Discrepancy among the published results.

Successful adipogenic, chondrogenic and osteogenic differentiation of UC-derived MSCs are exemplary presented in Fig. 2.10.
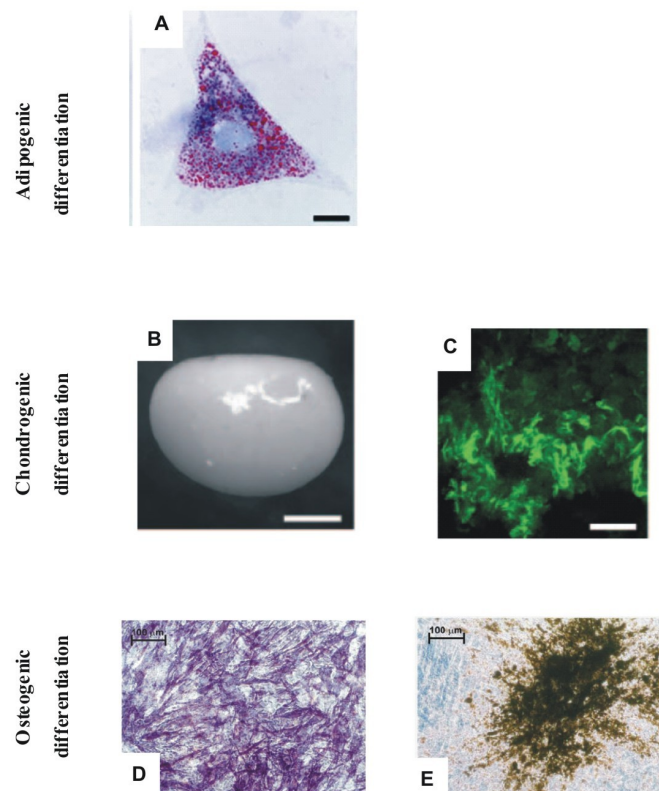
Fig. 2.10: Adipogenic, chondrogenic and osteogenic potential of UC-derived MSCs. A: formation of lipid droplets stained with oil red O in Wharton´s Jelly cells after adipogenic induction, scale bar = 20 μm; modified from [84], B: cell sphere obtained in droplet culture of chondrogenically induced UC-MSCs (scale bar = 500 μm) with abundant type II collagen expression (in C, scale bar = 50 μm); modified from [84], D: AP expression after osteogenic differentiation of umbilical vein derived MSCs; modified from [92]. E: mineralization of osteogenically induced culture of umbilical vein derived MSCs evidenced by von Kossa staining; modified from [92].

Adipogenic potential is usually demonstrated by the apparition of cells exhibiting intracellular lipid droplets (Fig. 2.10.A). The capacity to form chondroblasts is displayed by the formation of shiny cell-spheres with type II collagen expression in the extracellular matrix in droplet cultures (Fig. 2.10.B). Enhanced alkaline phosphatase (AP) expression and mineralization assayed by von Kossa or Alizarin red staining demonstrate osteogenic potency (Fig. 2.10.D and .E). It should be also mentioned that sub-populations of cells spontaneously exhibiting a functional osteogenic potential with mineralized bone nodules can be observed in UC-MSCs cultures [83]. Such bone nodules are presented in Fig. 2.11.
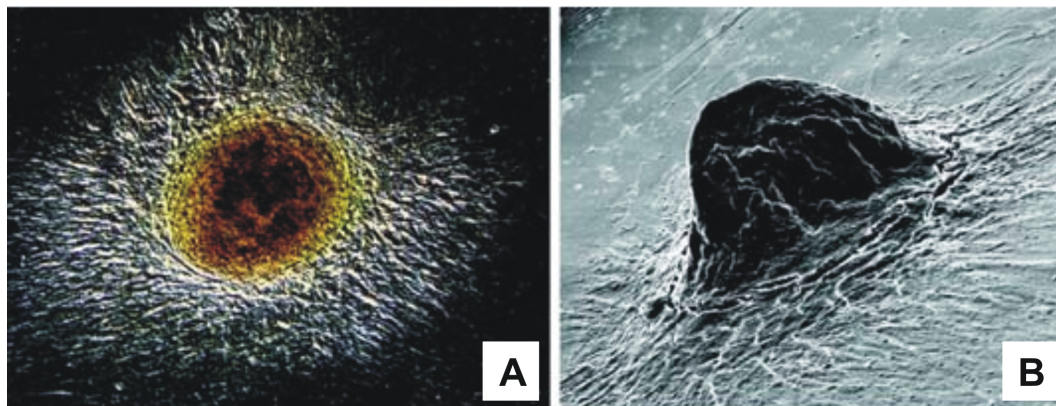
Fig. 2.11: Mineralized bone nodule in HUCPV cell culture, modified from [83]. A: nodule seen by phase contrast microscopy. B: nodule seen by scanning electron microscopy.

Moreover, it has been shown that UC-MSCs can successfully differentiate to endothelial cells after addition of VEGF and b-FGF [106, 114] and can form vessel-like structures in matrigel cultures [97, 114]. Furthermore, some UC-derived cell populations also seem to be able to differentiate to muscle cells. For instance WJCs could be induced to skeletal myocytes when placed in a myogenic medium [100]. Differentiation to cardiomyocytes was also reported but remains controversial. Whang *et al.* demonstrated for instance that WJCs could be induced to cells exhibiting cardiomyocyte morphology and expressing specific markers (*N*-cadherin and cardiac troponin) using 5-azacytidine or cardiomyocyte-conditioned medium [116]. Kadivar *et al.* observed cardiomyocyte-like cells expressing cardiac specific genes after 5-azacytidine induction of UC-MSCs isolated from the endothelium/subendothelium layer of the UC vein. In contrast to these results, Martin-Rendon *et al.* could not detect cardiac markers expression after *in vitro* induction of MSCs isolated from the WJs and perivascular tissues [119]. Furthermore, differentiated *in vitro* cultures of functional cardiomyocytes presenting beating clusters are poorly or not demonstrated. To our knowledge, only one group reported

differentiated cells exhibiting a slight spontaneous beating after 21 days of induction, however no quantitative data are presented in this study [141].

Recent findings suggested that UC-MSCs can differentiate into endodermal lineages. Campard *et al.* reported that UC matrix cells constitutively expressed markers of hepatic lineage, such as albumin, alpha-fetoprotein, cytokeratin-19, connexin-32, and dipeptidyl peptidase IV. After *in vitro* hepatic induction, cells exhibiting a hepatocyte-like morphology with hepatic features such as specific markers up-regulation and urea production were observed. However, the authors pointed out that their cells lacked important characteristics of functional liver cells and thus concluded that UC-matrix cells can be differentiated at least to immature hepatocytes [146]. Chao *et al.* were also able to induce WJCs using a four stage differentiation protocol to form islet-like clusters expressing pancreatic related genes and secreting insulin in response to glucose concentrations [145]. Recent results from Wu *et al.*, who successfully differentiated WJCs to pancreatic cells and observed higher differentiation potential compared to BM-MSCs [98], further reinforced these findings.

Finally, several groups observed the differentiation of WJCs to cells exhibiting morphological and biochemical characteristics of neural cells. This suggests that UC-MSCs are able to differentiate to a certain state of maturation along the neuronal lineage [81, 82, 84, 87, 117, 118, 142-144]. Mitchell et al. were the first to observe neuronal differentiation of WJCs after stimulation with bFGF and other neuronal differentiation reagents [82]. The differentiation was attested according to morphological changes and expression of neuron-specific enolase, βIII-tubulin, neurofilament M and tyrosin hydroxylase [82]. The differentiation potential was then confirmed by several other groups [84, 117, 118, 142]. Fig. 2.12 shows exemplary neuronal cells obtained by Karahuseyinoglu *et al.* after neuronal induction of a sub-population of WJCs [84]. Interestingly, it seems also possible to generate some sub-types of neurones as demonstrated by Fu *et al.*, who were able to obtain dopaminergic neurones from WJCs [118].
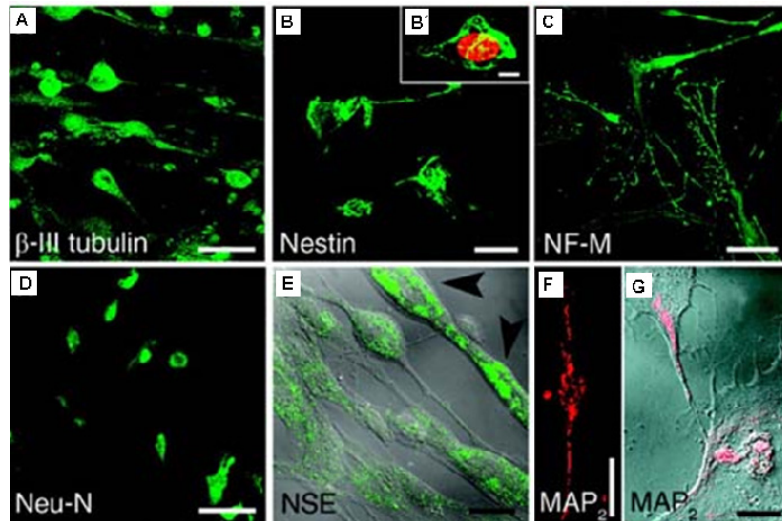
Fig. 2.12: Neuronal differentiation of WJCs, modified from[84]. A: β-III tubulin expression, B: Nestin expression located in the perinuclear cytoplasm in particular (B´), C: neurofilament-160 (NF-M), D: neuron-specific nuclear protein expression (Neu-N) restricted to the nucleus, E: neuron-specific enolase (NSE), F: microtubule-associated protein-2 (MAP2) detected as discontinuities along the cells. G: MAP2 distribution in cell-cell contact. Scale bars = 10 µm (B´), 20 µm (B, C), 50 µm (E), 100 µm (A, C, D).

Summarizing the published data, we find strong evidence to suggest that the human umbilical cord is a source of multipotent stromal cells that are capable of differentiating into mesodermal and non-mesodermal lineages. It remains unclear whether the differentiation potential of the UC-derived MSCs depends on their location in the UC-tissues. Recently, two sub-populations were found in cultures of Wharton´s Jelly-derived MSCs with regard to the expression of vimentin and pan-cytokeratin filaments [84]. Interestingly, cells expressing cytokeratin, predominently located in the perivascular tissue of the cord, did not differentiate into neurones *in vitro*. These findings are consistent with the results of Sarugaser *et al.*, who showed that perivascular UC-cells could not be induced to the neuronal lineage [83].

Many groups most likely investigate mixed populations of UC-MSCs, in particular if the cells are derived from whole umbilical cord or from the Wharton´s jelly. Thus, the results of studies comparing the differentiation potential of UC-derived MSCs with other sources (for example bone marrow) should be carefully interpreted [92, 112, 119, 135]. More work is needed to attest whether cells isolated from a defined compartment of the UC are more suitable for a specific differentiation lineage. This information would be of tremendous importance for the clinical applications of UC-derived MSCs.

2.2.5 In vivo and tissue engineering applications of UC-MSCs

Besides their multi-lineage differentiation potential, UC-derived MSCs have been shown to exhibit immune-privileged and immune-modulatory properties, which make them ideal candidates for cell-based therapies. Thus, several groups recently investigated the *in vitro* immune properties of umbilical cord-derived MSCs [126, 147, 148] and observed that the cells did not induce the proliferation of allogenic immune cells and even reduce the proliferation of activated peripheral blood lymphocytes in a dose-dependent way[147]. In this context, UC-MSCs may be used to reduce acute and chronic graft-versus-host disease (GvHD) occurring during allogenic transplantation, an approach which has been successfully applied with MSC derived from bone marrow[149, 150]. Currently, first clinical trials are conducted to demonstrate whether human UC-MSC have *in vivo* immune-suppressive effects and can be used for GVHD treatment (ClinicalTrials Identifier: NCT00749164).

Additionally, all reports of animal studies involving *in vivo* transplantation of UC-MSCs indicated low level of rejections and encouraging results in tissue repairs. In particular, supportive function through parakrine effects seems to be involved, i.e. that UC-MSCs support tissue repair by stimulating and modulating tissue-specific cells rather than differentiating into specialized cells. Yang *et al.* reported a positive modulation of microglia and reactive astrocytes activities by UC-MSCs when transplanted into rats after complete transection of the spinal cord [151]. They detected an elevated production of various cytokines around the lesion promoting spinal cord repair. Similar to these findings, Weiss *et al.* [85] hypothesized a supportive function of UC-MSCs mediated by various secreted trophic factors when used in a rodent model of Parkinson's disease. Liao *et al.* [152] used UC-derived MSCs in a rodent stroke model and observed that the cells, injected into the rat brain, survived for at least five weeks and reduced injury volume and neurologic functional deficits of rats after stroke. They assumed angiogenesis-promoting properties of the cells by the production of angiogenic cytokines. Koh *et al.* [153] used MSCs isolated from the umbilical vein sub-endothelium and induced first differentiation of the cells *in vitro* into neuron-like cells before transplantation into stroke rats. The cells were both morphologically differentiated into neuronal cells and able to produce neurotrophic factors, but have not become functionally active neuronal cells. Thus, the authors hypothesized that the observed improvement in neurobehavioral function might be related to the neuroprotective effects of UC-MSCs, rather

than to the formation of a new network between host neurons and the implanted cells. Analogical findings were reported by Lund *et al.* [101]. They suggested a supportive behavior of MSCs in a rodent model of retinal disease, where UC-MSCs were shown to contribute to photoreceptor rescue. In this study, the cells did not transform into neurons, but more likely secreted neurotrophic factors, as indicated by higher expression levels of these factors *in vitro*. The next generation of studies and first clinical trials will clarify if the benefit of UC-derived MSCs after transplantation experiments will rely on supportive effects or/and on differentiation *in vivo*.

One of the ambitious aims of regenerative medicine is the engineering of tissue *in vitro*. Few but very promising applications of UC-derived MSCs have been reported in this field. For instance UC-MSCs are believed to have potential in cardiovascular tissue engineering [154]. They grew very well on bio-degradable polymer for the elaboration of cardiovascular constructs[88] and could be used for the construction of human pulmonary conduits [155], for the engineering of biologically active living heart valve leaflets [156] and for the elaboration of living patches with potential for pediatric cardiovascular tissue engineering [157].

Considering the very encouraging results obtained in the recent years, it may be only a question of time until UC-derived MSCs will be routinely used for clinical and tissue engineering applications.

3 Establishment of CHO cell lines for the production of recombinant cytokines

Cytokines are key elements to control cellular fate of stem cells *ex vivo*. These proteins allow the maintenance of stem cell characteristics, i.e. the "stemness", and/or the directed differentiation into specific cellular lineages and are therefore essential tools for stem cell engineering. Cytokines contribute significantly to the costs of the cultures and might represent a bottleneck in process development, in particular if large scale approaches are needed.

In this work, a CHO platform was established for the expression of several recombinant cytokines of high interest in the field of stem cell technology. The establishment of stable recombinant CHO cell lines is a time consuming process. Classical methods for transgene delivery to eukaryotic cells, such as calcium phosphate precipitation, lipid-based or polymer-mediated transfection (see Section 2.1.1), are well established and mostly used for the transfection of CHO cells. However, the efficiency of these methods is variable and generally low. For instance, transfection efficiency for $CaPO_4$ precipitation or polyfection in serum-free condition was reported to be inferior to 1% [46]. The stable integration of the transgene in the host genome is inefficient and the simultaneous introduction of a gene conferring a selectable phenotype is necessary in order to select transfected cells. The selection of producing clones is necessary, as heterogeneous cell populations of producing and non-producing cells are usually obtained. Thus, several weeks are necessary for the establishment of a stable cell line [24].

Retroviral vectors allow a rapid and stable integration of an expression construct in the genome of mammalian cells. Lentiviruses, in particular, have been demonstrated to be an advantageous delivery system for the stable integration of a transgene into the genome of mammalian cells[158]. Their use has been proposed in the context of gene therapy and many advances in the recent years have made their application a safe and highly efficient technology [71].

In the following section, the approach used for the establishment of recombinant CHO suspension cell lines using lentiviral gene transfer is presented. The expression and the production of specific cytokines will be then discussed in more detail.

3.1 Establishment of CHO cell lines via lentiviral gene transfer

3.1.1 Lentiviral gene transfer

The CHO platform for the expression of recombinant cytokines used in this work was based on the parent cell line CHO^{SFS} clone II obtained from the company CCS Cell Culture Service (Hamburg, Germany). These cells were cultivated in a chemical defined serum-free medium in suspension (see Appendices 6.2.1). Master and working cell banks were established at the Institute of Technical Chemistry (Leibniz University of Hannover), providing the basic platform for all recombinant cell lines. The retroviral gene transfers to the CHO^{SFS} cells were performed in the BSL 2 laboratories of the Department of Experimental Hematology (Hannover Medical School) using lentiviral vector preparations established by Dr. Axel Schambach. The vector preparation, derived from Human Immunodeficiency Virus (HIV-I), was designed by Axel Schambach so that replication-defective viruses are used for the delivery of a self inactivating (SIN) retroviral vector, thus assuring the biosafety of the system. The details and the mechanisms of the gene transfer using this system are discussed in Section 2.1.2. An overview of the overall procedure is presented in Fig. 3.1.
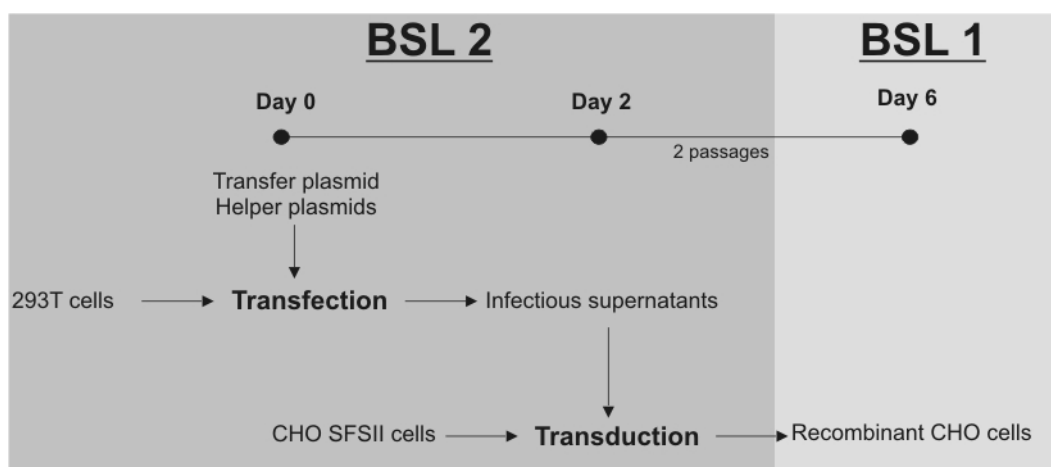
Fig. 3.1: Overview of the transduction procedure of the CHO^{SFS} cells. Virus production and cell transduction were performed in BSL 2 laboratories of the Department of Experimental Hematology (MHH). The recombinant CHO cells were transferred to the BSL 1 facilities of the Institute of Technical Chemistry after 2 passages, i.e. 4 days, following the transduction. BSL: biosafety level.

The lentiviruses were produced in HEK 293T cells. For this purpose, the cells were transiently transfected with four different plasmids using $CaPO_4$ precipitation. Three "helper" plasmids provided the sequences coding for the required viral proteins (gag/pol, REV and VSV-G proteins, see Section 2.1.2). The fourth plasmid, the so-called transfer plasmid or SIN vector, contained all regulatory sequences necessary for viral gene expression and packing of the viruses (5' LTR, SIN 3'LTRs, packaging signal ψ, RRE, PPT and PRE, see Section 2.1.2), as well as the construct containing the cDNA coding for the cytokine of interest. The transfer plasmid is presented in Fig. 3.2. Transcription is promoted in the CHO cells by the strong viral SFFV promoter guaranteeing a high gene expression. All cytokines were expressed fused to a His-tag at the C-Terminus for the purification of the proteins. No selection marker was introduced with the expression construct. The sequence of the plasmid representing the DNA sequence finally integrating into the CHO^SFS genome is schematically highlighted. It should be noted that in the CHO genome the 3'LTR will be partially exchanged with the 5'LTR of the presented sequence.
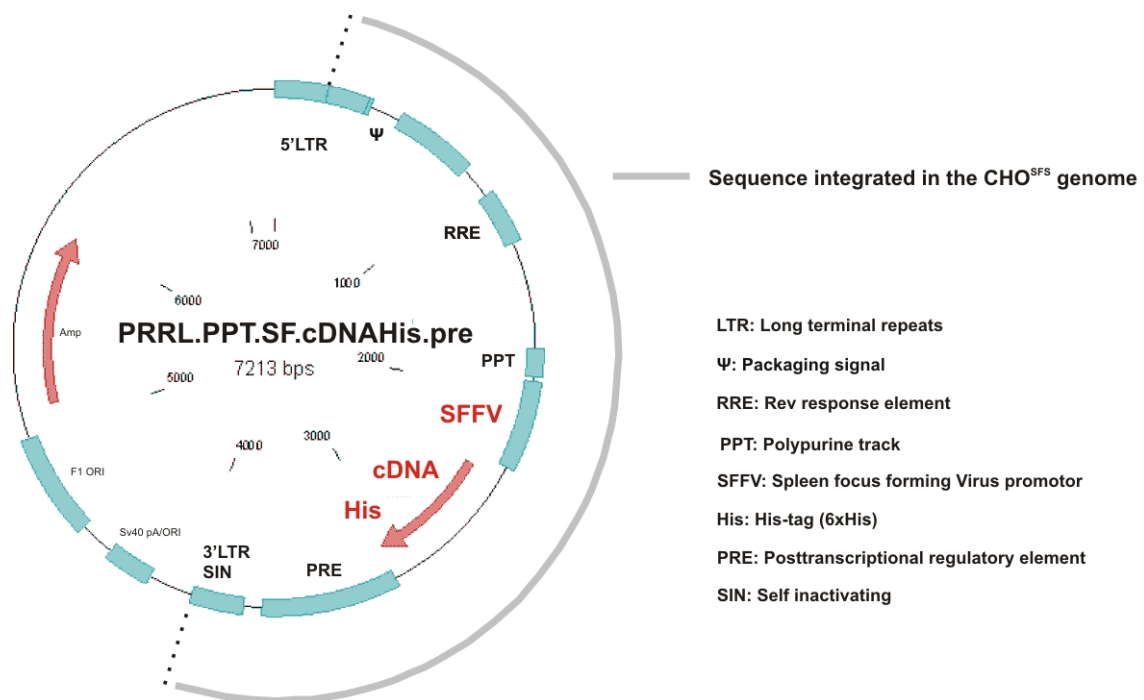
Fig. 3.2: Map of the transfer plasmid used for the transduction of the CHO^SFS cells.

The supernatants containing the infectious viruses were collected one day after the transfection of HEK 293T cells and used directly for the transduction of the CHO^SFS cells (Fig. 3.1). As a control of the transduction, the reporter protein GFP was delivered to the CHO^SFS cells under the same conditions as used for the delivery of the expression constructs designed for the cytokines. The infectious supernatants were removed by centrifugation two days

following transduction. The transduced cells were further cultivated for 2 passages to remove the remaining infectious viruses. Four days following transduction, the cells were transferred to the BSL 1 facilities of the Institute of Technical Chemistry. The overall procedure including the production of the viruses was performed within 6 days. At first, the efficiency of the procedure, i.e. the fraction of cells successfully transduced, was evaluated.

3.1.2 Transduction efficiency

The efficiency of the gene transfer to the CHO^{SFS} cells was evaluated using flow cytometry, typically 6 days following transduction. The efficiency was evaluated by measuring the fraction of GFP expressing CHO cells within the control cell population (see additional results in Section 6.3.1). The measurements indicated a high transduction efficiency of 98.8 ± 1.3 % (n=3). More specifically, intracellular staining of the expressed cytokines in the recombinant CHO cells was performed. The specific staining of the cytokines was performed using a mouse antibody directed against the His-tag of the recombinant proteins. The primary antibody was detected by a secondary goat anti Ig mouse antibody labeled with the fluorochrome PE (Phycoerythrin). As a control, untransduced CHO^{SFS} cells were stained under the same conditions. A detailed description of the procedure is given in Section 6.2.7. Fig. 3.3 shows typical results obtained for a CHO cell population transduced with a construct coding for the protein Angptl1 (in B), denominated as CHO^{Angptl1} subsequently. The expression of this cytokine will be further discussed in Section 3.2. The dot plots display the fluorescence intensity (FL2LOG) versus the forward scatter (FSC) signals of the cells. Positive staining was defined as the emission of a fluorescence signal that exceeded levels obtained by >99% of cells from the control population (in A).

In this example 99.3% of the CHO^{Angptl1} were found to express His-tagged recombinant proteins. The results demonstrated that the delivery of the expression construct to the CHO cells occurred with a high efficiency and also indicated that the translation of the His-tagged protein successfully occurred in the transduced cells. In the case of the cell line CHO^{Angptl1}, the transduction efficiency was evaluated to be 98.6 ± 0.7 % in triplicate measurements.
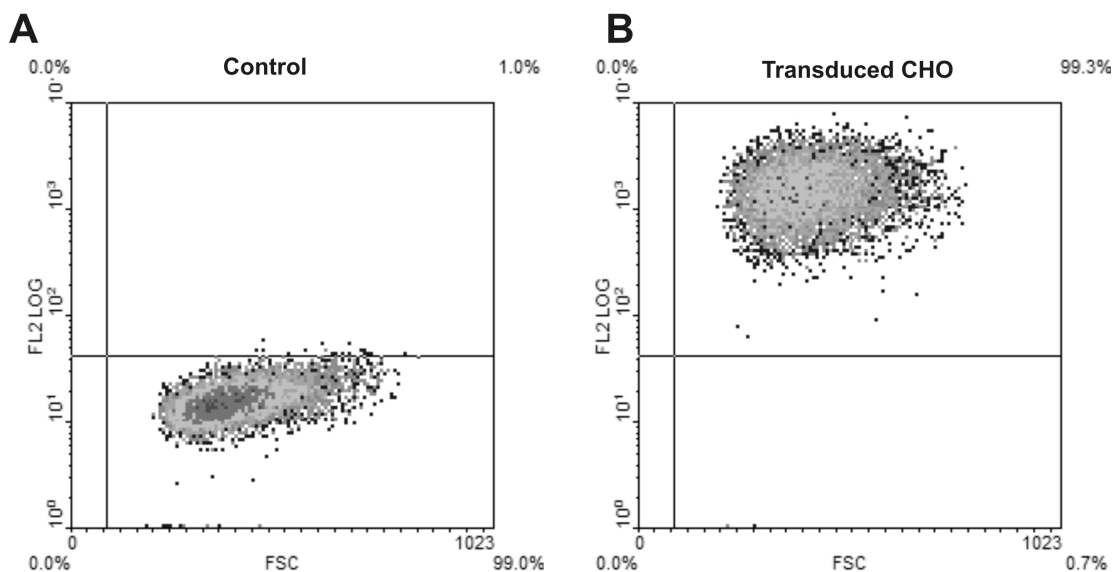
Fig. 3.3: Intracellular staining of His-tagged proteins in transduced CHO cells for the evaluation of the transduction efficiency. Measurements were performed 6 days after transduction. The cell population analyzed here were tranduced for the expression of the protein Angptl1. In A: untransduced CHO^{SFS} cells as control. In B: CHO cells transduced with the Anptl1 expression construct. At least 10 000 events are displayed. FL2LOG: fluorescence intensity of the PE-labeled antibody measured in the channel 2, FSC: Forward scatter signals.

Using this approach, the transduction efficiency of the cell lines established at the TCI for the production of recombinant cytokines was documented. Table 3.1 summarizes the results. The transduction efficiency evaluated using the GFP reporter CHO cell line is also given.

Table 3.1: Transduction efficiency of the lentiviral gene transfer to the CHO^{SFS} cells evaluated by intracellular staining of the recombinant protein or GFP fluorescence. The analysis were performed in triplicates (n=3). Angptl: angiopoietin-like protein; bFGF: basic fibroblast growth factor; hLIF: human leukemia inhibitory factor, TGF: transforming growth factor, VEGF: Vascular endothelial growth factor.

Cell line	Expressed protein	% positive cells
CHO^{Angptl1}	Angptl1	98.6 ± 0.7
CHO^{Angptl2}	Angptl2	96.3 ± 0.4
CHO^{Angptl5}	Angptl5	96 ± 1.1
CHO^{bFGF}	bFGF	96.8 ± 0.6
CHO^{GFP}	GFP	98.8 ± 1.4
CHO^{hLIF}	hLIF	n.d.
CHO^{TGF}	TGF	97.2 ± 0.4
CHO^{vEGF}	VEGF	95.4 ± 0.8

n.d. : not determined

31

The delivery of the expression construct to the CHO^SFS cells using lentiviral vectors was found highly efficient. Thus, more than 95% of the transduced CHO cells indeed expressed the recombinant protein. The efficiency of the transduction of the cell line CHO^hLIF could not be determined. This issue will be discussed further in Section 3.3. In the following part, the stability of the protein expression by the transduced cells is examined.

3.1.3 Cell line stability

Retroviruses have the ability to insert an expression construct into the host cell genome. In this regard, the transduced CHO cells may be considered as "stable" transduced cells. However, the stability of the recombinant protein expression is not solely depending on the integration in the host genome, but several other parameters, such as the site of integration, greatly influences the level and the stability of recombinant protein expression [61, 65]. Lentiviruses incorporate preferentially within active transcription areas of the host genome [70], so that the integration at sites exhibiting a high risk for gene silencing such as heterochromatin [159, 160], should be minimized. In this context, it was expected that the transduced CHO cell lines exhibit a stable recombinant protein expression. This hypothesis was verified in the following experiments.

The stability of recombinant protein expression by transduced CHO cells was evaluated using a reporter GFP cell line. Following lentiviral gene delivery, the fraction of GFP expressing cells (GFP+ cells) within the transduced CHO population was measured to be 98.8 ± 1.4 % (see Table 3.1). The cells were subsequently cultivated and repeatedly passaged in a serum-free and chemical defined medium (ProCHO5, Lonza). The fraction of GFP+ cells was monitored using flow cytometry over long-term cultivation (124 days). Fig. 3.4 shows the results of the investigations.
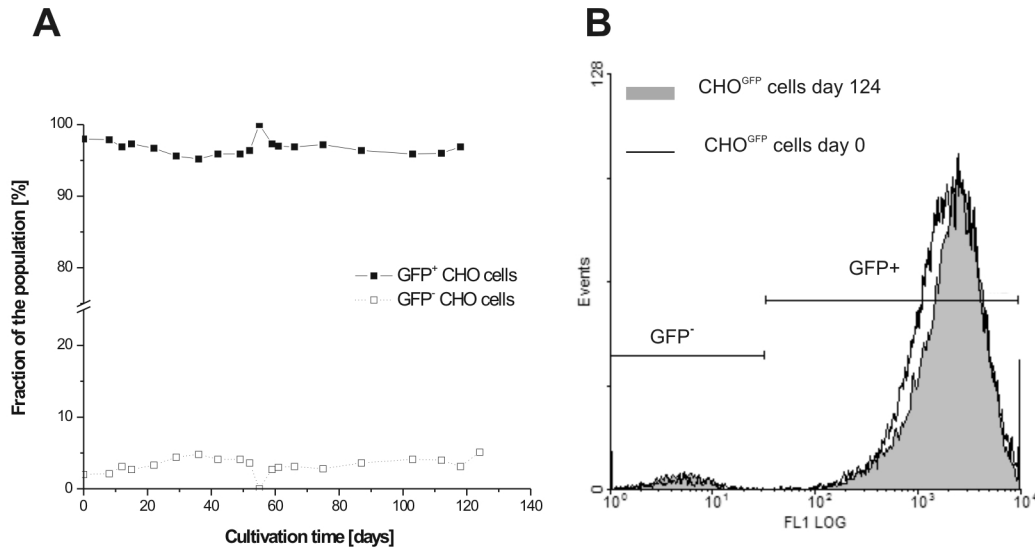
Fig. 3.4: Stability of the recombinant protein expression by transduced cells evaluated using a GFP reporter cell line. In A: evolution of the fraction of GFP$^+$ and GFP$^-$ cells within the transduced cell population. In B: Distribution of the GFP fluorescence on day 0 and day 124 of the experiment. All measurement were performed with cells buffered in PBS. At least 10 000 events are displayed.

The fraction of GFP$^+$ cells remained constant over the entire investigated time frame representing > 95 % of the overall population (Fig. 3.4.A). This indicates that the cells maintained GFP expression during prolonged cultivation and that no nonproducers arose within the transduced CHO population. In addition, comparable distributions of the GFP intensity were measured during the entire experiment, suggesting that the cells maintained a comparable recombinant protein level expression over long-term expansion. This point is illustrated in Fig. 3.4.B for the CHO population on day 0 and day 124.

Interestingly, the initial fraction of GFP$^-$ cells (approx. 2%) remained nearly constant during the whole cultivation, suggesting that non-producing cells do not exhibit a higher proliferation rate than producing ones, as in this case the non-producer fraction should have increased over long-term cultivation. This fact was confirmed in a co-culture experiment, where transduced GFP$^+$ cells were added to a culture of untransduced CHO^{SFS} (parent cell line) in a ratio of 1:1 (illustrated in Fig. 3.5.A). The co-culture was sub-cultivated for 50 days and monitored via flow cytometry. The evolution of the sub-populations (GFP$^+$ and GFP$^-$ cells) is plotted over time in Fig. 3.5.B.
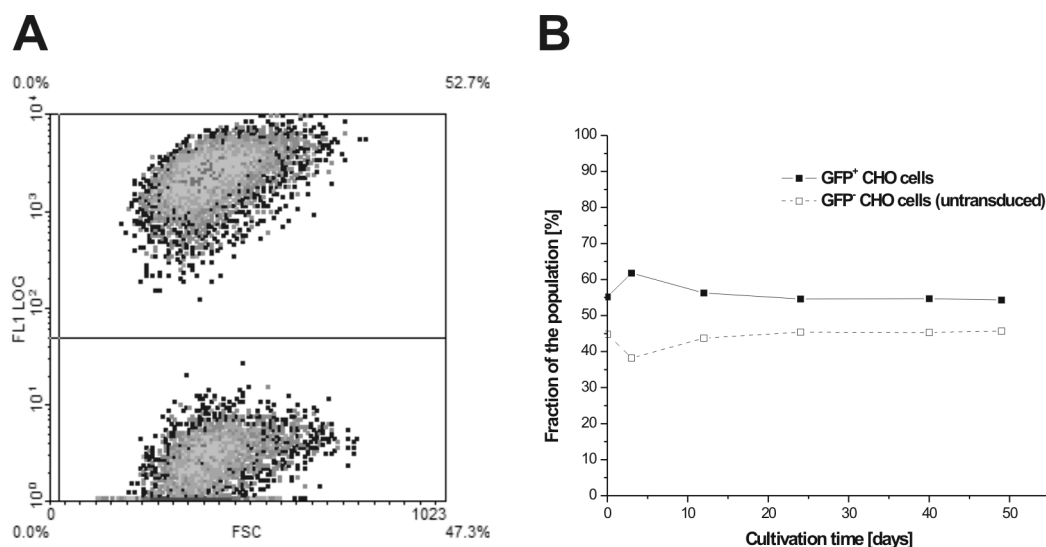
Fig. 3.5: Monitoring of the GFP expression in a co-culture of transduced and non-transduced CHO cells. In A: flow cytometric measurement of a co-culture of GFP expressing cells mixed at a ratio of approx. 1:1. In B: monitoring of the distribution of the co-culture over 50 days.

During the complete cultivation, the subset of untransduced cells (GFP⁻) did not overgrow the culture and the fraction of GFP⁺ cells remained nearly constant (Fig. 3.5.B). Accordingly, the expression of the recombinant protein does not seem to burden the cell metabolism and compromise the growth of recombinant CHO cells, so that no measurable change in the distribution of the co-culture was observed within 50 days.

The results indicated a stable expression of the recombinant protein over long-term cultivation. This fact was not restricted to CHO^GFP cells, as experiments performed with transduced CHO cells expressing the cytokine Angptl1 correlated well with these observations. Thus, 98.6 ± 0.7 % of the CHO^Angptl1 cells expressed the recombinant cytokine following transduction (see Table 3.1). The cell population was further cultivated for three weeks in serum-free medium and recombinant protein expression was monitored using intracellular staining of His-tagged protein as previously described (see Section 3.1.2). After three weeks of cultivation, no change in the distribution of the transduced cell population was observed and 98.8% of producing cells were measured in culture (data not shown).

The retroviral gene transfer method was found to be an efficient approach for the rapid establishment of recombinant CHO cell lines. Transduced cell populations containing more than 95% of cells expressing the recombinant cytokines were obtained within one week. The experiments confirmed that the expression constructs were integrated by the lentiviruses into active areas of the CHO genome, thus allowing a long-term expression of the transgene. The

34

stability of the protein expression in serum-free conditions was demonstrated for more than 16 weeks using a reporter GFP cell line. In the case of the cytokine Angptl1, a stable expression could be observed for at least 3 weeks. In addition, the experiments suggested that the metabolitic disadvantage of expressing cells in comparison to untransduced cells is minimal, as no changes in the distribution of CHO[GFP] or CHO[Angptl1] cell populations were observed over prolonged cultivation. Hence, we reasoned that 1-5 % of non-producing cells following transduction (see Table 3.1) could be tolerated and thus a time-consuming selection of producers or the generation of a clonal cell population could be avoided at first. In this context, the transduced cell populations were used directly for the expression and purification of the cytokines to rapidly characterize the expressed molecules and investigate the bioactivity. In the following part, the expression and the production of recombinant cytokines using established CHO cell lines are presented.

3.2 Expression of Angiopoeitin-like proteins (Angptl)

The Angiopoeitin-like proteins (Angptl) 1 and 2 were identified in 1999 by Kim *et al.*[161, 162]. The proteins induce *in vitro* the sprouting of vascular endothelial cells [161, 163], but their function during angiogenesis is not clarified yet [164]. Zhang *et al.* demonstrated in 2006 that Angptl2 stimulate the *ex vivo* expansion of mouse hematopoietic stem cells (HSC). These authors expressed the cytokine in adherent HEK 293T cells and demonstrated that the glycosylation of the protein is essential for the reported bioactivity [5]. These findings are highly interesting because HSC are rare stem cell populations, for instance representing one cell in 1-$10 \cdot 10^6$ cells in the bone marrow [165], which leads to cell dose limitation for clinical applications. E*x vivo* expansion of HSCs may overcome this problem, the procedure remains difficult however, mainly because of the lack of appropriate cytokines [166]. In this context, the use of Angptl2 protein as a growth factor for the *ex vivo* expansion of HSC is of tremendous interest. It is postulated that protein Angptl1 may likewise support the expansion of human HSC (Axel Schambach, personal communication).

The aim of this work was the production of the glycosylated cytokines Angptl1 and 2 using CHO suspension cell lines. The cell lines were established in the frame of the bachelor thesis of Ms. Sanketha Kenthirapalan [167] as described in section 3.1.1. The transfer plasmids used for Angptl 1 and 2 were constructed with the cDNA containing the coding sequences of the

human gene ("CDS" from NM_004673.3 and NM_012098.2, respectively) fused with a His-tag (6 x Histidines) at the C-terminus. The sequences comprise the native signal export peptide of both Angptls (first 21 amino acids of the translated proteins) at the N-terminus. Angptl1 and Angptl2 contain two coiled-coil domains (CC1 and CC2) and a fibrinogen-like domain (FD) highly conserved among angiopoietin family members [168]. Both unglycosylated proteins have a theoretical molecular weight of approx. 57 kDa. A schematic view of the translated proteins can be seen in Fig. 3.6. The established cell lines will be subsequently denominated as CHO^{Angptl1} and CHO$^{Angptl2.}$.
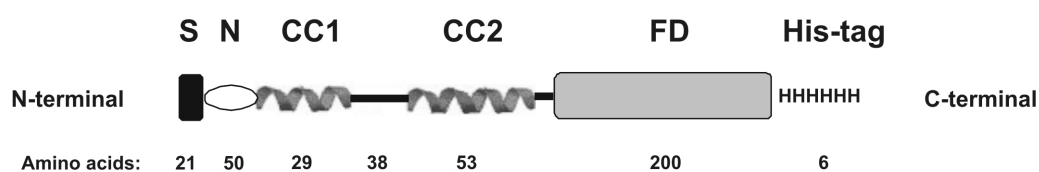
Fig. 3.6: Schematic protein structure of the recombinant Angptl1 and 2 expressed in the CHO^{Angptl1} and CHO^{Angptl2} cell lines. S: hydrophobic signal sequence (black square) for protein secretion. N: N-domain of unknown function (white oval) presenting structural homology to angiopoietin family members. CC1 and CC2: coiled-coil domains. FD: fibrinogen-like domain (grey rectangle). H: 6 x histidines at the C-terminus. Modified from Dhanabal et al.[168]

The transduction efficiency was evaluated to be 98.6 ± 0.7% (n=3) for the cell line CHO^{angptl1} and 96.3 ± 0.4% (n=3) for the cell line CHO^{Angptl2} by performing intracellular staining and flow cytometric measurement of His-tagged protein content (see Section 3.1.2). At first, the location of the recombinant proteins was investigated. Extracellular expression was analyzed in the supernatants of the CHO cultures using SDS-Page and Western blot. The analysis of the intracellular expression used supernatants after cell disruption by sonication and centrifugation (see 6.2.3). The specific detection of the protein on western blot was performed using a primary mouse anti His-tag antibody (see Appendices 6.2.2). Fig. 3.7 presents the obtained results.
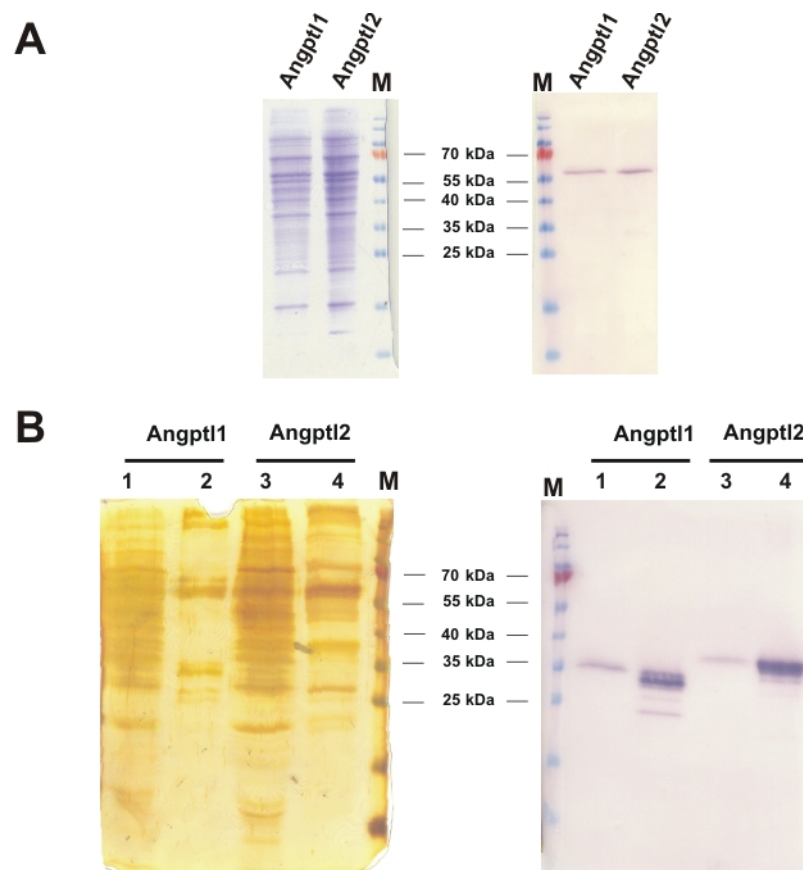
Fig. 3.7: Intra- and extracellular detection of Angptl 1 and 2 using SDS-PAGE (left part) and Western blot analysis (right part). Western blot detection was performed using a mouse anti His-tag primary antibody. In A: intracellular detection of His-tag protein in CHO^{angptl1} and CHO^{Angptl2} cell lysates. In B: extracellular detection of the recombinant proteins in the cell supernatant; 1: Angptl1, 10-fold concentrated supernatant (TCA precipitation). 2: Angptl1, purified supernatant using IMAC (Co^{2+}). 3: Angptl2, 10-fold concentrated supernatant (TCA precipitation). 4: Angptl2, purified supernatant using IMAC (Co^{2+}).

The analysis of the intracellular protein fraction by Western blot revealed His-tagged protein bands between 55-70 kDa (Fig. 3.7.A) that correspond to the expected size range for both Angptl1 and Angptl2 ($\approx$57 kDa). In contrast, the complete Angptl1 and Angptl2 proteins could not be observed in cell supernatants (Fig. 3.7.B). Only His-tagged fragments with a molecular weight of approx. 35 kDa were detected in the concentrated supernatants of both cell lines (see lines 1 and 3 in Fig. 3.7.B). The analysis of purified supernatants (via IMAC using Co^{2+}, see Appendices 6.2.4) presented in lines 2 and 4 confirmed the results.

The results indicated that both Angptl1 and Angptl2 are at least translated by the established cell lines, as His-tagged proteins exhibiting the expected size were detected in the intracellular protein fraction. However, the export of the entire proteins by the cells failed and solely C-terminal protein fragments > 35 kDa were detected in the culture supernatants. These peptides were not detected in the intracellular protein fraction (Fig. 3.7.A), which

suggests that these fragments are cleavage products of the complete Angptl proteins. This phenomenon is puzzling and it is not clear whether this cleavage occurred among the secretion pathway or once the Angptl proteins have been secreted. The exported fragments may comprise the fibrinogen domain (FD, theoretical MW$\approx$26 kDa), which is of limited interest as the super coiled coil domains (see Fig. 3.6) are more likely involved in the support of HSC expansion[5]. The purification of the intracellular Angptl protein may be possible, but is more complicated than the purification of secreted product. Furthermore, it is unlikely that the intracellular Angptl proteins are glycosylated, as glycosylation occurs first among the secretion pathway. This seems to be confirmed by the thin bands observed at the theoretical MW of both proteins in Fig. 3.7.A, suggesting that the detected Angptls are unglycosylated.

Currently, new CHO[angptl1] and CHO[angptl2] cell lines are being established. A new strategy for the better secretion of the recombinant cytokines is being investigated. Thus, the native export sequences of Angptl1 and Angptl2 have been exchanged with the signal sequence of proteins naturally secreted with high efficiency, such as the heavy chain of Immunoglobulin or interleukine-2. The signal peptide of the marine enzyme luciferase from *Gaussia princeps*, which was recently used efficiently in CHO cells[169], is also being investigated. Additional work currently performed should confirm whether the adopted strategy allows the export of the glycosylated Angptl1 and 2 proteins by the established CHO cells lines.

3.3   Production of human leukemia inhibitory factor (hLIF)

Human leukaemia inhibitory factor (hLIF) is a polyfunctional glycoprotein. Many functions of the cytokine have been reported, for instance actions in kidney[170] and in endocrine tissue such as breast epithelium[36]. The protein is involved in the regulation of osteogenic differentiation[171] and is essential for blastocyst implantation[172] and for neural development [173]. Human LIF was proposed for therapeutic uses and produced by Amrad[174] under the name "emfilermin". The protein reached phase II clinical trials for the treatment of chemotherapy-induced peripheral neuropathy[175] and for improving embryo implantation following in vitro fertilization (clinical trail NCT00504608).

In the context of stem cells, the cytokine is a key factor in maintaining the pluripotency of murine embryonic stem (ES) cells[47] and is also widely used for the culture of human ES

cells [8, 10]. In the latter case, hLIF more likely supports cell proliferation, as the cytokine is not necessary for the pluripotency of human ES cells [3].

In the context of ES cell expansion, it has been demonstrated that the glycosylation of hLIF is not essential for the bioactivity [176], so that the cytokine has been widely expressed in *E.coli*. However, the correct folding of the protein requires oxidizing conditions, so that strategies for the manipulation of the redox potential in the *E.coli* cytoplasm, such as the co-expression of thioredoxin or Glutathion-S-transferase, are necessary for the expression of the soluble cytokine. The elimination of the fusion partner implicates further purification steps for the isolation of the intracellular cytokine. In contrast, mammalian cells such as CHO cells are able to fold the protein correctly and export it directly in the culture medium. In addition, it is still not clear whether the glycosylated form of hLIF is more active and stable than the unglycosylated one.

In this work, a CHO cell line was established for the production of soluble glycosylated hLIF. Fig. 3.8 gives an overview of the approach followed for the establishment of the cell line and the production of the cytokine.
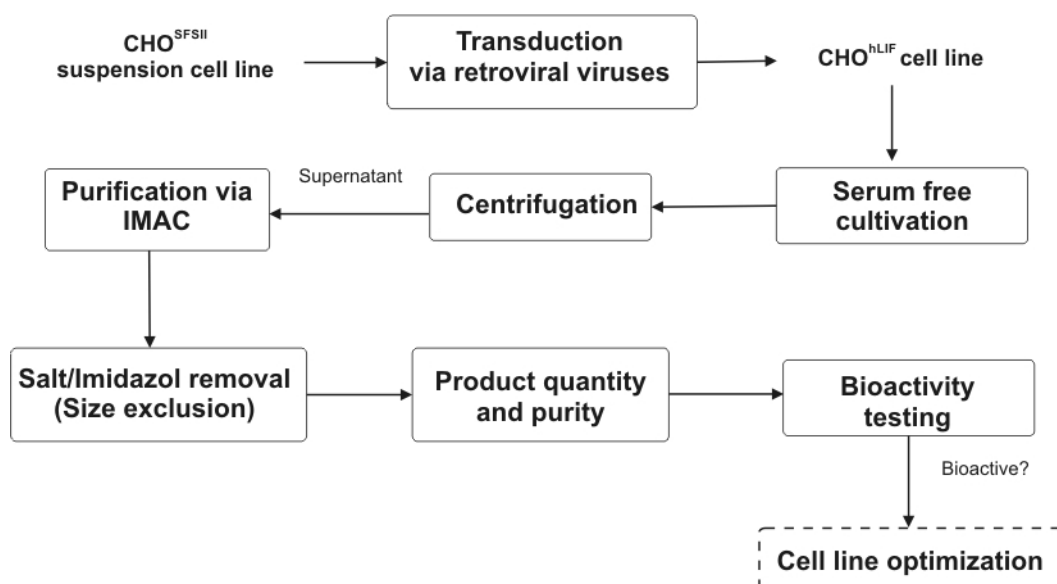
Fig. 3.8: Process flow chart for the production of hLIF. IMAC: Immobilized Metal Affinity Chromatography.

3.3.1 Expression of hLIF

The CHO cell lines for the hLIF expression, termed as CHO^{LIF} subsequently, was established as described in Section 3.1.1. In brief, the transfer plasmid was constructed with the cDNA

containing the coding sequence of the human gene (CDS from NM_002309), fused with a His-tag (6 x Histidines) at the C-terminus. The expression of hLIF by the established cell line was detected on the transcriptional level (see Fig. 3.9.A), and on the protein level in the culture supernatant. Fig. 3.9.B presents the SDS-PAGE and Western blot analysis of CHO[hLIF] of the intracellular protein fraction (line 2) and in culture supernatants (line 4). Untransduced CHO cells were used as a control (line 1 and 3). The specific detection on the Western blot was performed using an antibody directed against the His-tag of the recombinant protein.
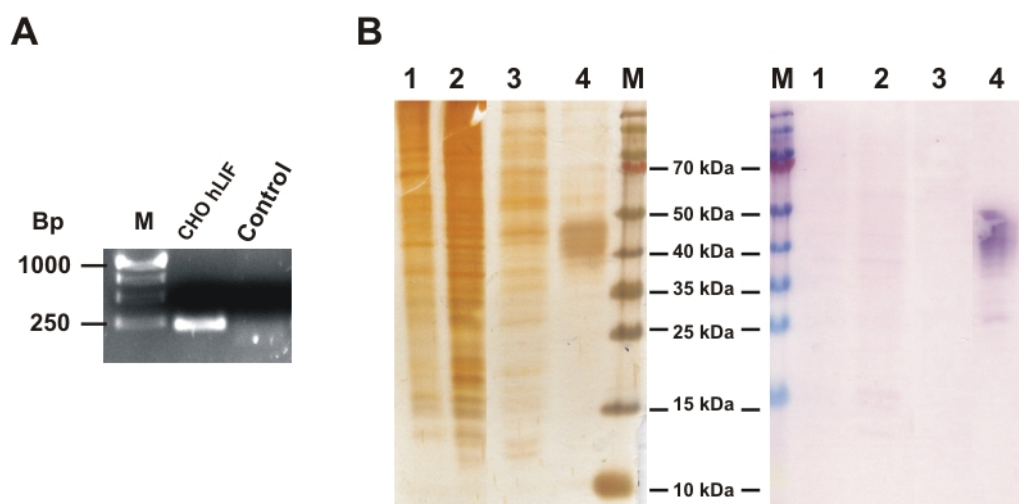
Fig. 3.9: Expression of hLIF by the established CHO cell line. In A: expression of hLIF on the transcriptional level, RT-PCR analysis of the transduced (CHO[hLIF]) and the untransduced CHO cells (control). In B: expression of hLIF on the protein level SDS-PAGE (left part), Western blot (right part). 1: intracellular protein fraction of control cells; 2: intracellular protein fraction of CHO[hLIF] cells; 3: supernatant of a control culture; 4: supernatants of a CHO[hLIF] culture.

The analysis of the CHO[hLIF] supernatants revealed several bands between 40-50 kDa on the SDS-PAGE gel (line 4, left), which were not found in the control supernatant (line 3, left). These bands were positively stained on the Western blot (line 4, right) indicating the presence of recombinant His-tagged proteins. The sensitive immunodetection revealed additional His-tagged proteins ranging from 25 kDa to approx. 50 kDa. Unglycosylated hLIF has a theoretical molecular weight of 19.7 kDa. Thus, the results indicate that the hLIF expressed by the established cell line is highly glycosylated and that several glycoforms are secreted by the cells. Interestingly, no hLIF was detected in the intracellular protein fraction of the CHO[hLIF] (lines 2) suggesting that the intracellular content of the recombinant protein is under the detection limit of the immunodetection. Flow cytometric measurements confirmed these observations, as a very low, if detectable, level of intracellular His-tagged proteins was

measured in the CHO^{hLIF} using this method (see Appendices 6.3.2). In this work, the determination of the transduction efficiency relied on the intracellular staining of His-tagged proteins. It was consequently not possible to determine the fraction of hLIF expressing cells within the CHO^{hLIF} population. It was first assumed that similar high transduction efficiency was achieved as demonstrated in Section 3.1.2 for all others recombinant cell lines established under identical conditions. The topic will be discussed further in Section 3.3.4.

The results suggest that the established CHO^{hLIF} cell line efficiently secreted hLIF, as the recombinant protein was only detected in culture supernatants. In this context, the purification of the cytokine from the culture supernatants was performed.

3.3.2 CHO^{hLIF} cultivation and hLIF purification

For the production of hLIF, CHO^{hLIF} cells were cultivated in two 250 mL Spinners each containing 100mL serum-free ProCHO5 medium. Batch cultures were started with a cell concentration of $4 \cdot 10^5$ cells$\cdot$mL^{-1}. The cells were harvested after 4 days in the late growth phase at a cell concentration typically $>1.5 \cdot 10^6$ cells/mL and a high viablilty (> 85 %). After cell separation by centrifugation, 160 mL supernatant were concentrated to a final volume of 10 mL using centrifugal concentrators with a size exclusion limit of 10 kDa (Vivaspin20, Sartorius Stedim). The concentrated supernatant was then purified via Immobilized Metal Affinity Chromatography (IMAC) using Co^{2+} immobilized on a Sartobind Metal Chelate Membrane Adsorber (IDA75, Sartorius Stedim). The detailed procedure is presented in Section 6.2.4. The obtained chromatogram (in A) as well as the SDS-PAGE analysis of the eluted fractions (in B) can be seen in Fig. 3.10.

The analysis of the eluted fractions revealed bands ranging from 25 to 50 kDa corresponding to the previously discussed band profile detected by Western blot (see Fig. 3.9.B). The fractions containing hLIF were collected (Fraction 56 to 61) and sterile filtrated (0.2 μm). In addition, the elution buffer was exchanged to PBS using a centrifugal concentrator (10 kDa exclusion limit, Vivaspin6, Sartorius Stedim) and the collected fractions were concentrated to a final volume of 1.5 mL.
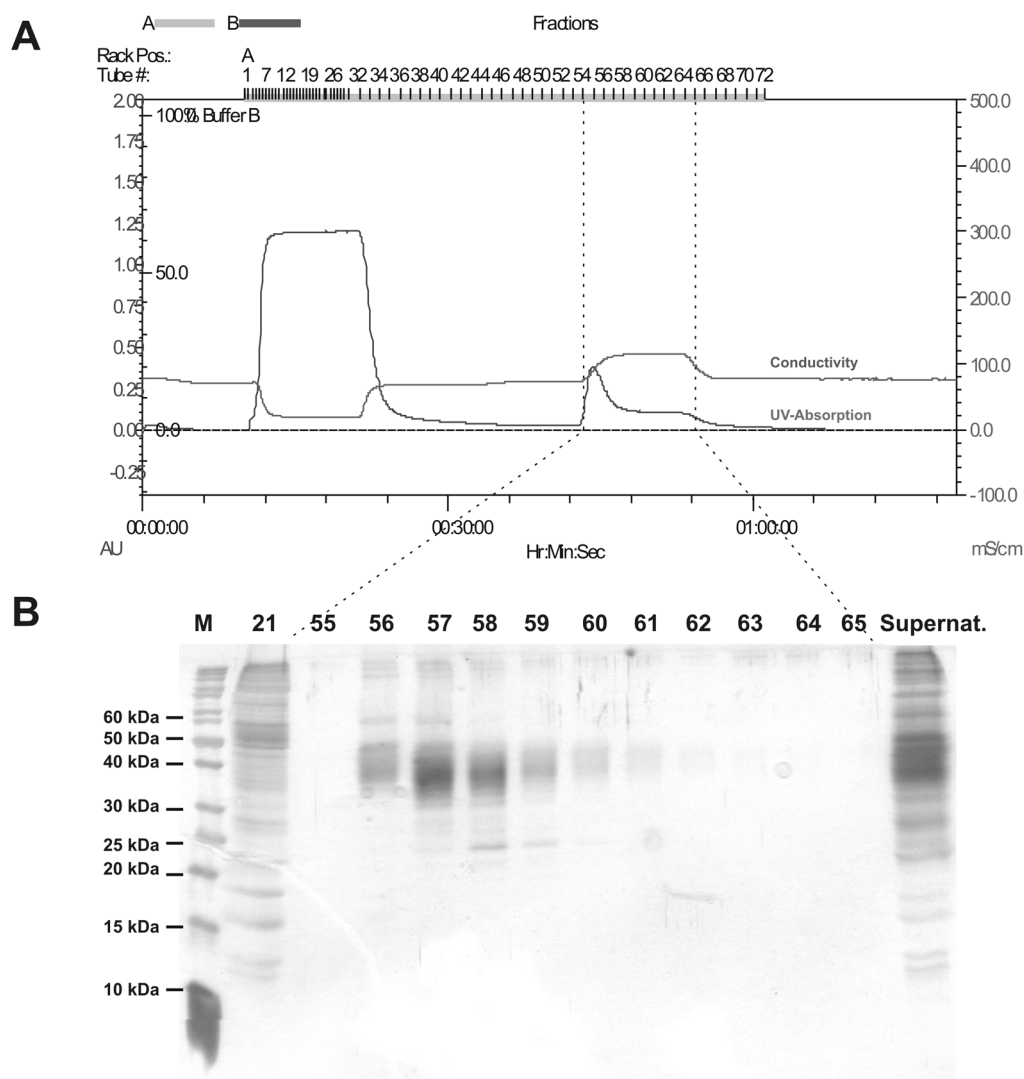
Fig. 3.10: Purification of hLIF via IMAC. In A: FPLC chromatogram. In B: SDS-PAGE analysis of the eluted fractions. Fraction 21: flow through. Supernat. = concentrated culture supernatants.

The protein purity of the final product was evaluated by SDS-PAGE and Western blot analysis. In this case, the specific detection was performed using a primary antibody directed against the hLIF protein. For a comparison, unglycosylated hLIF produced in *E.coli* was also analyzed. The results are presented in Fig. 3.11. The analysis confirmed the previous observation, namely that the cell line CHO[hLIF] expressed a heterogeneous pattern of glycosylated hLIF ranging from approx. 25 kDa to 50 kDa. The comparison with the protein expressed in *E.coli* (at approx. 20 kDa, Fig. 3.11.) makes the glycosylation of the secreted protein obvious. Interestingly, no unglycosylated hLIF is expressed by the CHO[hLIF] cell line, as no protein band was detected at 20 kDa. The considerable post-translational modification can be explained by the fact that hLIF contains at least six potential N-glycosylation sites [177]. The variable glycosylation of the protein was also described in previous reports for instance for

hLIF expressed in CHO cells with a molecular weight ranging from 40 to 60 kDa [178] or in COS cells ranging from 20 to 50 kDa [178].

The determination of the protein purity was difficult because of the heterogeneous expression pattern of hLIF. However, all protein detected on the SDS-PAGE gel were also detected by specific immunodetection following Western blotting. In this context, the protein purity was assumed to be high and evaluated from the gel to be at least > 90%.
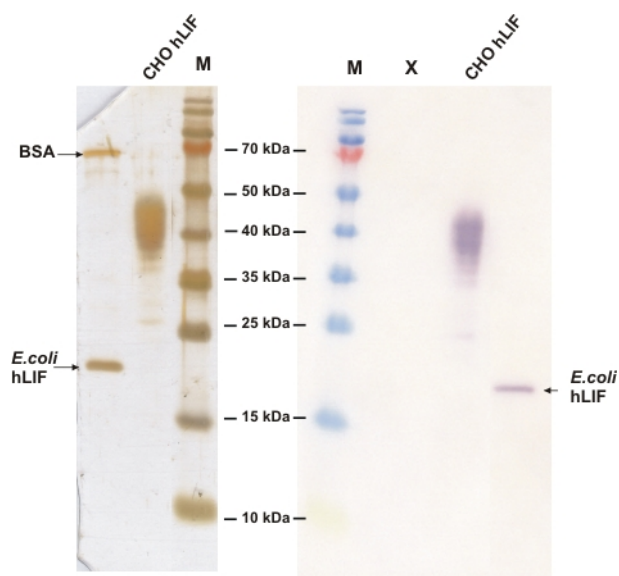
Fig. 3.11: Product purity evaluated by SDS-PAGE (left part) and Western blot (right part) analysis. The specific detection was performed using a primary antibody directed against the hLIF protein. Unglycosylated hLIF expressed in *E.coli* is displayed as a control.

The protein concentration of the final product was measured to be 193.6 µg·mL^{-1} using Bradford assay, which corresponds to approx. 310 µg purified protein from 160 mL supernatant. Thus, 1.9 mg hLIF could be theoretically obtained from a 1L culture. An analysis using a hLIF-specific detection method such as ELISA should be performed to confirm these findings.

In the following section, the testing of the bioactivity of hLIF expressed by the CHO^{hLIF} cell line is presented.

3.3.3 Bioactivity testing of hLIF expressed by CHO cells

The biological activity of the hLIF produced by the CHO^{hLIF} cells was investigated using suspension cultures of murine embryonic stem (ES) cells. The suspension cultures were established by Magda Tomala by adapting adherent Brachyury ES cells to suspension and dynamic culture conditions[179]. The experiments were performed in close collaboration with

Magda Tomala and Nina Bahnemann. The activity of the CHO hLIF was compared to the activity of a commercially available LIF protein (ESGRO, Millipore) expressed in *E.coli*. Each cytokine was added to the culture media to a final concentration of 10 ng·ml^{-1} respectively. As a negative control, cells were cultivated in the absence of LIF.

Erlenmeyer flasks containing 25 ml medium were inoculated with $2 \cdot 10^4$ cells·ml^{-1} each and shaken orbitally at an agitation rate of 110 rpm. The cells were passaged after 4 days in culture. The cultures were monitored daily by determination of the cell concentration and viability. Apoptosis measurements were performed using the Annexin-V assay and flow cytometry (See Appendices 6.2.2). In parallel, suspension cultures in petri dishes were conducted for morphological observations.

Growth curves and viability of the cells cultivated in the three different culture media are shown in Fig. 3.12. Whereas cells proliferated normally in the presence of ESGRO LIF and purified hLIF (CHO LIF), the negative control cultures showed a significantly reduced proliferation.
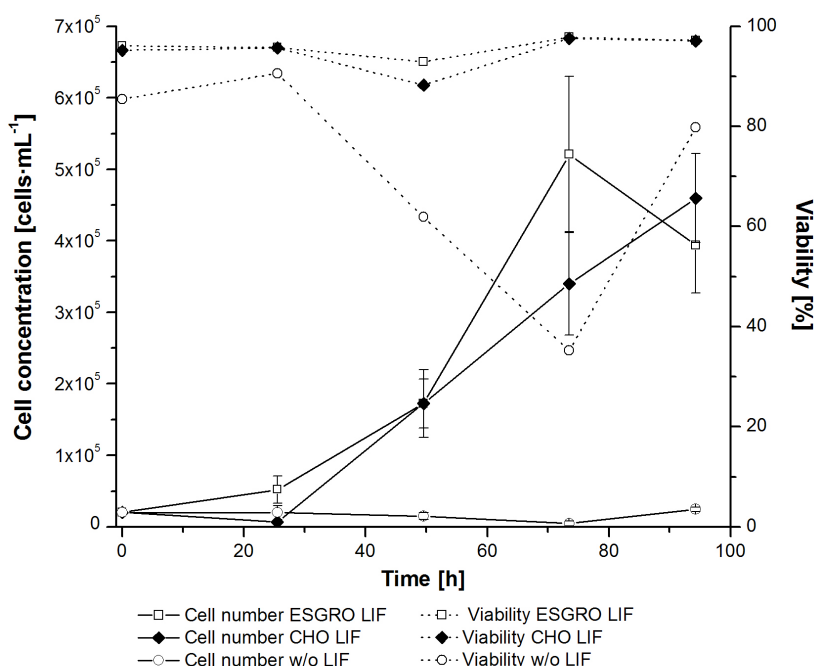
Fig. 3.12: Cell growth and viability of the ES cells Brachyury cultivated in the presence of CHO hLIF, control LIF (ESGRO) and w/o LIF. The data are presented for cells in passage 2.

The viability assayed by trypan blue exclusion (Fig. 3.12) and Annexin-V apoptosis assay (Fig. 3.13.A and .B) was comparable for both LIF cultures. In contrast, cultures without LIF displayed a significant lower viability (Fig. 3.12) and massive apoptosis was demonstrated via

Annexin-V assay (Fig. 3.13.C). It was not possible to maintain the Brachyury ES cell line in suspension culture without LIF for more than 2 passages.
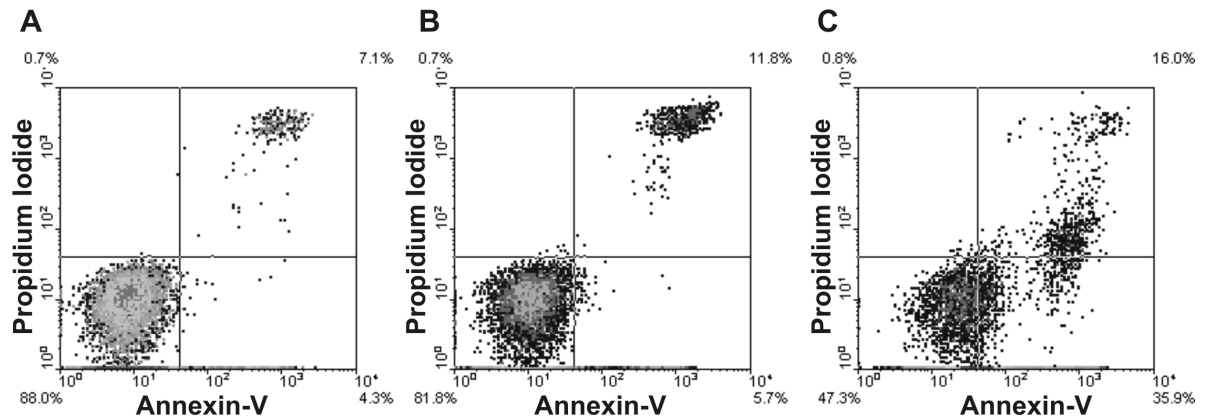
Fig. 3.13: Flow cytometric apoptosis measurements using the Annexin-V assay in ES cell cultures in the presence of the purified CHO hLIF (in A), in the presence of ESGRO LIF (in B) and w/o LIF (in C). The analysis were performed after 4 days of the suspension cultivation in passage 2. Lower quadrant left: living cells. Lower quadrant right: early apoptotic cells. Higher quadrant right: late apoptotic or necrotic cells. At least 10 000 events are displayed.

With regard to growth and viability, the purified CHO hLIF was comparable with commercially available ESGRO LIF. The maintenance of cell pluripotency, however, is another important aspect for the characterization of the purified cytokine.

The maintenance of cell pluripotency in the presence of the purified hLIF was evaluated by expression analysis of the pluripotency marker SSEA 1. The expression level of the surface molecule was determined via flow cytometry using a monoclonal antibody labeled with FITC. Marker expression level was evaluated in comparison to a matched isotype control, i.e. an identically labeled antibody of the same isotype class and used in the same quantity as the test antibody, but presenting no affinity for murine cells (see Appendices 6.2.6). In Fig. 3.14 the histograms representing SSEA-1 expression of Brachyury ES cells derived from each culture are shown. Cells cultivated throughout 2 passages in the presence of the CHO hLIF retained high SSEA-1 expression levels (> 94 % positive cells, in Fig. 3.14.A), fully comparable with the positive control ESGRO LIF (Fig. 3.14.B). The expression remained high and stable over 14 subsequent passages (93 % for CHO LIF and 94 % for ESGRO LIF). In contrast, cells cultivated without LIF showed a decrease in SSEA-1 expression (only 77 % positive cells) already after two passages (Fig. 3.14.C).
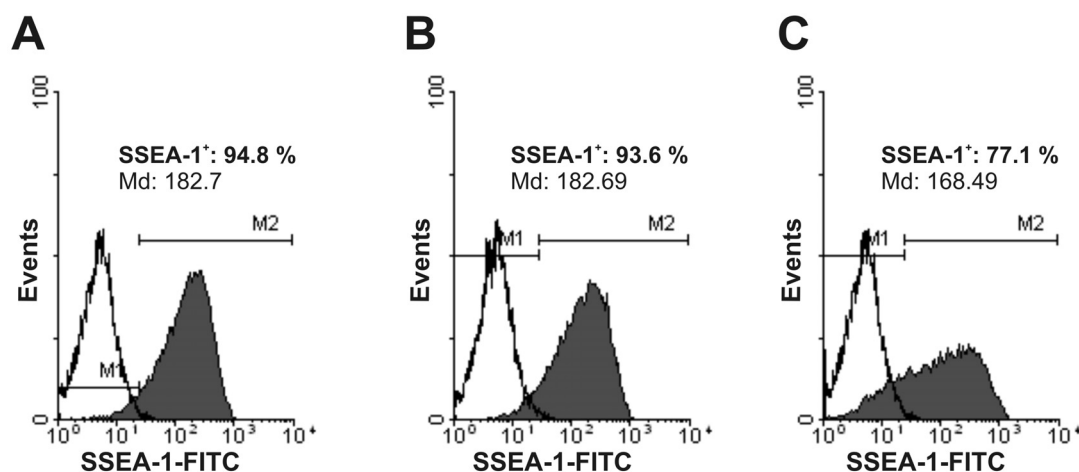
Fig. 3.14: Expression of the pluripotency surface marker SSEA-1 by ES cells cultivated in the presence of the purified CHO hLIF (in A), in the presence of ESGRO LIF (in B) and w/o LIF (in C). Analyses were performed on day 3 of the suspension cultivation for cells in passage 2. Unfilled histograms: matched isotype control. Filled histograms: SSEA-1 expression. At least 10 000 events are displayed.

Microscopic observations of the morphology of suspension ES colonies cultivated in petri dishes also confirmed the undifferentiated phenotype of the cells cultivated in the presence of the purified hLIF. Thus, round shaped spheres were observed in the cultures supplemented with CHO hLIF and ESGRO LIF. The examination of the negative control, on the other hand, clearly revealed adhering and sprouting cells in the petri dishes, indicating that the cells differentiated when LIF was omitted.
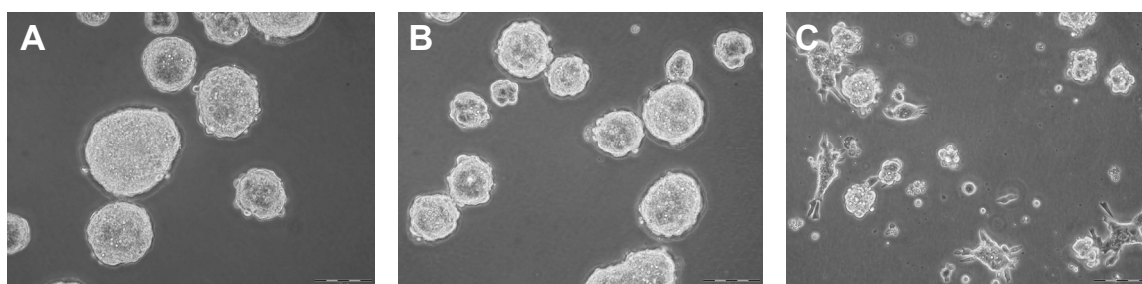
Fig. 3.15: Morphology of ES suspension cell cultures (petri dishes) in the presence of the purified CHO hLIF (in A), in the presence of ESGRO LIF (in B) and w/o LIF (in C). Pictures were taken on day 4, passage 2 (phase contrast, 100 x magnification)[180].

The experiments demonstrated that the purified hLIF was active in maintaining the proliferation potential of murine embryonic stem cells as well as their pluripotency. The approach described here for the biological testing of LIF, namely the use of suspension cultures of ES cells was found very advantageous. Thus, feeder cell free and suspension conditions allowed for a strong and immediate response of the ES cells to the absence or

presence of LIF already after one to two passages (8 days). In particular, apoptosis was found to be rapidly triggered in the suspension cultures cultivated without LIF. As a comparison, biological testing of hLIF performed by the group of Dr. Tobias Cantz (Junior Research Group Stem cell biology, MHH) using adherent cultures with feeder cells are performed over 5 passages (24 days) to attest the activity of the cytokines. The use of feeder cells in the experimental set-up may in this case provide additional cytokines, which prolonge the culture of the ES cells. Thus, the functional testing of the bioactivity using suspension cultures may allow reducing the screening time of the purified cytokines.

The experiments confirmed that the hLIF produced by the established CHO[hLIF] cell line is able to support the growth and maintain the pluripotency of ES cells. In this context, first step of the optimization of the hLIF production process were conducted. At first, the isolation of producing cells was performed for the generation of clonal cell populations. The use of a homogenous cell population for the production process of hLIF may be desirable, in particular if clones exhibiting superior growth or production characteristics can be identified within the transduced cell population. In the following section, the isolation and the characterization of CHO[hLIF] from the clonal cell population is presented.

3.3.4   Isolation and characterization of CHO[hLIF] cell clones

In the previous section, the establishment of a CHO cell line expressing bioactive hLIF was demonstrated. As mentioned in Section 3.3.1, the intracellular detection of hLIF was not possible and the fraction of producing cells within the transduced cell population could not be determined. In addition, the expression of hLIF was found to be heterogeneous with regard to the molecular weight, indicating that several glycoforms of the cytokine are expressed by the CHO cells. It was hypothesized, that the glycosylation of the protein may be cell clone dependent. In this context, cell clones issued from the transduced population were isolated. The analysis of the hLIF expression of the isolated cells was subsequently performed to identify producing cells and to observe if individual cell clones exhibited different glycosylation patterns.

Generation of CHO[hLIF] clones using flow cytometric cell sorting

Cell cloning was performed using Fluorescence Activated Cell Sorting (FACS). Exponentially growing CHO[hLIF] cells were harvested and cloned using the single cell sorting modus of a FACS Vantage SE. Thus, 180 cells were sorted in 96-well plates containing fresh cultivation medium. The efficiency of the procedure was evaluated by counting the number of growing cells 6 days after cell sorting and was determined to be 33% (60 growing cell populations). All cultures were further expanded by Nina Bahnemann in the course of her Master thesis [180]. Eventually, 25 living clonal cell populations were obtained after 8 weeks, leading to an overall cloning efficiency of approx. 14%.

Characterization of isolated clones

The expression of hLIF by the isolated CHO clones was analyzed semi quantitatively by SDS-PAGE. Culture supernatants were purified utilizing small scale IMAC (Vivawell 8-strips, Sartorius Stedim, see Appendices 6.2.5) and subsequently analyzed for hLIF expression using SDS-PAGE. The volume of purified supernatant was adjusted according to the measured cell concentration in the culture, so that the purified volume of medium contained the same number of cells. This approach allowed a semi-quantitative comparison of the hLIF expression between each clone. The results are displayed in Fig. 3.16. All 25 clones were found to be producers, which strongly supports the hypothesis that high transduction efficiency was achieved during the establishment of the cell line, as demonstrated in Section 3.1.2. In addition, a similar heterogeneous expression of hLIF was observed on the gels for all isolated clones (Fig. 3.16), indicating that the protein was similarly glycosylated by all cells. Thus, the observed heterogeneous glycosylation pattern is not cell clone dependent and is more likely caused by the changing chemical environment in the culture. The maintenance of defined and controlled culture conditions may allow manipulating glycosylation by the CHO[hLIF] cells. This may be advantageous, if a particular glycoform of hLIF is found to be more suitable for a defined field of application of the cytokine.

Interestingly, two clones (6 and 21) exhibited more pronounced and intense bands on the SDS-PAGE gel. These results, confirmed by Coomassie staining (data not shown), suggested a higher expression level of the recombinant protein by these clones.
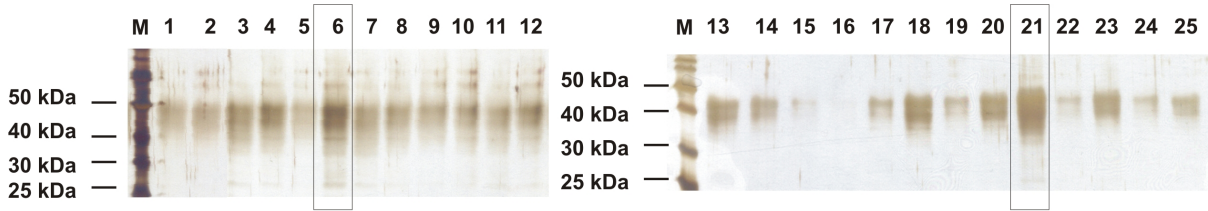
Fig. 3.16: Analysis of the hLIF expression by CHO^{hLIF} clones isolated by FACS. The purified volumes of the supernant for the analysis was determined occording to the cell concentration.

In addition, microscopic observation of the two clones revealed a significant higher cell size compared to untransduced cells. This fact is illustrated in Fig. 3.17 for CHO^{hLIF} clone 21 (in A) in comparison to untransduced CHO^{SFS} cells (in B).
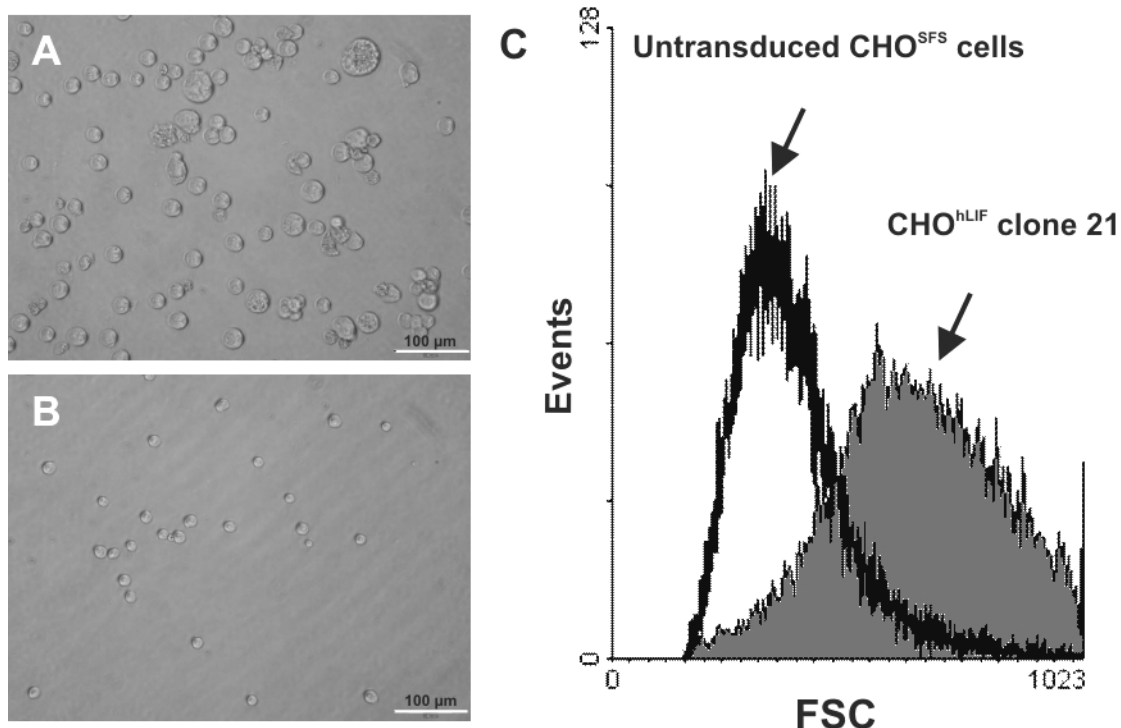
Fig. 3.17: Comparison of the cell size of the isolated CHO^{hLIF} clone 21 with untransduced CHO^{SFS} cells. In A: CHO^{hLIF} clone 21 (200 x magnification), In B: untransduced CHO^{SFS} cells (200 x magnification); In C: flow cytometric measurement using FSC signals as a measure of cell size. FSC: Forward Scatter.

Thus, from the digital images cell diameter was estimated to be approx. 31.4 μm (± 9.2 μm, n = 10 cells) for CHO^{hLIF} clone 21 and 15.5 μm (± 2.2 μm, n = 10 cells) using the Olympus software Cell^2. The results were confirmed by flow cytometric measurement using the forward scatter signals (FCS) as measure of cell size (see Fig. 3.17.C). This phenomenon may be explained by the fact that producing cells increase the size of some intracellular organelles, such as the

endoplasmic reticulum or the golgi apparatus for the secretion of the recombinant cytokine. Cell size is an intrinsic parameter requiring no staining. Thus, this criterion may be used as a selection parameter during cell sorting by FACS in order to isolate high producing clones more selectively from the established CHO[hLIF] population. Further experiments should be performed to elucidate if a correlation exists between the size and the specific productivity of the transduced CHO cells.

Based on the hLIF expression observed on SDS-PAGE, new cell banks (CHO[hLIF] clone 6 and CHO[hLIF] clone 21) were established for further investigation. The growth characteristics as well as the specific productivity should be determined for these homogenous cell lines using a quantitative method such as ELISA. Ideally, the cell line will exhibit a high growth rate and a high specific productivity, so that the volumetric productivity of the production process of hLIF could be increased.

3.4 Summary and perspectives

In this work, recombinant CHO cell lines were established for the production of cytokines of high interest for stem cell technology. For this purpose, lentiviral vectors were used for the delivery of expression constructs to the CHO cells. This approach was found to be very efficient. Within one week, transduced cell populations harboring more than 95% of producing cells were obtained. The expression constructs were integrated by the lentiviruses in the CHO genome, allowing a stable expression of the recombinant proteins.

During this work, the production of the proteins Angptl1 and 2, two cytokines that may have a high potential for the *ex vivo* expansion of hematopoietic stem cells, was intended. The expression of both recombinant proteins by the established CHO cell lines was confirmed. However, only intracellular expression was detected leading to the conclusion that the cytokines were not properly exported by the CHO cells. The use of new export signals for both proteins may allow overcoming this problem.

In contrast, the CHO cell line established for the expression of hLIF, a key cytokine for ES cell cultures, efficiently secreted the protein. The heavily glycosylated cytokine could be purified from CHO supernatant with a yield of approx. 190 μg from 100 mL. A rapid functional assay involving suspension cultures of murine ES cells was established in cooperation with Magda

Tomala and the bioactivity of the expressed hLIF was demonstrated. Additional testing performed by Tobias Cantz at the Hans-Borst-Zentrums für Herz- und Stammzellforschung (Rebirth Junior Research Group, MHH) confirmed the activity of the protein using adherently growing ES cells on feeder layers. This experiment also suggested that the glycosylated form of hLIF may be still active at lower dilutions compared to hLIF expressed in *E.coli*. This point may indicate that the glycosylated form of hLIF may be more bioactive or stable than the unglycosylated one. This should be confirmed and investigated in more detail in a comparative study.

Eventually, CHO[hLIF] clones were generated using flow cytometric cell sorting from the original transduced CHO cell pool. On the basis of semi quantitative analysis of the hLIF expression, two clonal populations were selected and used for the establishment of new cell banks. The specific productivity as well as the growth characteristics of these clones should be investigated. A high specific productivity and a high specific growth rate, if demonstrated, may allow increasing the volumetric productivity of the hLIF production process.

The efficiency of lentiviral preparations for a stable transgene transfer to CHO cells observed in this work raises the question of the applicability of this approach for the establishment of industrial cell lines and will be here briefly discussed. For the production of small amounts of recombinant protein, transient transfections are usually performed to rapidly characterize a molecule and screen its bioactivity[24]. For the large scale production of a bioactive protein, the establishment of a stable cell line for a long-term and reproducible expression is performed subsequently. The use of lentiviral gene transfer combines in our opinion both approaches, as a stable transduced cell population is obtained within one week, allowing thus the rapid production of a recombinant protein for screening purposes. If the bioactivity of the expressed protein is attested, a stable transduced cell population is already available for large scale production purposes. If necessary, the generation of clones and the selection of high producers within the originally transduced cell pool can be performed. Screening and production are performed using the very same cell line, thus variations due to the change of host cell or to the change of gene transfer method are reduced. In addition, the transduction of CHO cells can be performed in serum-free condition, as both virus production and CHO infection do not require the presence of serum or any additives of animal origin. The use of human derived viruses requires a level of biosafety 2, which may represent a difficulty, as it implicates the

availability of dedicated facilities. However, the use of murine-based lentiviruses for instance, may allow reducing the biosafety level to 1. In this context, the efficient technique of lentiviral gene transfer may play a role for the establishment of recombinant CHO cell lines of industrial relevance.

4 Characterization of mesenchymal stromal cells isolated from human umbilical cord tissue

Pioneer works of several groups during the last decade demonstrated that the tissues of the umbilical cord harbor mesenchymal stromal cell (MSC) populations exhibiting potential for clinical and tissue engineering applications (see Section 2.2). The development of suitable biotechnological protocols for the isolation, expansion and differentiation of MSC is now a challenge for the delivery of cells to a patient.

MSC have been derived from umbilical cord tissue by various approaches using non-human serum such as fetal calf serum (FCS) for isolation and expansion of the cells. The use of sera of animal origin raises some safety concerns in particular the potential transmission of infections e.g. viruses and prions from animals to man. The prominent example of the Bovine Spongiform Encephalopathy (BSE) in the late 90's brought the FDA to recommend the use of fetal-calf serum originating from a country certified free of this disease [181].

In this context, the use of human serum (subsequently abbreviated HS) would be preferable for the delivery of cells of clinical grade. Furthermore, HS-based isolation and expansion protocols would open possibilities for the use of allogenous strategies, i.e. the use of a patient's own serum for the production of therapeutic MSCs.

In this work, primary cells derived from human umbilical cord under xeno-free conditions were characterized. In particular, flow cytometry was used as an analytical tool to specify the identity of the isolated cells and to monitor their growth or differentiation. Experiments were partially performed in collaboration with co-workers, as mentioned subsequently. A xeno-free isolation procedure using HS for the isolation of the cells is first presented. The procedure was evaluated with respect to the capability to yield MSCs and its reproducibility. Investigations were conducted to determine the nature of observed sub-populations within the isolated cultures. The growth characteristics as well as the expansion capacity of the cells cultivated with HS were studied. Finally, the osteogenic potential of the isolated cells was evaluated.

4.1 Isolation of mesenchymal stromal cells from human umbilical cord tissue under xeno-free conditions

Several strategies have been applied for the isolation of Mesenchymal Stromal Cells (MSC) from human umbilical tissue (reviewed in Section 2.2). The challenge of the procedure is the release of primitive cells widely distributed in the tissue and their separation from other suspension (blood cells) or adherent (endothelial cells, blood or endothelial progenitors) cell populations also contained in the cord.

Within the framework of this thesis, six human umbilical cords were processed in close collaboration with Stefani Boehm [182] and Tim Hatlapatka [183]. Because MSCs are found in nearly all compartments of the umbilical cord (see Section 2.2.1), the isolation approach chosen by our group did not focus on a particular region, but involved the processing of the entire umbilical tissue. No enzymatic treatment was used for the release of cells from the tissue. More importantly, the complete isolation procedure was performed under xeno-free conditions using HS as a supplement. The HS used in this study was obtained from the Institute of Transfusion Medicine (Hannover Medical School) and consisted of a pool of sera without regard to blood type or Rhesus factor. Fig. 4.1 illustrates the isolation procedure.
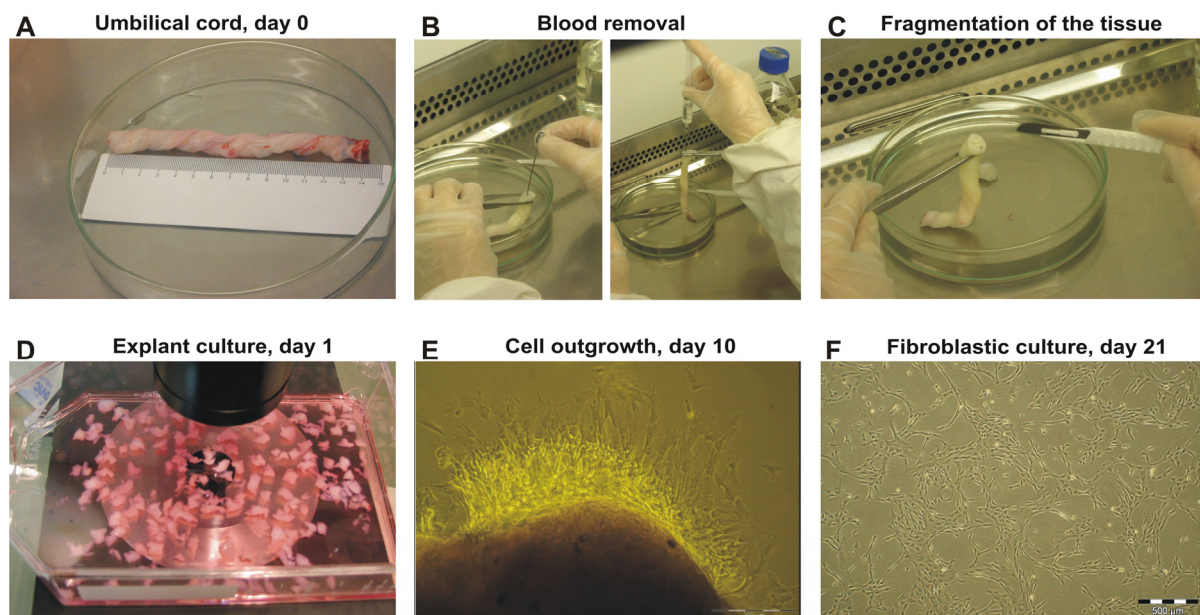
Fig. 4.1: Isolation of plastic adherent cells from human umbilical cord tissue, modified from [184].

The umbilical cords were obtained from consenting patients delivering full-term (38–40 weeks) infants by cesarean section. Immediately after birth the cords were fragmented into 10-15 cm long segments (Fig. 4.1.A) and stored for transport in PBS containing 5 g·l^{-1} glucose supplemented with 50 µg·ml^{-1} gentamicin, 2.5 µg·ml^{-1} amphotericin B, 100 U·ml^{-1} penicillin and 100 µg·ml^{-1} streptomycin to prevent bacterial or fungal contaminations. The cord segments were then transported and processed within 48 hours. Blood from the arteries and the vein was first removed by flushing PBS through the vessels using blunt needles and a sterile syringe (Fig. 4.1.B). The tissue was then chopped in small pieces (termed here as explants) in order to enhance the contact surface of the tissue and transferred to cell culture flaks (Fig. 4.1.C and D). Explant cultures were incubated in αMEM supplemented with 15% HS and 50 µg·ml^{-1} gentamicin at 37°C in a humidified atmosphere with 5% CO_2. The medium was changed every second day.

After few days, an outgrowth of adherent cells from the explants could be observed as illustrated in Fig. 4.1.E (day 10). After 2 weeks the tissue was removed and the attached cells were washed several times with PBS. The adherent cell population was further cultivated in αMEM with 10% HS avoiding the formation of confluent colonies by enzymatic treatment if necessary. On day 21 a culture of sub-confluent plastic adherent cells presenting predominantly a fibroblastic morphology was finally obtained (Fig. 4.1.F). However, microscopic examination revealed colonies exhibiting an endothelial morphology within the fibroblastic cell population in one of the six isolated cultures (Fig. 4.2.A and B).
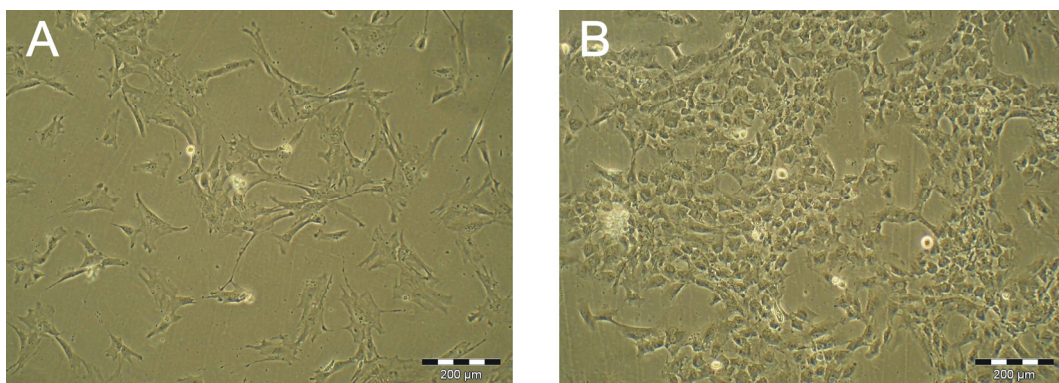
Fig. 4.2: Endothelial contamination in a UC-derived adherent culture. A: fibroblastic adherent cells. B: colony of cells exhibiting an endothelial morphology (100 x magnification).

The identity of this subset of adherent cells was investigated on the single cell level via flow cytometry. For this purpose, the expression of the surface antigen CD31, designating the protein PECAM-1 (Platelet endothelial cell adhesion molecule) was measured, as this antigen is known to be expressed on endothelial cells[185]. CD31 expression was detected using a monoclonal mouse anti-human FITC-labeled antibody. The detailed staining procedure is described in Appendices 6.2.6.
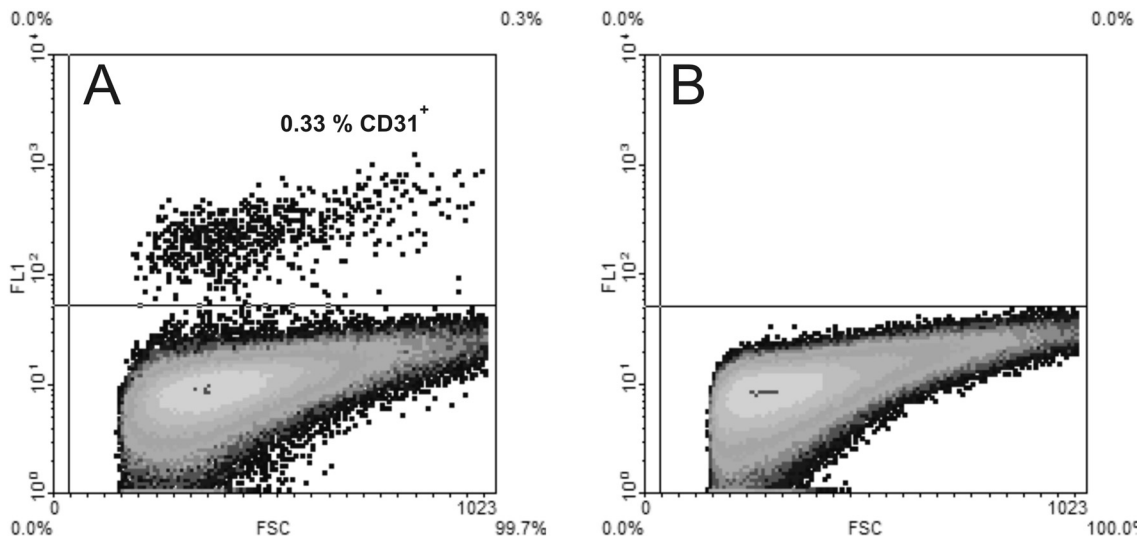
Fig. 4.3: Identification of an endothelial (CD31$^+$) sub-population in UC-derived cultures via flow cytometry. CD31 expression was detected using a mouse anti-human FITC-labeled antibody in the FL1 channel (BP: 505-545 nm). A: CD31 analysis before cryopreservation (> 2·10^5 events displayed); B: CD31 analysis after revitalization (> 4·10^5 events displayed). FSC: Forward scatter signals.

The isolated culture was found to harbour a subset of CD31 expressing cells at a frequency of approx. 0.33% total living cells. This sub-population can be seen in a density plot FL1 vs FSC in Fig. 4.3.A. The result of the analysis confirms the fact that endothelial cells are possible contaminants during the isolation procedure of fibroblastic cells from umbilical tissue. However, only a very low frequency of such cells could be detected in one of six isolated cultures. More importantly, CD31$^+$ cells could not be longer detected after cryopreservation and revitalization (illustrated in Fig. 4.3.B) suggesting that the subset of endothelial cells did not survive the freezing procedure.

The process flow chart presented in Fig. 4.4 summarizes the isolation and highlights some selection features observed during the applied procedure.
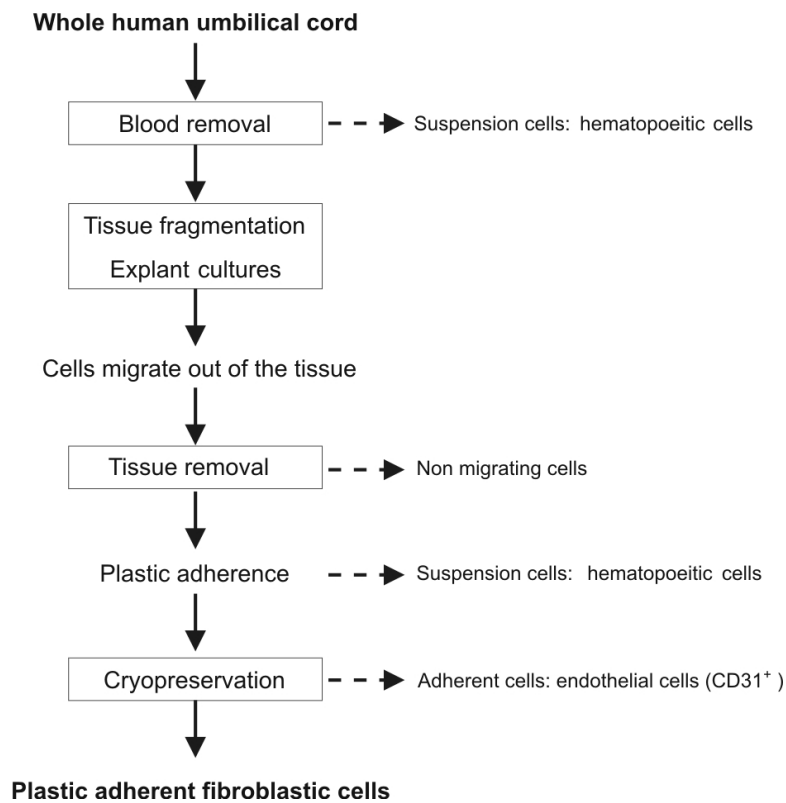
Fig. 4.4: Process flow chart summarizing the isolation of plastic adherent fibroblastic cells from umbilical cord tissue. Dashed arrows indicate removal of unwanted cells.

Hematopoietic cells (blood cells) present in great number in the cord at birth are removed by washing the blood vessels and subsequently during repeated medium changes and washing steps of the explant cultures. The isolation procedure relies primary on the fact that adherent cells grow out of the fragmented umbilical tissue in the presence of medium. This can be explained by a passive phenomenon: the direct contact of the chopped tissue with the cell culture vessel allows superficial cells to adhere to the plastic surface. An active migration of the cells out of the explants is however the most likely involved mechanism. Chemotaxis may be driven by the increasing nutrient gradient from tissue to the surrounding medium but also by specific cytokines present in the medium. In particular, chemokines such as HGF (hepatocyte growth factor) and SDF-1 (stromal-derived factor) known to be secreted by injured tissue were found to induce the migration of bone marrow and umbilical cord blood derived MSCs [186, 187]. In this procedure, these cytokines must be secreted into the medium after tissue fragmentation and drive MSC migration out of the explants. This phenomenon, if verified, may be used for the optimization of the isolation process. Medium, supplemented

with specific cytokines may accelerate cell migration und reduce the duration of the procedure.

Using a simple approach, fibroblastic plastic adherent cell populations were successfully isolated from 6 umbilical cords. Numerous cells could be derived from each cord and cell banks were established with a minimum of $21 \cdot 10^6$ cells.

Plastic adherence and fibroblastic morphology belong to the characteristics of mesenchymal stromal cells. However, these two criteria are not sufficient for the identification of MSC in cultures derived from human tissue. The UC-derived fibroblastic cells were further investigated with regard to the expression of specific molecular markers. Analyses on the single cell level were performed to investigate the heterogeneity of the cell population and to determine the identity of the isolated cells.

4.2 Characterization of stromal cells isolated from human umbilical cord on the single cell level

4.2.1 Immunophenotyping of the UC-derived cells

The UC-derived cell populations were investigated with regard to the expression of specific molecules reported to be present on MSC. In contrast to other progenitor cells, for instance hematopoeitic stem cells, there is currently no unique marker available for defining human MSCs. The expression of a set of markers combined with the demonstration of *in vitro* multi-lineage differentiation potential (discussed later and in Section 4.5) is necessary to identify MSCs derived from human tissue.

The expression of several intra- and extracellular specific proteins were reported for UC-derived MSC (reviewed in Section 2.2.3). The surface glycoprotein endoglin also termed as surface antigen SH2 or CD105, the extracellular 5'-nucleotidase (SH3 or CD73), and the Thy-1 membrane glycoprotein (CD90) are widely used for the identification of UC-derived stromal cells (see Section 2.2.3), as these markers were proposed by the International Society for Cellular Therapy (ISCT) in 2006 as positive markers for human MSCs [94]. However, these surface molecules may also be expressed on haematopoietic and endothelial cells, which are two potential contaminants in UC-derived cell populations. Consequently, it is necessary to

carefully examine the haematopoietic or endothelial nature of the isolated cells using surface markers such as the transmembrane tyrosin phosphatase CD45 (leukocyte common antigen), CD34 (antigen expressed on hematopoietic progenitors and endothelial cells) and CD31 (endothelial cells, already discussed in 4.1). The hyaluronic acid (HA) receptor CD44 is also a commonly used positive marker and may be expressed by UC-derived MSCs as the extracellular matrix of the UC is one of the highest HA-containing tissue in humans [188]. Cell surface markers will be subsequently denominated using the "CD" nomenclature.

Analytics for the detection of the antigens CD31, CD34, CD45, CD73, CD90 and CD105 using fluorescence labeled antibodies was established in this work. Fig. 4.5 illustrates for instance the expression of CD90 on the membrane of UC-derived adhering cells detected with a FITC labeled antibody.
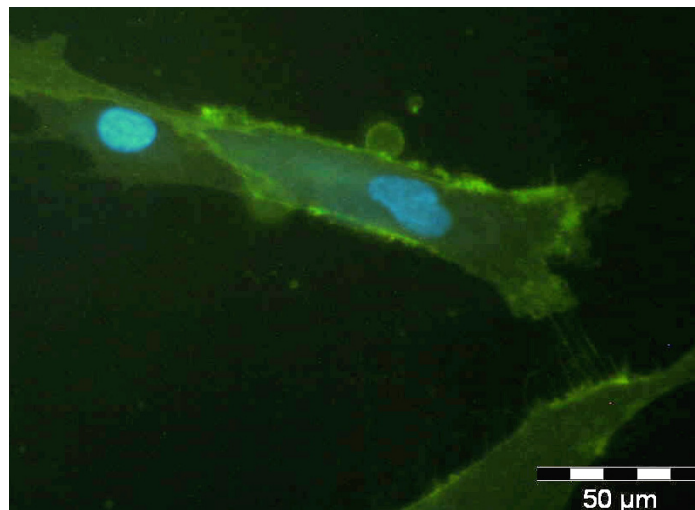
Fig. 4.5: Thy-1 (CD90) expression on the membrane of UC-derived cells. CD90 is detected using a mouse anti-human FITC labeled monoclonal antibody (green fluorescence). Cell nuclei are visualized using the nucleic acid dye DAPI.

The heterogeneity of the isolated cell populations was investigated via flow cytometry. Considering the fact that a set of cellular markers have to be combined to identify MSC, assays allowing the simultaneous analysis of several markers were established. Accordingly, the fluorophores FITC, PE and the tandem dye PE-Cy5 were used in three color experiments (detailed in Appendices 6.2.6).

The results of the analysis of UC-derived fibroblastic cells after revitalisation (termed in the following as passage 1 or P1) can be seen in Fig. 4.6.A-C. The analysis was validated by the use of a mix population of UC-derived and Jurkat cells (D, E and F). The Jurkat leukaemia human

cell line was found very convenient as a control population, as these hematopoietic cells express CD45 [189], lack the expression of CD73 [190], CD44 [191] and CD105 [192] and showed a heterogeneous expression for CD34 and a low CD90 expression level.
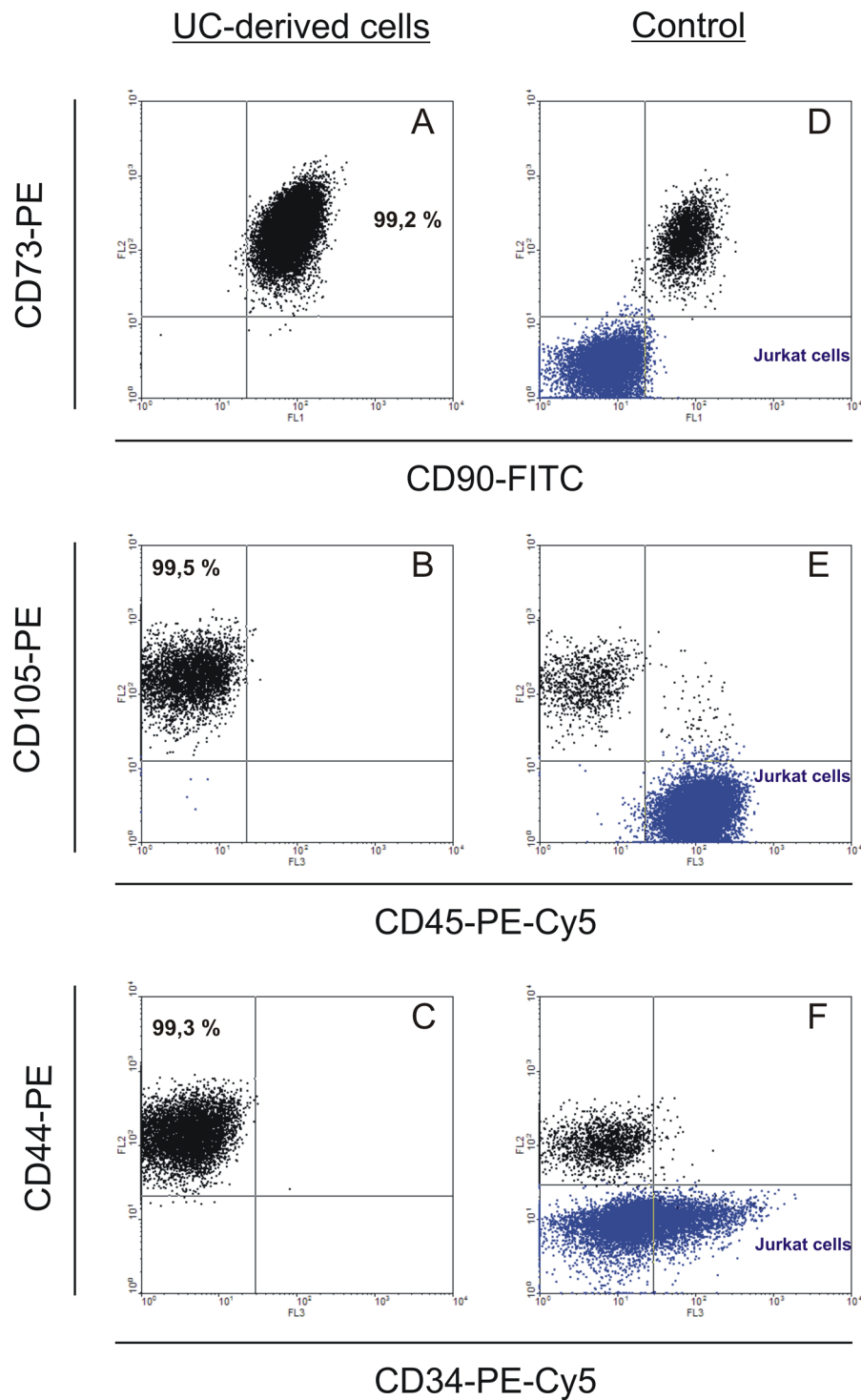
Fig. 4.6: Multicolor analysis of a UC-derived fibroblastic cell population in P1 (A, B and C) and control mixed sample containing leukaemia Jurkat cells (blue dots in D, E and F). Data were obtained from three staining experiments combining detection of CD90, CD73 and CD45 (A and D), detection of CD90, CD105 and CD45 (B and E) and detection of CD90, CD44 and CD34 (C and F). At least 10 000 events are displayed.

The UC-derived cell populations were found surprisingly homogenous with regard to all investigated cell markers as demonstrated in the dot plot A, B and C in Fig. 4.6. Compared to the control cell population, the isolated cells were found positive for the MSC markers CD90 and CD73 (A), CD105 (B) and CD44 (C), but lacked the expression of the markers CD45 (B) and CD34 (C).

The expression of each surface molecule was confirmed and quantified in monoparametric measurements. Marker expression level was evaluated in comparison to a matched isotype control, i.e. an identically labeled antibody of the same isotype class and used in the same quantity as the test antibody, but presenting no affinity for human cells (see Appendices 6.2.6). The conditions for flow cytometric analysis were optimized in additional experiments. Thus, cell harvest using the enzymatic solution accutase (a mixture of proteolytic and collagenolytic enzymes) was preferred to trypsin or to non-enzymatic methods, since a reduced antigen detection was measured after treatment with the latter two detachment procedures (see Appendices 6.3.3). All assays were validated on the transcriptional level via RT-PCR using Jurkat cells as control (Appendices 6.3.4).

The typical immunophenotype of a UC-derived cell population in P1 is presented in Fig. 4.7 (filled histograms). Positive staining was defined as the emission of a fluorescence signal that exceeded levels obtained by >99% of cells stained with isotype control antibodies (unfilled histograms). In addition, medians of the fluorescence distributions are displayed. The analyses confirmed that the isolated cells lack the expression for CD31, CD34 and CD45. The isolated cells are consequently neither from endothelial (CD31$^-$ and CD34$^-$) nor from hematopoietic (CD45$^-$) nature. More importantly, the cells were found positive (>99.8%) for the MSC markers CD44, CD73, CD90 and CD105.
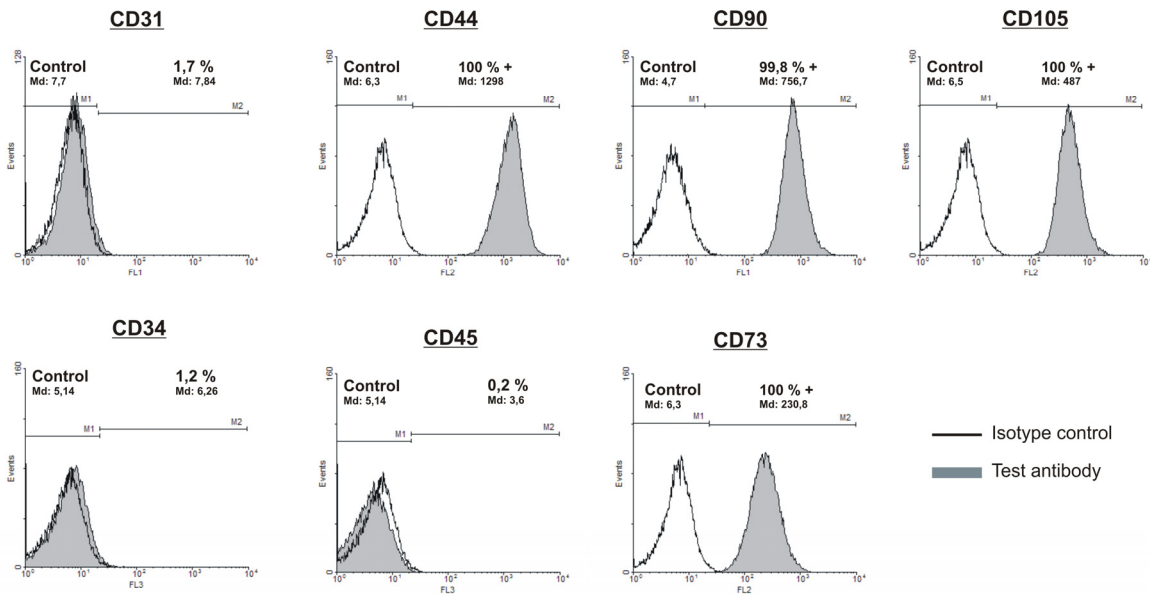
Fig. 4.7: Immunophenotype of UC-derived cells (in P1).

Table 4.1 summarizes the measured immunophenotype of all cell populations isolated by our group during this work (n=6 umbilical cords). The reproducibility and the efficiency of the isolation procedure are demonstrated since fibroblastic cells exhibiting a MSC immunophenotype could be derived from all processed cords. Additionally, *in vitro* differentiation studies performed by Tim Hatlapatka demonstrated the adipogenic and chondrogenic potential of the isolated cells [183]. The osteogenic potential will be discussed in more detail in section 4.5. Consequently, it can be stated that the isolated cells meet the basic criteria defining Mesenchymal Stromal Cells (MSC) as proposed by the ISCT [94]: the adherence to plastic, the expression of a set of specific surface antigens and a multi-lineage differentiation potential. Accordingly, the isolated cells will be termed subsequently as UC-MSC.

Table 4.1: Overview of the measured immunophenotype of primary cells isolated from 6 umbilical cords.

Surface marker	[%] Positive cells
CD31	0,9 ± 0,8
CD34	1,4 ± 0,2
CD44	99,9 ± 0,2
CD45	0,4 ± 0,4
CD73	98,9 ± 1,8
CD90	99,9 ± 0,2
CD105	98,9 ± 2,3

To date the identification of MSC in human tissue isolates requires the combination of several characteristics (morphology, surface marker profile and differentiation potential). In this context, the identification of a universal marker defining primitive human MSCs remains challenging. Recent works described surface molecules allowing the identification of MSC in bone marrow aspirates[75, 130, 131]. In the following section, the analysis of the expression of these cellular markers in UC-MSC culture is presented.

4.2.2   Expression of newly described MSC markers in UC-derived MSC cultures

Several markers were described to uniquely distinguish MSC from other bone marrow cell populations. Thus, the surface antigens CD271[130, 131], MSCA-1[131] and the neural ganglioside GD2[75] were successfully used for the isolation of multipotent cells from bone marrow aspirates. The analysis of the expression of these antigens in MSC isolated from other sources is highly interesting in order to elucidate whether these markers are universally expressed on human MSC or restricted to the bone marrow.

In this work, the expression of CD271 and MSCA-1 were analyzed using PE-labeled monoclonal antibodies. The protein GD2 was stained using a primary antibody and PE-labeled secondary antibody (see Section 6.2.6).

The analysis of the isolated cell population did not reveal cells expressing the surface antigen MSCA-1 and CD271 (see additional results in Section 6.3.5). For the protein GD2 however, a few positively stained cells were detected at a frequency <0.1%. At such a low frequency, the determination of significant results is challenging and the signal to noise ratio of the method used for detection has to be carefully examined. This particular field of flow cytometry is called "rare event flow cytometry" and technical aspects have to be scrutinized in order to obtain reliable results[193]. In particular, dead cells and cell aggregates have to be excluded from the analysis to prevent the measurement of false positive events. Fig. 4.8 summarizes the approach used for the analysis. First living cells were gated in a density plot of the FSC versus SSC signals (region R1 Fig. 4.8.A) and according to propidium iodide exclusion (R2 in Fig. 4.8.B). In addition, cell aggregates were excluded of the analysis using pulse height and pulse integral measurement (region R3 in density C displaying pulse high versus pulse area of the measured FSC signals). In this example 122 positive cells were measured (Fig. 4.8.D). The

background noise of the detection was evaluated measuring the same number of cells treated with the secondary antibody under identical conditions as the test sample, but omitting the primary anti-GD2 antibody (17 events in Fig. 4.8.E). Thus, subtracting the background from the number of measured events, 105 ± 26 cells positive for GD2 in a total population of $5 \cdot 10^5$ cells were measured. The counting error was determined using Poisson statistic (standard deviation SD = 26 cells) and corresponds to a coefficient of variation (CV) of 11.2%. Using this method, frequencies of GD2$^+$ cells ranging from 0.02 – 0.1 % were measured in three isolated cell populations.
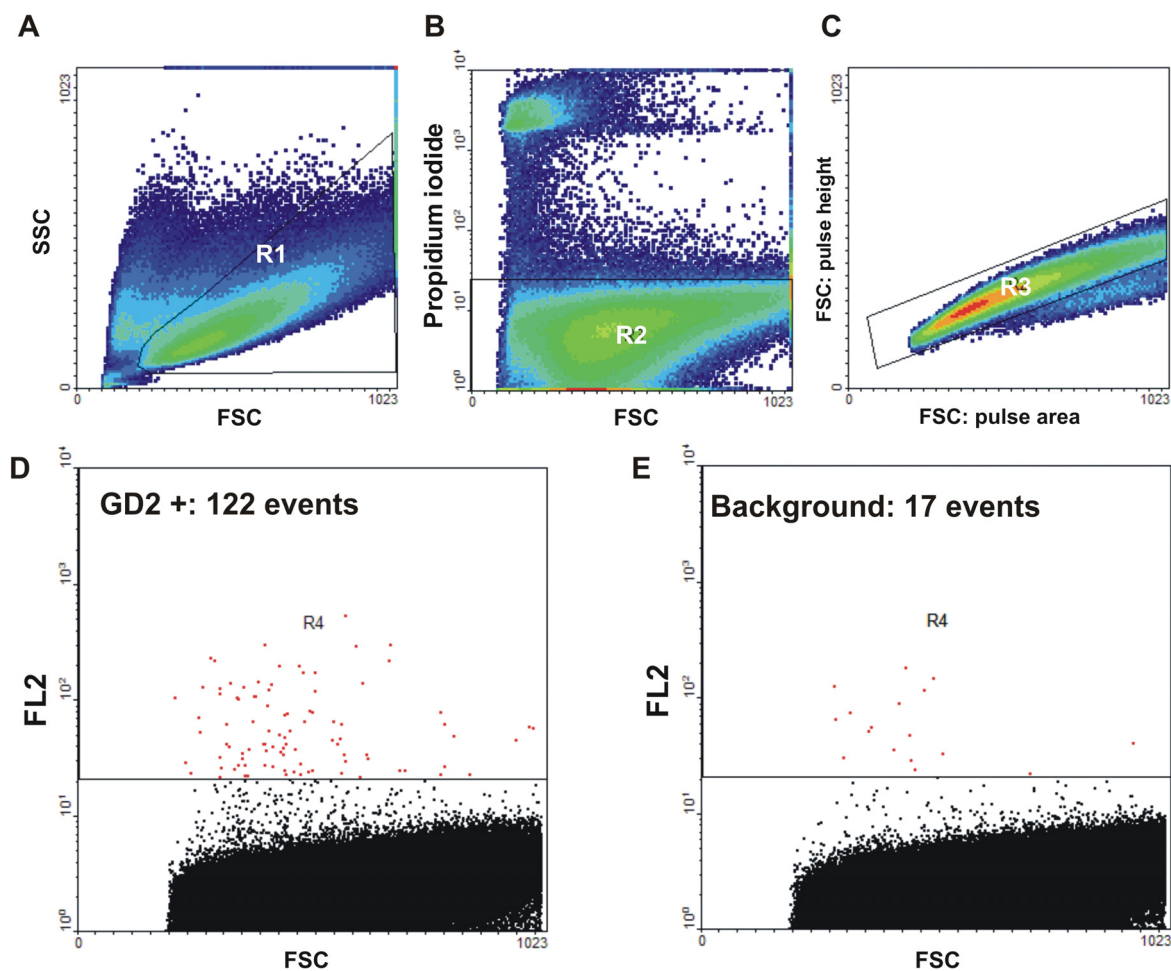
Fig. 4.8: Rare event analysis of GD2 expressing cells within a UC-derived MSC population. Dead cells were excluded of the analysis according to FSC and SSC signals (in A) as well as Pi exclusion (in B). Aggregates were excluded using pulse processing analysis (in C). GD2 was detected using a primary and secondary PE-labeled antibody detected in channel FL2 (dot plots D and E, a total of $5 \cdot 10^5$ living cells are displayed). The background noise of the procedure was evaluated measuring cells solely stained with the secondary antibody.

A higher number of events of interest (GD2$^+$ cells) should be acquired to improve the statistical relevance of the results. For instance, the acquisition of 10000 events of interest

would allow the counting of GD2$^+$ cells with a CV of 1%. With a measured frequency of 0.02%, a total of $50 \cdot 10^6$ living cells should be measured, which is barely possible using a conventional flow cytometer such as the Epics XL used for this study (acquiring approx. 1000 cells/s, approx. 14 hours of analysis would be necessary). Thus, the measured frequency should be confirmed using an experimental setting appropriate for rare event flow cytometry, in particular a high speed analysis system.

The results of the analysis suggest the presence of GD2$^+$ cells within the isolated population at very low frequency. These findings are supported by a very recent report from Xu et al.[124]. In this work, GD2$^+$ cells were detected using immunohistochemistry in the tissue of the umbilical cord. Using an enzymatic isolation approach and cell separation by magnetic-activated cell separation (MACS), a sub-population of GD2$^+$ cells was obtained. Interestingly, flow cytometric analysis of the GD2$^+$ cells demonstrated the expression of pluripotent markers usually expressed by human embryonic stem cells such as Oct3/4, SSEA-4, Sox-2 and Nanog[124]. In addition, these cells exhibited a higher differentiation potential than GD2$^-$ cells. According to these recent findings, GD2$^+$ may represent a more primitive cell population within the umbilical cord tissue. This subset of cells may be of interest for clinical applications and deserves further investigation. However, the explant isolation approach used in this thesis is not efficient to derive this sub-population, as only a very low frequency of GD2$^+$ cells (< 0.1%) was detected in the isolated cultures. A more specific isolation procedure using monoclonal antibodies and MACS or FACS approaches may be more efficient for this purpose. In the following section the analysis of surface proteins of the major histocompatibility complex (MHC) is presented to specify the immune status of the isolated UC-MSCs. The MHC antigens are involved in the recognition and the rejection of transplanted tissues. Thus, the analysis of the expression of these molecules is of high interest to evaluate the potential of the isolated cells for allogenic transplantation.

4.2.3 Analysis of MHC molecules expression: immune status of UC-MSCs

The molecules of the major histocompatibility complex (MHC) are polymorphic glycoproteins expressed on the surface of human cells. There are two class of molecules MHC class I and MHC class II, which are subdivided according to the product of the Human Leukocyte

Antigen (HLA) genes. Thus, the antigens HLA-A, -B, -C belong to the MHC class I, HLA-DL, -DQ and DR to MHC class II [194]. The function of the MHC molecules is to present peptide fragments derived from foreign organisms (viruses, bacteria) to T-lymphocytes and trigger the immune response against infected cells in the body. MHC molecules are also involved in the recognition of non-self (allogenic) molecules[194]. Thus, rejection of transplanted tissues from a donor usually results from T-cell responses to allogenic MHC molecules expressed by the grafted tissues.

During pregnancy, the foetus, which can be seen as a semi-allogenic engraftment[195], is protected from the maternal immune system by a cell barrier in the placenta (see Fig. 4.9)[196]. In particular, trophoblast cells in the chorion display several defence mechanisms against maternal T-cells. For instance they harbour a reduced expression of MHC class I molecules [195, 197], i.e. these cells do not express HLA-A, HLA-B and HLA-C only weakly. On the other hand, they specifically express the HLA-G antigen, a non classical molecule of the MHC class I group [198-200].
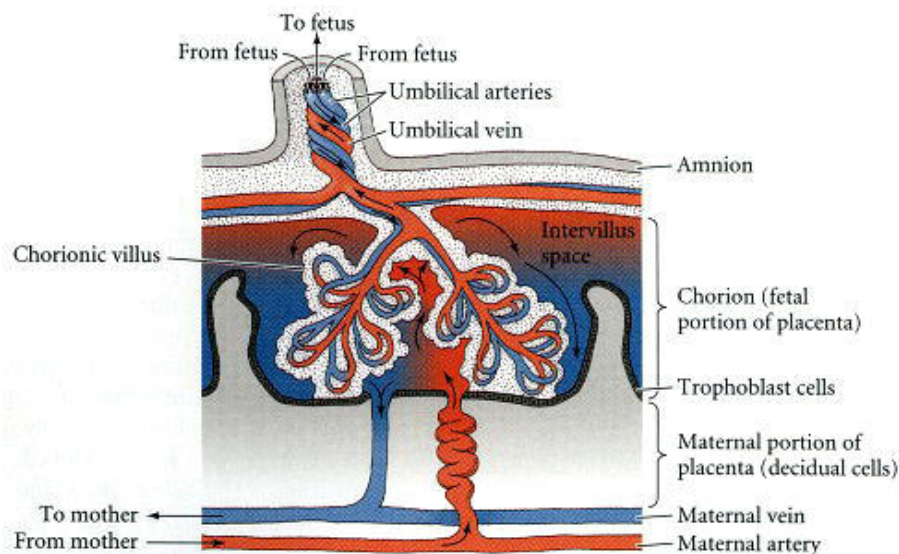
Fig. 4.9: The interface between maternal and foetal tissue in the placenta. Immuno-privileged trophoblast cells in the chorion protect the foetus from rejection by the maternal immunsystem [196]

The human umbilical cord links the trophoblastic tissue to the foetus (Fig. 4.9). For this reason, it has been postulated that the tissue of the cord or at least a part of it may possess similar immune properties as trophoblasts[126]. In this context, the analysis of MHC molecules expression of UC-derived cells is highly interesting to elucidate if the isolated cells harbour

similar properties. The issue is of particular interest with regard to the potential of UC-MSCs for allogenic transplantation.

In the frame of this work the expression of the MHC class I molecules was investigated on the protein level via flow cytometry. For this purpose, a FITC-labeled monoclonal antibody (clone TÜ149) reacting with HLA-B, - C and some HLA-A molecules[201-203] was used for detection. Fig. 4.10 illustrates typical results obtained for UC-derived MSCs (P1).
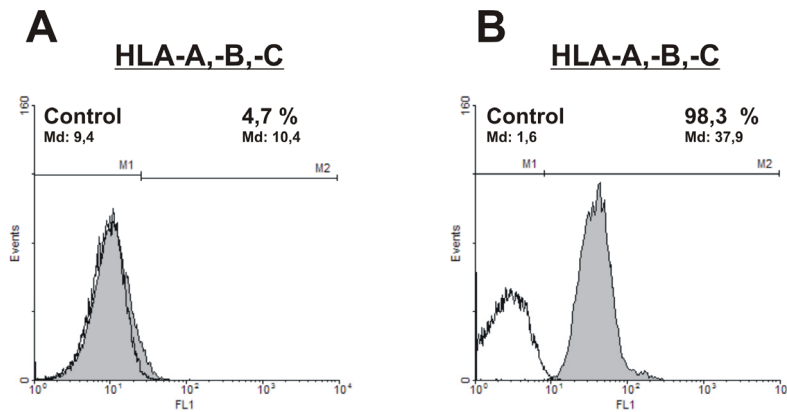
Fig. 4.10: Flow cytometric analysis of HLA-A, -B and –C (MHC class I) expression on UC-derived MSC in P1 (in A) and on a positive control population (PBMCs; in B). Filled histogram: FITC labeled anti HLA-A,-B and –C monoclonal antibody; unfilled histogram: matched isotype control. At least 10 000 living cells are displayed.

Histogram A in Fig. 4.10 shows the expression of the HLA antigens on UC-derived MSC. The fluorescence distribution (filled histogram) overlaps the distribution of the matched isotype control (unfilled histogram) and no significant HLA-I expressing cells could be measured (the relevance of the 4.7 % positive cells measured in the histogram is questionable considering the distribution of the fluorescence). Similar results were obtained for all isolated cell populations (2.5 ± 1.9 % measured positive cells, n=6). The validation of the staining procedure through the analysis of human peripheral blood mononuclear cells (HLA-I expressing cells) is displayed in Fig. 4.10.B.

The results indicate that the isolated cells do not express HLA-A, -B and C antigens, or at least in an undetectable level, and suggest a similar immune status of UC-derived MSC as other extra-embryonic tissues of the placenta. The lack of HLA-A, -B and –C antigen contradicts published data for UC-derived MSCs [83, 85, 87, 100, 101, 104, 106, 108-111, 115, 125]. Indeed, a low level of expression of HLA-I molecules could be detected in all reviewed studies. However, in these

works UC-MSC were isolated and cultivated in Foetal Calf Serum (FCS). Giving credit to the fact that the use of HS for the isolation and expansion of the cells may allow a superior maintenance of the original status of UC-MSC than a xeno-serum, the data presented here may provide a more accurate picture of the HLA-I expression compared to groups working with FCS. This hypothesis was strengthened by the observation of the antigens expression of UC-MSC cultivated in parallel using 10 % HS or 10 % FCS (Fig. 4.11). A significant higher expression of the antigens was observed for cells cultured in presence of FCS compared to cells cultivated with HS (illustrated here for cells in passage 3 and 5). However, the expression level in the presence of FCS diminished over the cultivation time, so that a similar expression was observed at passage 8 in the presence of HS and FCS. In contrast, in the presence of HS HLA-I expression remained negative over all cell passages. The influence of the used serum on HLA-I expression of UC-MSC should be further clarified in comparative studies.
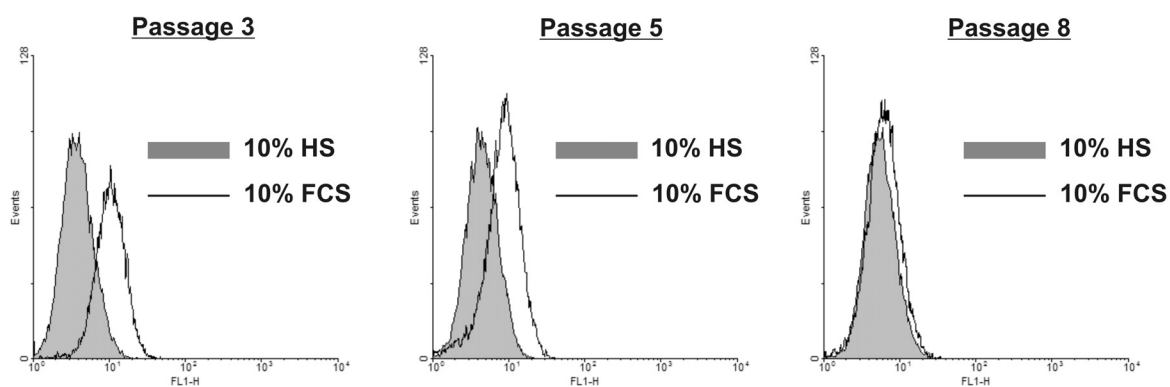
Fig. 4.11: HLA-I antigens expression level in the presence of human or fetal calf serum. UC-MSCs were cultivated in α-MEM supplemented with 10% serum. The cells were cultivated in T-flasks at a seeding density of 4000 cells/cm².

The results of these experiments indicate that UC-derived MSC, like other extra-embryonic tissue of the placenta, may not express some molecules of the MHC class I (HLA-A, -B and – C), suggesting immune-privileged properties of the isolated cells. The investigation of other molecules of the MHC class I and II must be carried out to further specify the phenotype of the cells. For instance, the expression of the non classical HLA-G molecule (MHC-I) is of particular interest as the expression of this antigen may inhibit the cytolytic activity of natural killer (NK) cells [204]. In a recent study, the expression of HLA-G on UC-derived MSCs has been demonstrated on the transcriptional level [126]. The expression remains to be demonstrated on the protein level.

The exciting topic of immune properties of UC-derived stromal cells is currently the subject of further investigations conducted by Tim Hatlapatka [183]. In co-culture experiments of UC-MSC and allogenic human peripheral blood mononuclear cells (PBMC), the immune privileged status of the isolated cells should be confirmed. For further information on the topic, the reader is encouraged to read the work of Tim Hatlapatka.

4.2.4 Conclusion

In this work it was demonstrated that MSC could be isolated efficiently from human umbilical cord tissue under xeno-free conditions. The isolated cells exhibit a homogeneous MSC phenotype (CD34$^-$; CD44$^+$; CD45$^-$. CD73$^+$; CD90$^+$; CD105$^+$) and a mutilineage mesodermal differentiation potential. Interestingly, the cells lack the expression of markers found on bone marrow MSCs such as MSCA-1 and CD271, suggesting that these markers are restricted to the bone marrow MSC niche. The isolated MSCs may harbor a rare population of GD2$^+$ cells. The frequency of this subset of cells should be confirmed using an experimental setting allowing for rare events flow cytometry. Finally, the isolated MSC cell population did not express typical MHC-I molecules, suggesting immuno-privileged properties for these cells. Experiments using UC-MSCs in co-culture with human peripheral blood cells, may confirm this hypothesis. Table 4.2 summarizes the phenotype of the isolated cells

Table 4.2: Overview of the immunophenotype of the isolated UC-MSCs

Cellular marker	Expression	Detection methods
CD31	-	Flow cytometry, RT-PCR
CD34	-	Flow cytometry, RT-PCR
CD44	+	Flow cytometry, RT-PCR
CD45	-	Flow cytometry, RT-PCR
CD73	+	Flow cytometry, RT-PCR
CD90	+	Flow cytometry, RT-PCR
CD105	+	Flow cytometry, RT-PCR
CD271	-	Flow cytometry
GD2	< 0.1% *	Flow cytometry
HLA-A,B,C	-	Flow cytometry
MSCA-1	-	Flow cytometry

* rare event analysis

4.3 Identification of sub-populations in UC-derived MSC cultures

In the previous sections it was demonstrated that fibroblastic cells exhibiting a homogenous MSC immunophenotype could be successfully isolated from human umbilical cord tissue. Despite a homogenous surface marker profile, heterogeneity could be recognized within the isolated population, in particular with regard to morphology. Thus, broad cell size distribution and marked morphological differences were observed in isolated UC-MSCs cultures. This fact is illustrated in Fig. 4.12. Cell cytoplasm is visualized via total protein staining (FITC), while cell nuclei are stained using the nucleic acid dye DAPI.
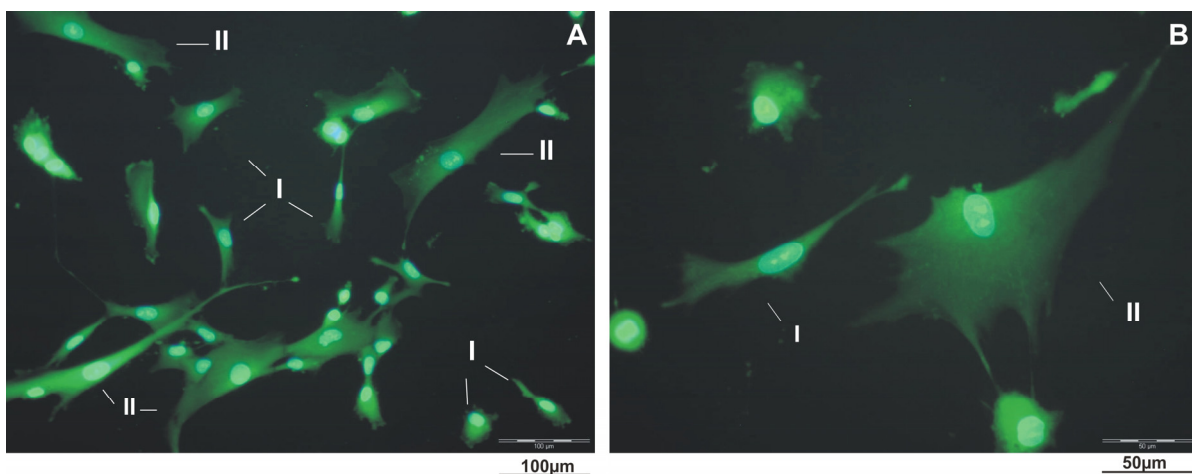
Fig. 4.12: Morphological and size heterogeneity of UC-derived stromal cells. Small cells (type I) with low cytoplasm-to-nucleus ratio and large cells (type II) can be observed. Cell nuclei are visualized via DAPI staining. Cytoplasm is visualized via total protein staining using FITC. A: 200 x magnification. B: 400 x magnification.

Besides small sized cells exhibiting a relatively low cytoplasm-to-nucleus ratio (type I in Fig. 4.12.A and B), large cells exhibiting an elongated to broad morphology (type II) with a higher proportion of cytoplasm could be observed in the cultures. Cell size and morphological heterogeneity in animal cell cultures may be a normal phenomenon related for instance to the cell cycle status of the cells. Cell division being imminent, cells are usually larger because protein content has been enhanced over precedent cell cycle phases. Increased cytoplasm may be also the result of migration phenomena in the cultures vessels: MSC extend their cytoplasm searching for cell-cell contact.

However, cell size/morphology heterogeneity may have another biological explanation indicating the presence of real sub-populations. To examine this hypothesis, UC-derived cells

were separated according to their size and subsequently characterized. These experiments were performed in close collaboration with Prof. Ralf Hass (AG Biochemie und Tumorbiologie, Klinik für Frauenheilkunde und Geburtshilfe, Medical School Hanover) [89]. The results are presented subsequently.

4.3.1   Cell separation using Counterflow Centrifugal Elutriation (CCE)

Counterflow Centrifugal Elutriation (CCE) was chosen as a separation technique, as CCE allows a high throughput separation with minimal perturbation of cellular function. The technique has been widely used for the synchronization of cell populations for biochemical studies[205]. In brief, cells suspended in an elutriation fluid are led to a rotating separation chamber (Fig. 4.13.A). A size gradient is obtained in the separation chamber as a result of the balance between the centrifugal force and the counterflow of elutriation buffer (B). The cells are then eluted from the chamber by increasing the flow rate of the elutriation fluid, where small cells are obtained first followed by larger ones (C).
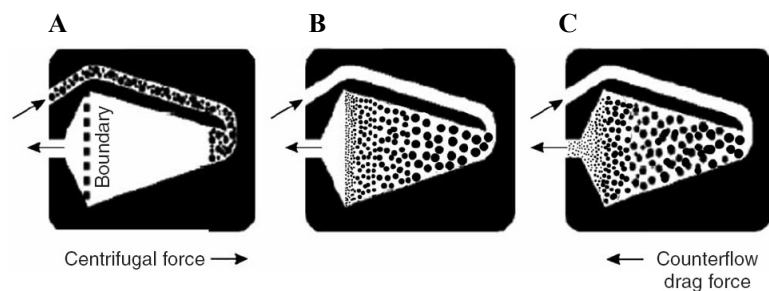
Fig. 4.13: Principle of cell separation via Counterflow Centrifugal Elutriation (CCE) [205]

For this experiment, UC-derived MSC were first expanded in a cell factory (Nunc, Thermo Fischer). Approximately $6 \cdot 10^8$ cells were harvested and elutriated in the laboratory of Prof. Ralf Hass at the Medical School in Hannover. Fractions the elutriated sample were collected upon progressive increase of the pump speed (flow rates are presented in Appendices 6.2.9). Cell concentrations and viability of every fraction was documented (Appendices 6.2.9).

Cell size distribution within the elutriated fractions was then directly analyzed via flow cytometry using forward scatter signals (FSC) as a measure of cell size. Additionally, the distribution of the cell diameter was analyzed utilizing the image analyzer Vi-CELL Series (Beckman Coulter). During the elutriation procedure six separate cell fractions with

continuously increasing cell sizes were obtained (Appendices 6.2.9). The first elutriated fraction consisting of the smallest and the last fraction containing the largest cells were further characterized. Fig. 4.14 illustrates the size differences of the elutriated cells.
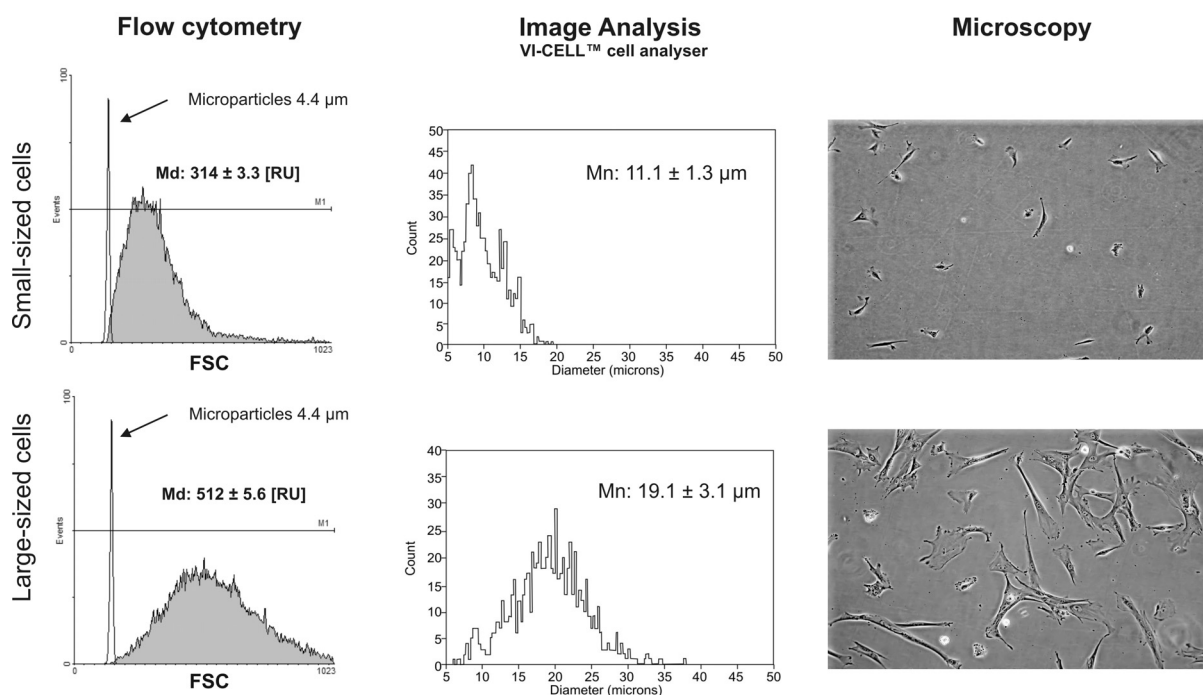
Fig. 4.14: Cell size distribution of small-sized and large-sized cells obtained after CCE. The cells were analyzed in suspension via flow cytometry (FSC) and digital image analysis (Vi-Cell analyzer). After adherence size and morphological differences were observed via phase contrast microscopy (100 x magnification). Flow cytometry: the median (Md) of the FSC signals is given [RU: relative units]. The standard deviation results from 6 independent measurements (n=6). Microparticles with a diameter of 4.4 μm were measured as reference. Vi-cell analyzer: the mean of the calculated diameter is given. The standard deviation results from 3 independent measurements (n=3), modified from [89].

Flow cytometric analysis of the cells confirmed the success of the elutriation procedure. A population of small cells, termed subsequently as small-sized cells, was obtained in the first fraction. The central tendency of the distribution is here given as the median of the FSC signals (Md = 314 ± 3.3 RU, n = 6). The last fraction yielded a population of significantly larger cells (Md = 512 ± 5.6 RU, n = 6), termed subsequently as large-sized cells. The flow cytometric data correspond well with the cell diameter distribution measured via digital image analysis (Vi-cell analyzer, Fig. 4.14). An average diameter of 11.1 ± 1.3 μm could be measured for the small-sized cells and 19.1 ± 3.1 μm for the large-sized cells. Eventually, microscopic observations of the adherent cultures confirmed the morphological differences. The high proportion of cytoplasm in the large-sized cell fraction is remarkable.

In addition, the cell cycle distribution in the elutriated samples was measured in order to investigate whether the observed size variation was a cell cycle related feature. It is commonly observed that cell size increases among the cell cycle phases[206]. DNA content analysis was performed using propidium iodide (Pi) as previously described[207]. Aggregates were excluded of the analysis using pulse height and pulse integral measurement. The generated histograms were analysed with the software WinCycle (Phoenix Flow Systems, San Diego, CA). Fig. 4.15 presents the cell cycle distribution of the small-sized and large-sized cells after elutriation.
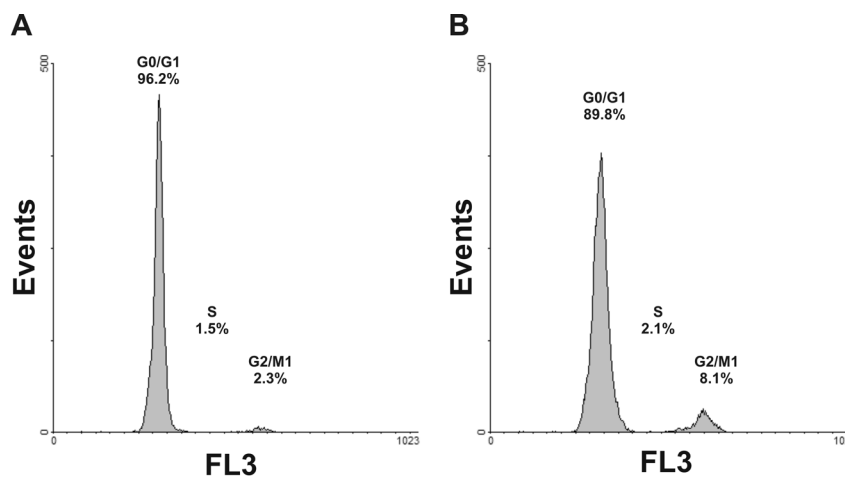
Fig. 4.15: Cell cycle distribution of the elutriated small sized (in A) and large sized (in B) cell populations.

The analysis demonstrated that small-sized cell fraction consists of 96.2% G1/G0, 1.5 % S and 2.3 % G2/M cells. In the large-sized cell fraction approx. 8 % of the cells are in the G2/M phases suggesting a poor enrichment of G2/M cells compared to the small-sized cell population. However, more than 90% of the cells are in the G0/G1 phase. It is therefore unlikely that the observed increase of cell size was cell cycle related, as the low enrichment of G2/M cells can not explain the clear cell size differences observed between the two elutriated fractions.

4.3.2 MSC antigen expression level of elutriated cultures

The aim of this experiment was the comparison of the expression level of MSC surface antigens between the elutriated cell fractions. Flow cytometric measurement of the antigens CD44, CD73, CD90 and CD105 demonstrated that all cells, regardless of the fraction, do express the surface MSC markers (see Appendices 6.3.6). These results were to be expected, as

it has been already demonstrated in Section 4.2.1 that all isolated UC-MSCs express the surface molecules. However, slight but significant differences were observed suggesting that large-sized cells express fewer surface antigens than small-sized cells (see Appendices 6.3.6). This point was surprising as it might be expected that larger MSC would express comparatively more surface antigens.

To confirm this observation, the ratio of antigen expression (immunofluorescence) and total protein content was measured. Since a good correlation ($R^2 = 0,893 \pm 0,011$; n = 6) could be observed between the total protein content measured via the fluorescence dye FITC and the side scatter signals (see Fig. 4.16.A and Appendices 6.3.6), the SSC signals were found to be a good approximation of the total protein content of UC-derived cells. Thus, the ratio of immunofluorescence to SSC signals was used here as a parameter representative of the surface antigen expression normalized on total protein content. To the best of our knowledge, this is an original approach for making comparisons of the surface antigen expression between two cell populations. Fig. 4.16.B and .C present the ratio of CD73/SSC and CD90/SSC measured for the small- and large-sized cells.
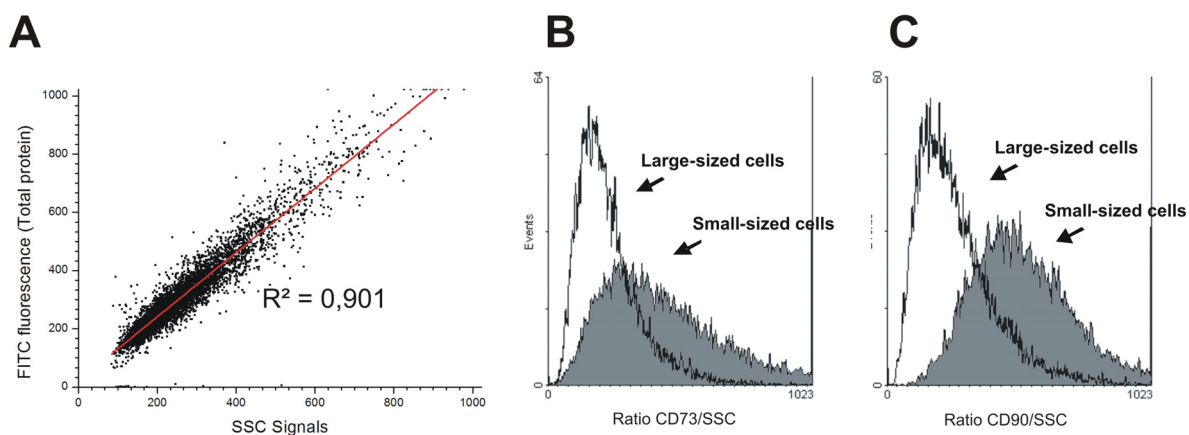
Fig. 4.16: Correlation between SSC signal and total protein content (A). Comparison of antigen surface expression normalized on total protein content (CD73 in B; CD90 in C). All signals were measured on linear scale. Ratios were measured using the ratio circuit of an Epics XL MCL flow cytometer (Beckmann coulter).

The obtained histograms clearly indicate that small-sized cells exhibit a higher ratio of surface antigen (CD73 and CD90) to total protein than large-sized cells (Fig 4.17.B and .C). Similar results were observed for the antigen CD44 and CD105, however in a less extend (see Appendices 6.3.6).

Flow cytometric ratio measurements demonstrated that large-sized cells do not express MSC antigens proportionally to their size and confirmed the lower expression level of specific MSC antigens compared to small-sized cells. The reduced expression of the specific cellular surface protein may indicate altered cellular functions. The comparison of the proliferation and the senescence level of the elutriated cultures eventually brought explanations for this phenomenon.

4.3.3   Comparison of the proliferation and senescence level of the elutriated fractions

The proliferation as well as the level of senescence of elutriated populations were investigated by Majore *et al.* [89]. The proliferation potential of parallel cultures was evaluated by calculating the average number of cell doublings and the resulting theoretical total cell number obtained over several passages. Fig. 4.17.A presents the growth of the elutriated small-sized and large-sized cells. As a control, the initial UC-derived primary population was cultured in parallel.
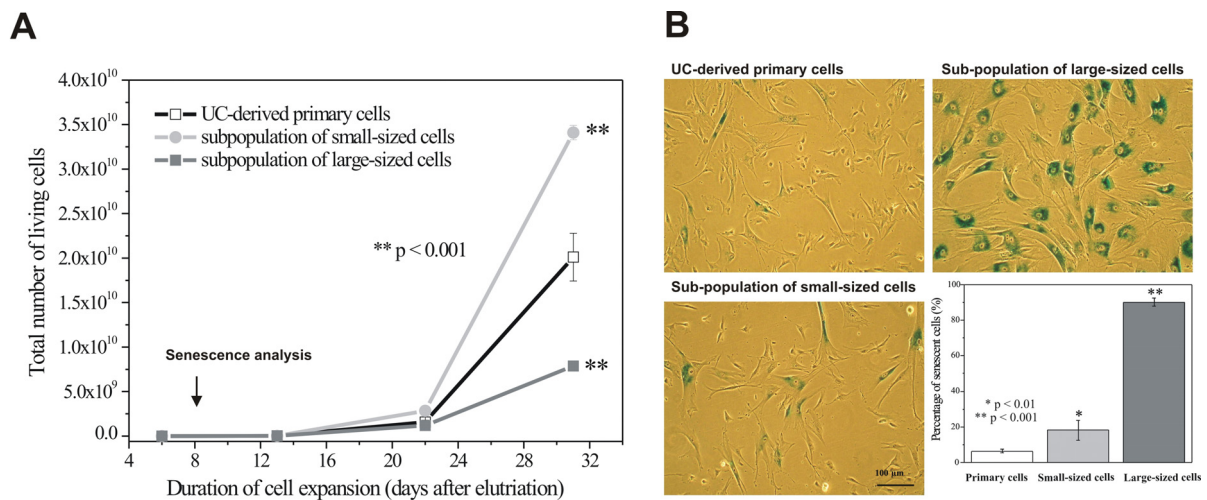
Fig. 4.17: Proliferation potential and detection of senescence in elutriated cultures. A: proliferation potential of the control, small- and large-sized cell populations over three passages. The experiment was performed 6 days after elutriation. The theoretical total number of cells was calculated at each passage. B: detection of senescent cells via β-galactosidase staining (100 x magnification). Quantitative results were obtained from the analysis of 4 microscopic images (n=4). The experiment was performed 8 days after elutriation, modified from [89].

The growth of the cells issued from the small-sized sub-population was significantly higher than the start population and the large-sized sub-population. This fact was illustrated by higher numbers of cell doublings and thus higher total cell number at each passage (Fig. 4.15.A). Large-sized cells exhibited in contrast the lowest proliferation potential.

Senescence associated β-galactosidase activity was measured in culture 8 days following the elutriation using the substrate X-gal (Appendices 6.2.2). Typical images of the cultures can be seen in Fig. 4.17.B. Senescent cells are marked by cyan dye surrounding the nucleus. The fraction of senescent cells was determined by manual counting of stained cells in the cultures. The analysis revealed $6.3 \pm 0.9\%$ (n = 4) of senescent cells in the original primary culture and $18 \pm 5.5\%$ of senescence in the small-sized sub-population. In contrast, $90.1 \pm 2.3\%$ of the large-sized sub-population displayed features of a senescent phenotype.

This experiment demonstrated that the large-sized cell fraction predominantly consists of senescent cells. These results explain the low growth observed for the elutriated sub-population, as senescent cells are growth arrested[208]. The data are in good agreement with the observed cell cycle distribution (Fig. 4.15.B), where > 90 % cells were measured in the G1/G0 phase. The growth of the culture over 32 days relies consequently on a sub-population of non-senescent cells (8 % in G2/M after elutriation in Fig. 4.15.B, or 10 % of non-senescent cells 8 days after elutriation in Fig. 4.17.B). Furthermore, the altered cellular function of senescent cells may explain the observed reduced expression of MSC surface antigens.

4.3.4 Conclusion

Senescence is a normal protective mechanism leading to the elimination of aged cells and occurs after a certain number of cell divisions. It may be also the result of oncogenic stimuli[208, 209]. Spontaneous immortalization of human cells in culture has been reported[210]. This process involves the escape of cells from senescence leading to the emergence of immortal cell clones. Thus, in the perspective of clinical applications aged cultures containing senescent cells are undesirable and may represent a risk for the patient. We demonstrated here that an increased cell size and a reduced surface antigen expression are related to the appearance of senescent cells in UC-MSC cultures. This two cell characteristics are measurable using high throughput single cell analysis such as flow cytometry and may be useful for the monitoring of the *ex vivo* cell expansion procedure. In particular, cell size measurement is an interesting parameter, as in this case no staining is required. Considering the fact that high nucleus to cytoplasma ratios are observed in senescent cells, this feature may serve for the detection of senescence in cultures. The combination of phase contrast microscopy and automated digital image analysis

for the calculation of this ratio may represent an interesting approach for the non-invasive monitoring of adherent UC-MSC cultures.

4.4 Growth characteristics of UC-MSC under xeno-free conditions

The proliferation potential and the expansion capacity are prominent characteristics for cells dedicated to clinical applications. Before delivery to a patient, MSCs will have to be generally expanded, so that a sufficient amount of undifferentiated cells can be obtained for therapeutic doses or for cell differentiation for tissue repair. How fast a clinical dose can be obtained is depending on the proliferation of the cells and their stability during the expansion process.

In this work the successful isolation of MSCs cells from umbilical cord tissue using a medium supplemented with HS was already demonstrated (section 4.1-2). In the following part, the growth characteristics of the isolated cells cultured with HS are presented.

4.4.1 Cell cultivation with human serum

UC-derived MSC have been mostly cultivated and characterized in FCS [83, 84, 129, 211]. To the best of our knowledge, the cultivation of MSC derived from umbilical cord tissue using HS has not been investigated yet. However, it has been demonstrated that HS does not optimally support the growth of bone marrow derived MSCs [212]. In this context, a comparative study performed in close cooperation with Tim Hatlapatka was conducted to establish whether HS supports the growth of the isolated UC-MSCs in a comparable manner to FCS. For this purpose, UC-MSCs were cultivated in a basal medium (αMEM) supplemented with 10% serum. Five cultures issued from the same isolated UC-MSC population were started in parallel in the presence of HS and four commercially available FCS (type "standard quality", "gold quality", "heat inactivated" and "pre-tested for amnion cells", all obtained from PAA Laboratories). The influence of the different sera on cell growth, cell morphology and on the expression of MSC markers was observed over 31 days. The detailed results of this study are presented in the PhD thesis of Tim Hatlapatka [183]. The results of the flow cytometric analysis and the major conclusion are briefly presented subsequently.

The UC-derived MSCs were able to grow in the presence of all sera. However, important morphological changes could be observed in cultures supplemented with FCS. Particular

attention was paid to cell size, as it was demonstrated in section 4.3 that the size of UC-MSC can be considered as a quality parameter for the cultures. Cell size was assayed utilizing flow cytometry (Forward Scatter signals, FSC). Fig. 4.18.A and B presents the cell size distribution of the start population (filled histogram) compared with the size distribution of the final population (unfilled histogram) obtained after 8 passages in FCS type "standard" (in B) and 9 passages in HS (in A) (respectively 31 days and 28 days of cultivation). Fig. 4.18.C summarizes the cell size evolution of all cultures over the entire experiment. The central tendency of the distributions (median, Md) is plotted for every culture (measurements were made in triplicates, n=3).
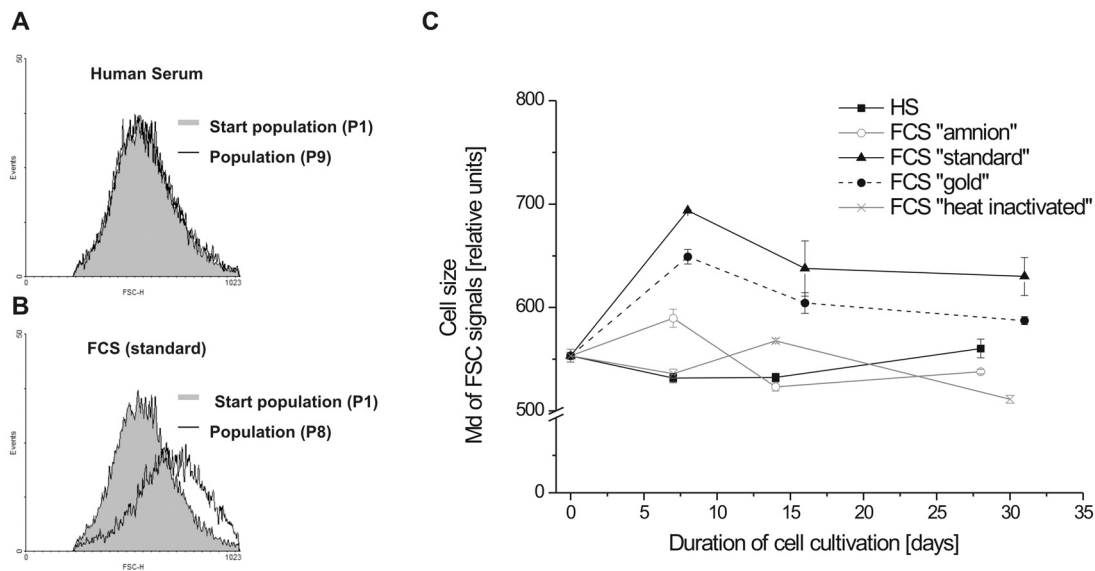
Fig. 4.18: Influence of serum on the size of UC-derived MSC. Cell size was measured by flow cytometry (FCS signals) in the presence of 10% human serum (in A) and 10% FCS "standard" (in B). The median (Md) of the distribution is given in diagram C for all cultures over the cultivation time. The plotted standard deviation was calculated from triplicate measurements, n=3.

While cells cultivated in HS maintained a comparable size over the entire investigated time frame (Fig. 4.18.A and C), FCS type "standard" and "gold" induced a significant increase of cell size (Fig. 4.18.B and C). These observations were confirmed by microscopic observation and cell size measurements utilizing a CASY cell analyzer instrument (see Tim Hatlapatka's thesis).

Cell size increase was accompanied by a significant loss of MSC marker expression, which supports the observations made in section 4.3.2. This fact is illustrated in Fig. 4.19 for FCS type "standard". In contrast, cells cultivated in HS exhibit a stable immunophenotype over the

entire investigated time frame (the stability of the immunophenotype of cells cultivated with HS will be discussed in more details in section 4.4.2).
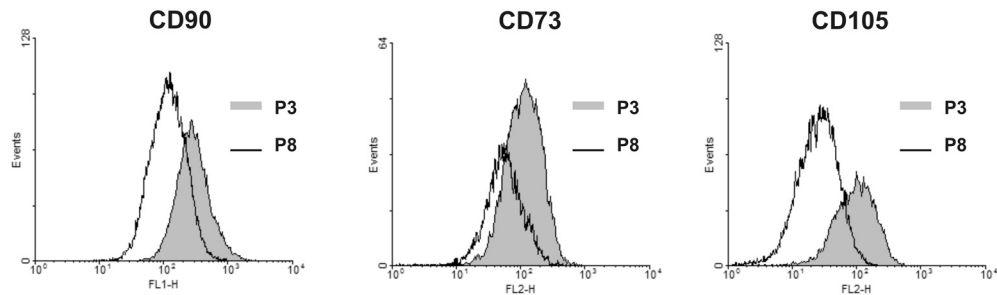
Fig. 4.19: Down regulation of MSC marker expression in the presence of FCS type "standard". P3: passage 3; P8: passage 8.

Cells cultivated with "heat inactivated" and "amnion pre-tested" FCS were found more stable with respect to cell size (Fig. 4.18.C) and to MSCS marker expression. However, with regard to the proliferation potential of the UC-MSC, HS was superior to all tested FCS. Thus, higher numbers of cell doublings were measured at every passage during the expansion using HS. These results are presented in more detail in the PhD thesis of Tim Hatlapatka [183].

The study demonstrated that not all fetal calf sera are able to maintain a stable morphology and immunophenotype of UC-derived MSCs. Moreover, a higher proliferation was observed in the presence of HS compared to cells cultivated with FCS.

In conclusion, it was demonstrated that UC-MSC could be efficiently cultivated in HS. On the basis of these results, the expansion protocol for the isolated UC-MSCs was established using 10% HS as a basal medium supplement. In the following section, a detailed analysis of the growth characteristics of the UC-MSCs cultured under these conditions is presented.

4.4.2 Growth characteristics of UC-MSCs

The growth characteristics of UC-derived cells were investigated in 175 cm² T-flask cultures. Cells in an early passage (P4) were cultivated in basal medium (α-MEM) supplemented with 10% HS. Six identical cultures were started in parallel with a cell density of 4000 cells/cm² (=$7 \cdot 10^5$ cells). Cultivation medium was replaced daily. After harvest through enzymatic treatment using accutase, total cell number, viability, cell cycle distribution as well as glucose, lactate and glutamine concentrations were determined (Analytics described in Appendices 6.2.2). Fig. 4.20.A presents the growth curve of UC-MSC and the measured cell cycle distribution over the cultivation time.
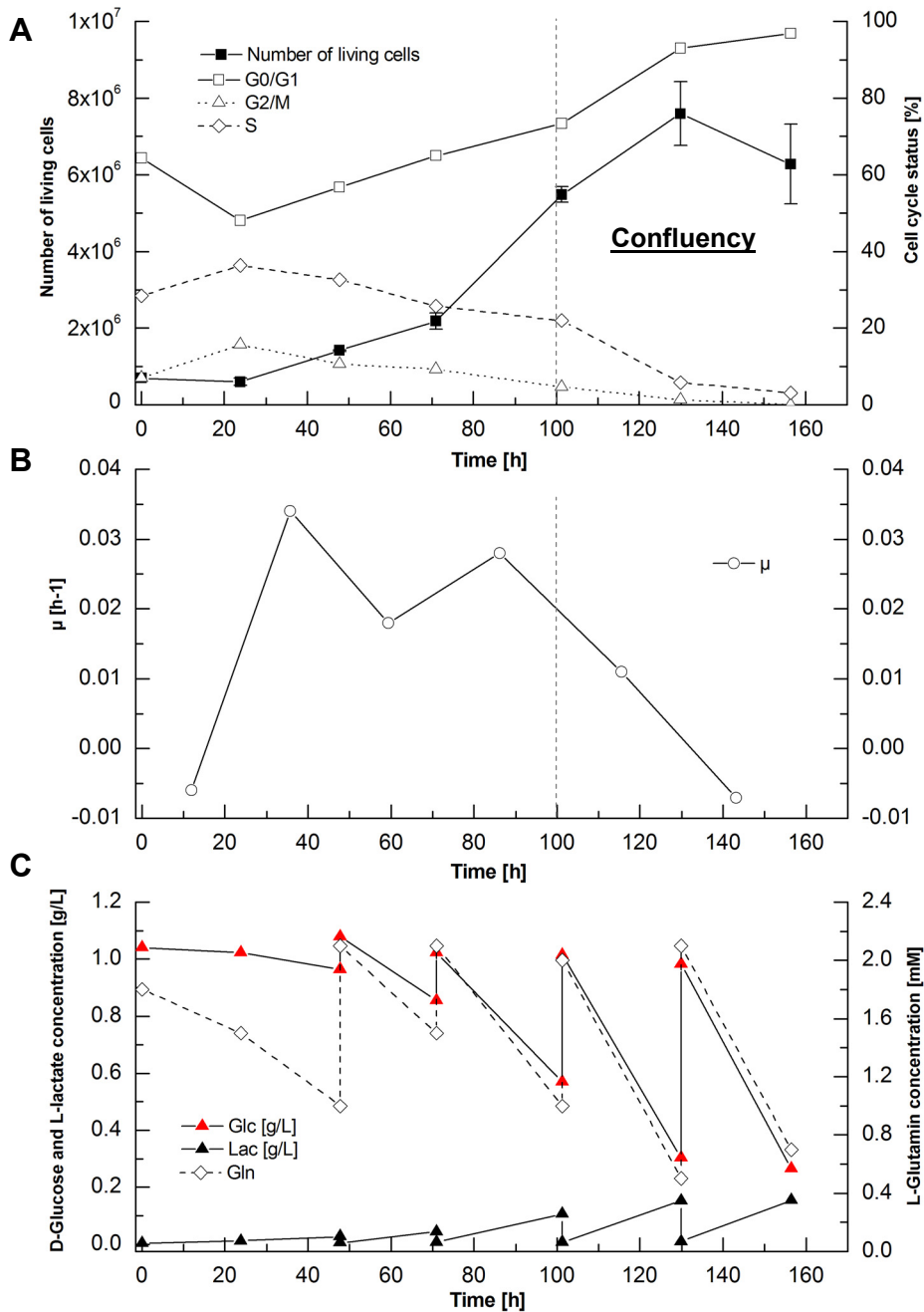
Fig. 4.20: Proliferation of UC-derived cells in α-MEM supplemented with 10% HS. A: cell growth and cell cycle distribution, B: specific growth rate μ over the cultivation time, C: D-Glucose (Glc), L-lactat (Lac) and L-glutamin (Gln) concentrations.

After a short lag phase of approx. 24 hours, the cells grew until confluency was reached after approx. 100 hours. During this phase, the specific growth rates observed were ranging between $0.2 - 0.35$ h^{-1} (Fig. 4.20.B). After 100 hours, the growth rate of the cell decreased rapidly. A maximum of $7.6 \cdot 10^6$ cells could be measured after 130 hours, which represents an approx. 11-fold expansion compared with the initial cell number. Post-confluent cultures were interrupted after 6 days. The viability of the cultures at this point remained high (87%).

The results of the cell cycle distribution analysis of the cultures were consistent with the observed growth curve (Fig. 4.20.A). The highest proportion of proliferating cells (here defined as cells in the S and G2/M phases) were observed during the growth phase (t=24 - 100 hours) ranging from 52.1 % to 27%. Once confluency was attained (t > 100 hours), the proportion of proliferating cells rapidly decreased, so that > 90 % of the population with a G0/G1 DNA content were measured in post-confluent cultures (t ≥ 130 hours). This result is illustrated in Fig. 4.21, where the cell cycle distribution of a post confluent culture (day 6) is plotted in comparison to the distribution of proliferating cells (day 2). The accumulation of G0/G1 cells indicates cell growth arrest.

The analysis of D-glucose and L-glutamine concentrations over the cultivation time confirmed that no limitation of the main energy sources occurred during the experiment, as fresh medium was daily provided to the cells (Fig. 4.20.C). Moreover, L-lactate concentrations were found low(<0.2 g·L^{-1}) over the entire time frame, so that a cytotoxic effect on the cells due to L-lactate accumulation can be excluded. Therefore, the reduction of cell growth after 100 hours is not due to nutrient limitation or lactate accumulation but can be reasonably explained by the fact that the cells reached confluency. In this context, it can be concluded that UC-derived MSCs are contact inhibited.

The proliferation potential of a cell population is often described by the population doubling time. Strictly considered, the population doubling time is calculated under unlimited growth (exponential cell growth), which may correspond here to the growth between 24 and 71 hours. However, most of the published studies performed on MSC report the average population doubling time, i.e. the entire cell growth within a cell passage is considered. In order to compare the proliferation potential of our cells with other investigators, the average population doubling time (T_d) was determined accordingly using five cultures (P4) in T-flasks. T_d was calculated using the initial and final number of cells obtained within one passage from day 0 to day 4 (see Appendices 6.2.10). Thus, the average population doubling time of UC-derived MSC was found to be 31.4 ± 3.5 hours (n = 5). This T_d value indicates a high proliferation potential comparable for instance with the potential of human embryonic stem cells, as T_d values of approx. 24-36 hours have been reported for these cultures[213-215]. According to the calculated T_d, UC-MSC exhibit a higher proliferation potential than adult MSC isolated from other human tissue such as bone marrow or adipose tissue. Thus,

81

population doubling times ranging from 40 hours [216] (using 10% FCS) to 80 hours [212] (using 10% HS) were reported for human bone marrow MSCs and T_d values of approx. 70 hours were found for MSC derived from human fat [125, 217](10% FCS).
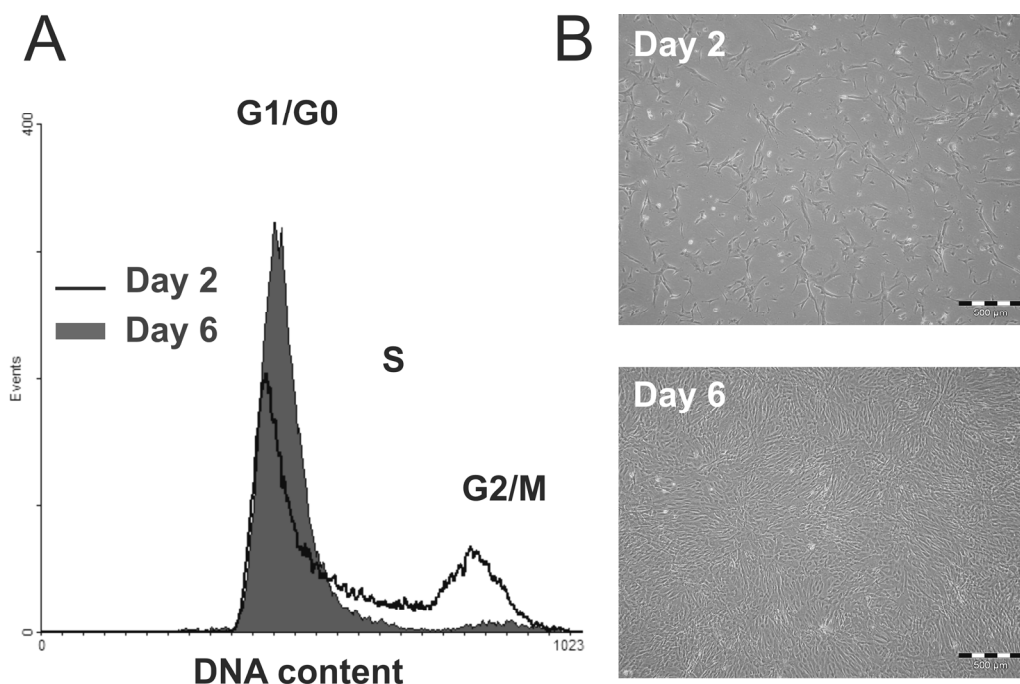
Fig. 4.21: DNA content distribution of proliferating (day 2) and confluent (day 6) UC-MSC cultures. In A: flow cytometric analysis. In B: phase contrast microscopic pictures of the corresponding cultures.

The high proliferation potential demonstrated here underlines the primitive nature of UC-MSC cells. Since UC-MSCs are isolated at birth, the cells exhibit a superior proliferation potential compared to aged cells. This feature should also be critically evaluated, as a high proliferation potential is often associated with a tumour phenotype and may be the result of the transformation of primary to immortalized cells during the isolation procedure. However, two features demonstrated in this study contradict this hypothesis. First, flow cytometric analysis of the DNA content revealed a diploid cell population with a normal distribution in G1/G0, S and G2/M phases (Fig. 4.21). DNA aneuploidy, which in some cases is associated with the appearance of tumor-like cells[218, 219], could not be detected (see Fig. 4.21 and Appendices 6.3.7). Furthermore, the isolated cells demonstrated contact inhibition, which is also a primitive cell characteristic that may be lost during cell transformation [220-222].

Finally, the stability of the cells during expansion was evaluated with regard to the MSC phenotype. Cell size and the expression of the MSC surface markers CD44, CD73, CD90 and

CD105 were monitored by flow cytometry. For this purpose, cells were expanded in T-flasks over several passages in α-MEM supplemented with 10% HS. The cells were passaged when the cultures were evaluated to be 80%–90% confluent by phase contrast microscopy. The experiments were all started with revitalized isolated cells (P0), which were first cultivated over one passage and then plated in T-flasks (P1). The experiments were performed at two different seeding densities 4000 cells/cm² and 500 cells/cm².

The stability of the cell phenotype was investigated over 28 days of cell expansion. Cell size remained stable over the investigated time frame (data not shown), which confirmed the results already presented and discussed in section 4.4.1. In addition, the expression of all MSC markers remained stable regardless of the seeding density, as demonstrated in Fig. 4.22.
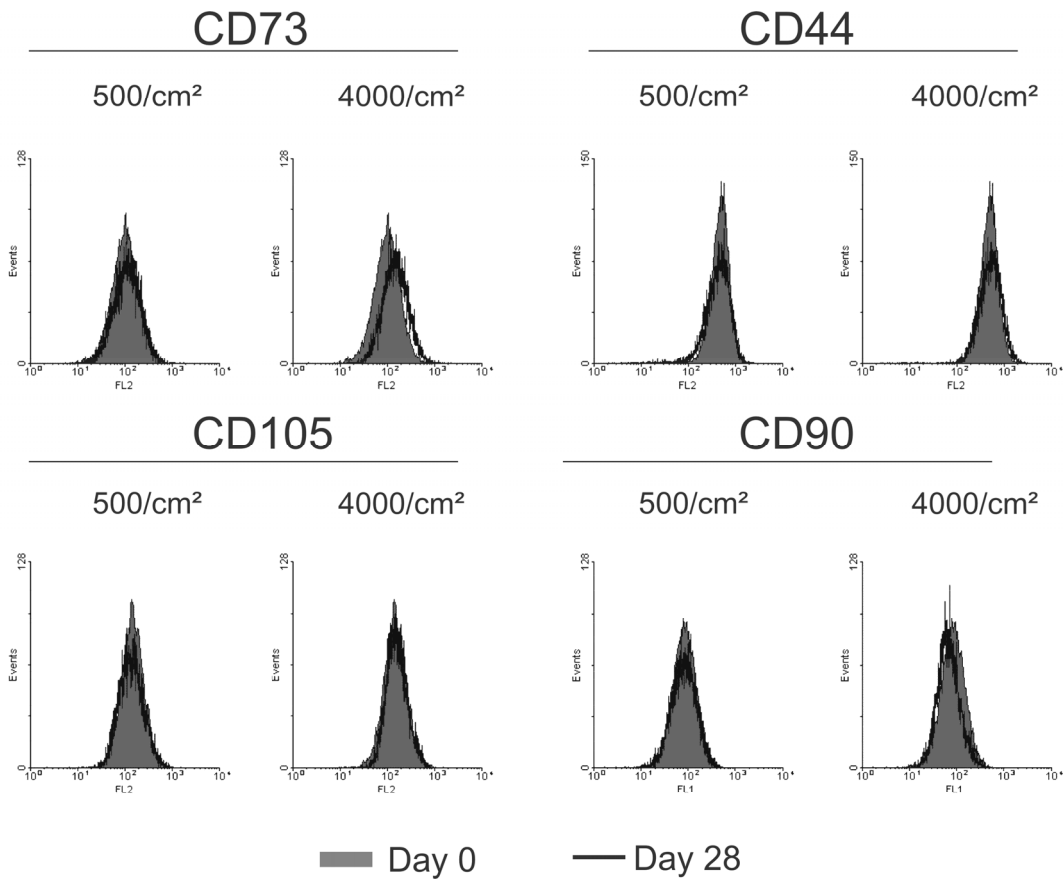
Fig. 4.22: Stability of the immunophenotype of UC-MSC over cell expansion. Cultures were started with cells in P1 (day 0). Day 28 correspond to P8 for the cultures seeded at 4000 cells/cm² and to P5 for the cultures seeded at 500 cells/cm².

Thus, the cells maintained their MSC immunophenotype. The results suggest that no biological alterations occurred during cell expansion. The data obtained during this study demonstrated that UC-MSCs can be expanded at least over 28 days (approx. 18 cell

generations) with a stable phenotype. In addition, the expression of all MSC markers remained stable regardless of the seeding density, as demonstrated in Fig. 4.22. This fact is advantageous, as a low density seeding reduced the number of passages and thus enzymatic treatments required for cell expansion. This may be considered for the development of a large scale expansion procedure.

4.4.3 Conclusion

During this work it was demonstrated that human serum was superior to fetal calf serum for the cultivation of UC-MSCs. The growth and the expansion capacity of the UC-MSCs using HS were characterized. The investigations confirmed the primitive nature of the isolated cell population, as demonstrated by a normal DNA content, contact inhibition, a high proliferation potential with an average population doubling time of approx. 31 hours.

The rapid cell growth combined with a possible expansion without loss of the MSC phenotype at least during 28 days are very advantageous features in terms of cell engineering. A high number of cells may be rapidly obtained for the delivery of clinical doses, thus limiting the duration of the *ex vivo* cultivation and the cellular damages, which may occur during this process.

Clinical cell doses, i.e. the number of cells required for cell therapy, is difficult to estimate and mostly not yet determined. However, available data from clinical studies involving human MSC, which have shown successful results, can be used for a rough estimation of required cell numbers. Thus, bone marrow MSC were transfused into patients and showed positive results for instance for the treatment of graft versus host diseases (GVHD) [223, 224], for hematopoietic recovery [225] or for the treatment of osteogenesis imperfecta [226]. In these studies, MSC doses ranging from $1 - 5 \cdot 10^6$ cells/kg body weight were used. Thus, for a patient weighing 75 kg (average weight in Germany 2005, published by the Gesundheitsberichterstattung des Bundes) cell numbers ranging from $7.5 \cdot 10^7$ to $3.75 \cdot 10^8$ may be required for transfusion. It can be calculated from our data, that starting with a cell population of $7 \cdot 10^5$ cells (number of cells required for the seeding of 175 cm² T-Flask at 4000 cells/cm²), a population of approx. $3.4 \cdot 10^{11}$ cells can be theoretically obtained after 28 days of expansion. This would represent approx. 900 clinical doses ($3.75 \cdot 10^8$ cells/dosis) of highly qualitative MSC.

For some applications, MSCs will have to be induced *in vitro* to differentiated tissue before delivery to a patient. The potential of the cells to differentiate in a particular lineage and the efficiency of the applied procedure will be determining factors in this case. In the frame of this work, the osteogenic potential of the isolated UC-MSCs was studied. The results are presented in the following section.

4.5   Osteogenic potential of UC-derived MSCs

The multi-lineage differentiation potential of UC-MSCs was demonstrated by Tim Hatlapatka. Thus, the isolated cells could be induced *in vitro* into adipogenic and chondrogenic lineages [183]. In this work, the osteogenic potential of UC-derived MSCs was investigated in more detail. An efficient induction into the osteogenic lineage is of high interest, especially in the context of bone tissue engineering applications.

4.5.1   Evaluation of the osteogenic potential of UC-derived MSCs

The osteogenic potential of UC-MSCs was first perceived as very promising, since gene expression analysis of the isolated cell population revealed that non-induced cells spontaneously express typical osteogenic markers, such as the key osteogenic transcription factor RUNX2, alkaline phosphatase (AP), collagen type I (Col I), osteocalcin (OCN) and osteopontin (OPN). These observations are demonstrated in Fig. 4.23.
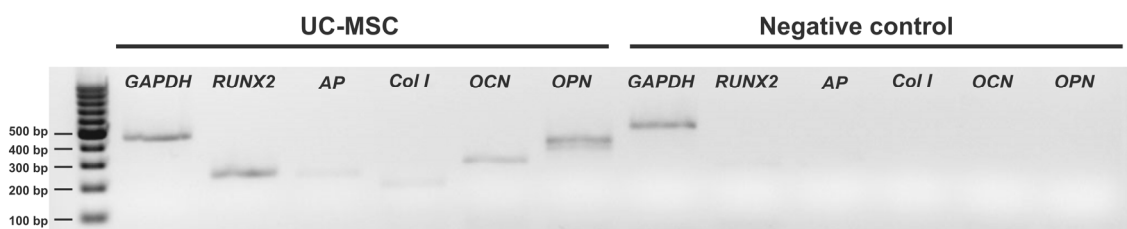
Fig. 4.23: Transcriptional analysis of osteogenic markers of a non-induced UC-MSC population. As a negative control, mRNA from the leukemia cell line Jurkat was used for the RT-PCR analysis.

The reverse transcriptase PCR (RT-PCR) analysis indicates that all cells express a basal level of osteogenic markers, or at least that these genes are expressed by a subset of cells within the population. In addition, the isolated cells spontaneously demonstrated morphological features associated with osteogenic differentiation. Thus, bone nodule-like cell colonies were observed

occasionally in non-induced cultures, suggesting that a subset of cells may differentiate spontaneously. Such bone nodule is presented in Fig. 4.24. A similar phenomenon was already described and extensively characterized by Sarugaser *et al.* for MSCs derived from perivascular tissue of the umbilical cord, and moreover a high osteogenic potential could be demonstrated for these cells in standard differentiation experiments[83].
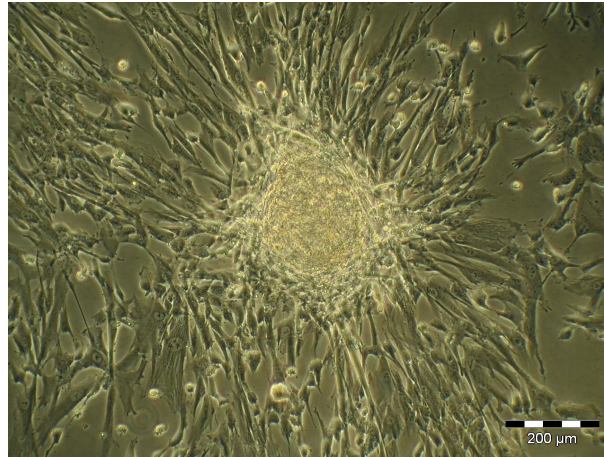
Fig. 4.24: Bone nodule-like cell colony observed by phase microscopy (200 x magnifications) in a non-induced UC-MSC culture (P3).

In vitro differentiation experiments were performed to confirm the osteogenic potential of the UC-derived MSCs. The detailed protocol and differentiation medium are presented in Appendices 6.2.11. Briefly, UC-cells in P1 were induced using the synthetic hormone dexamethasone (100 nM) in the presence of L-Ascorbat-2-Phosphat (0.2 mM) and β-Glycerophosphat (5mM). The cells were seeded at 4000 cells/cm² in 6-well plates and cultivated in osteogenic medium over 28 days. These conditions correspond to standard osteogenic differentiation assays widely described in the literature [80, 83, 84, 136]. Alkaline phosphatase (AP) expression, as well as the ability of the extra cellular matrix to undergo mineralization were investigated to attest the osteogenic phenotype of the induced cultures. Mineralization of the extra cellular matrix was assayed by Von Kossa and Alizarin red S staining (Appendices 6.2.12). The differentiation procedure was validated using MSCs isolated from human adipose tissue (kindly provided by the group of Prof. Martijn van Griensven) as a positive control.

Fig. 4.25 shows typical UC-MSC cultures obtained after 28 days of induction. The positive control cells (MSCs from adipose tissue) could be successfully differentiated, as demonstrated by AP expression (Fig. 4.25.D) and by the mineralization of the extra cellular matrix revealed by Von Kossa staining (black area in Fig. 4.25.E) and by Alizarin red S staining (red area in

Fig. 4.25.F). In contrast, the induction of UC-MSCs to mineralized cultures failed, a major difficulty being the loss of adherence over the differentiation experiment (Fig. 4.25.A – C). UC-MSC cultures reached confluency typically after 4 – 5 days. A considerable extra cellular matrix production was observed in post-confluent cultures. However, this feature was not restricted to osteogenic induced cells, but was generally observed in non-induced UC-MSC cultures. Confluent cultures could be maintained over a maximum of 10 days. After this time period, the cells rapidly detached from the culture vessels and aggregated (Fig. 4.25.A – C).
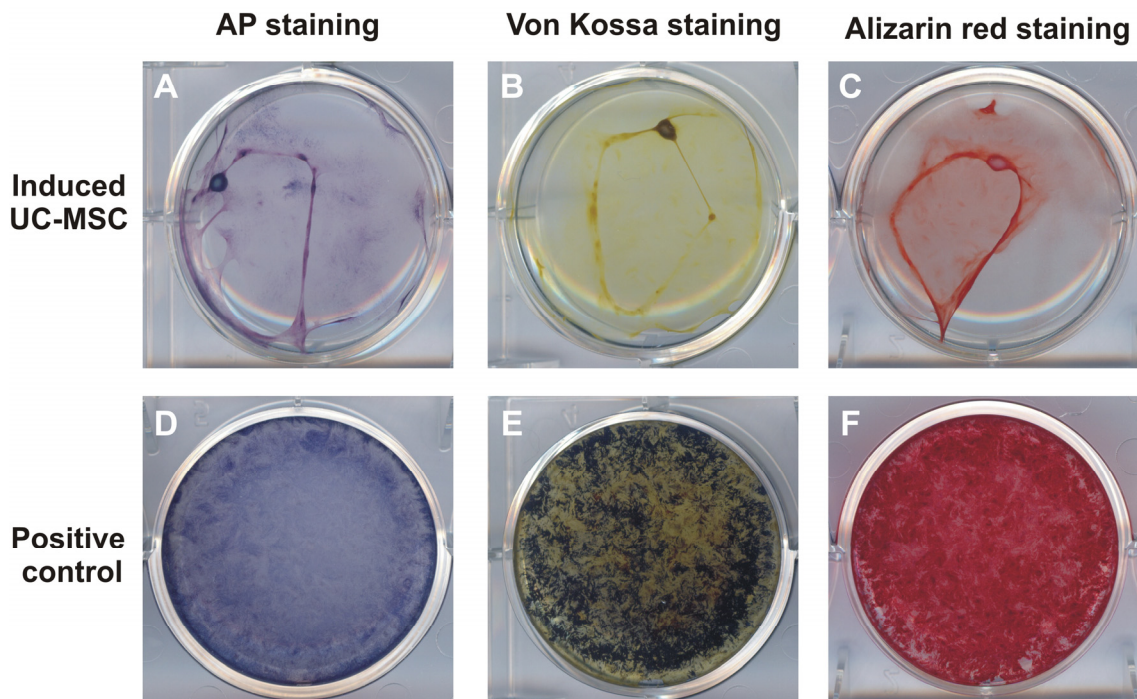
Fig. 4.25: Osteogenic potential of UC-MSCs evaluated by *in vitro* differentiation assay. Alkaline phosphatase (AP) staining as well as mineralization (Von Kossa and Alizarin red S staining) of the post-confluent cultures were assayed after 28 days. At this stage, the cultures were 24 days post-confluent.

Some areas of the UC-MSC cultures showed persisting adherent cell layers after 28 days of induction. However, microscopic observations of these cells did not reveal any biomineralization of the extra cellular matrix as illustrated in Fig. 4.26.A - C.

Phase contrast	Von Kossa staining	Alizarin red staining
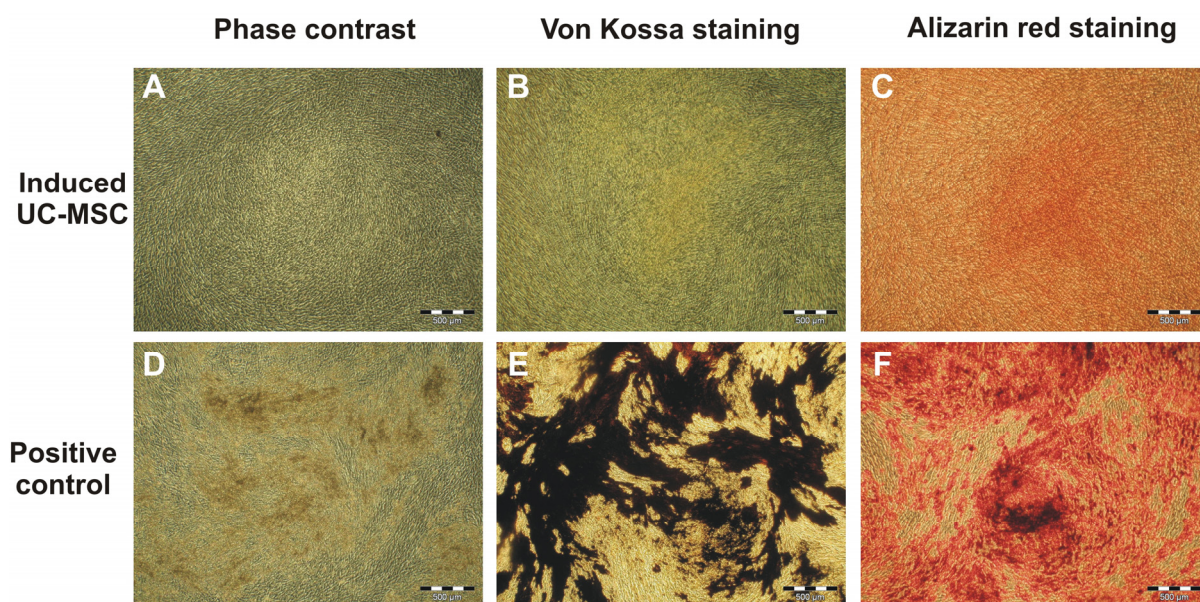
Fig. 4.26: Comparison of the biomineralization of osteogenic induced UC-MSC cultures with a positive control (MSC from human adipose tissue) after 28 days of induction (24 days post-confluent cultures). A, D: phase contrast observation of the culture; B, E: Von Kossa stained cultures; C, F: Alizarin red S stained cultures. (40 x magnification)

Additional differentiation assays were performed using culture vessel surfaces coated with proteins naturally found in the extra cellular matrix. During these experiments, it was hypothesized that a culture surface mimicking the extra cellular matrix would increase cell interaction with the culture vessel and would thus prolong cell adherence. In the frame of this work, Collagen type I coated plates were used, as this collagen is the main constituent of the bone extra cellular matrix [227]. In addition, it was demonstrated in Section 4.2.1 that UC-MSCs express the transmembrane adhesion protein CD44. Specific interaction between CD44 and collagen type I has been reported in the literature [228, 229].

After several differentiation assays, it was observed that cell adherence was not significantly improved by the collagen type I coated surface. Similarly to the experiment performed on non-coated cell surfaces, UC-MSCs detached from the culture surfaces shortly after confluency was reached (data not shown). No mineralization could be detected in the induced cultures.

A functional osteogenic phenotype of UC-MSCs, i.e. mineralizing cultures under osteogenic stimulation, could not be demonstrated during this work. The loss of cell adherence of post-confluent cultures constituted a major problem during the differentiation experiments. Further investigations with coated surfaces should be performed to improve cell adhesion. Other proteins of the extra cellular matrix such as fibronectin or laminin may lead to better results in this respect.

A statement about the osteogenic potential of the isolated UC-MSCs using standard differentiation procedures was problematic to achieve, mainly because of the difficulty in maintaining a post-confluent monolayer. In this context, the response of UC-MSCs to the osteogenic stimulus was investigated in sub-confluent cultures. In particular, flow cytometry was used to monitor cell response on the single cell level to elucidate whether all or a fraction of UC-MSCs respond to osteogenic conditions.

4.5.2 Monitoring of cell response to osteogenic induction in sub-confluent cultures

During this experiment, UC-MSCs were maintained under osteogenic conditions and passaged before cell confluency was attained. The cellular response to the osteogenic stimulation was first evaluated with regard to the expression of specific surface proteins. It was demonstrated in Section 4.2.1 that undifferentiated UC-MSCs express the marker CD44, CD73, CD90, and CD105. It was hypothesized that the expression of these specific surface antigens may be modulated during osteogenic cell differentiation. This hypothesis seemed reasonable, as some of these markers are used to monitor the differentiation or maturation of other cell types. For instance, CD73 and CD90 are used to monitor the differentiation state of cells in the T-lymphocyte lineage [230-232]. In the particular case of human MSCs, some reports described a reduced expression of CD73 and CD105 for adipogenic and osteogenic differentiated bone marrow MSCs [233]. Also a loss of CD90 expression was reported on a subset of bone marrow MSCs under angiogenic stimuli[234]. More recently, a down regulation of CD105 associated with multi lineage differentiation was also described for MSCs isolated from umbilical cord blood [235].

Surface protein expression was quantitatively monitored using flow cytometry. UC-MSCs were maintained in osteogenic medium (see Appendices 6.1.9) for 28 days and successively passaged. In parallel, cells were cultivated in culture medium (α-MEM containing 10% HS) as a control.

UC-MSCs cultivated under osteogenic conditions did not significantly modulate the expression of the surface markers CD44 and CD105 compared to the control conditions (see Appendices 6.3.8). In contrast, the expression of the surface protein CD90 was definitely influenced by the osteogenic medium. A reduced amount of the CD73 antigen was also

measured under osteogenic conditions (see Section 6.3.8), however to a lesser extend than CD90. Fig. 4.27 illustrates the results assayed by multicolor flow cytometry measuring simultaneously CD90 and CD73.
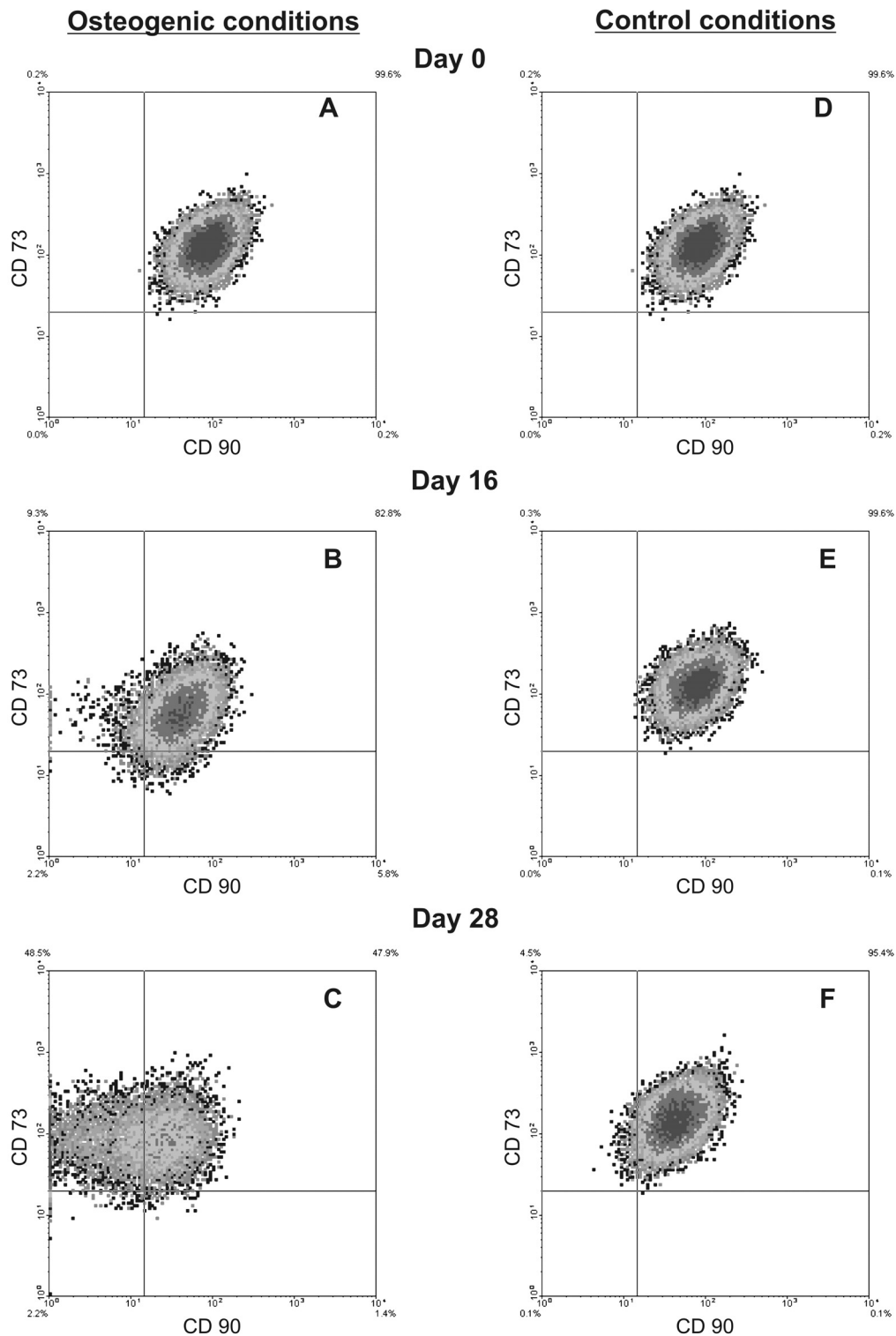
Fig. 4.27: CD90 expression under osteogenic (left) and control conditions (right). UC-MSCs were maintained in sub-confluent cultures. CD90 and CD73 expression was assayed using a FITC- and PE-labeled monoclonal antibody respectively. At least 10 000 events are displayed.

Under osteogenic conditions a subset of UC-MSCs gradually lost CD90 surface expression. This sub-population was evaluated to be 11% after 16 days of induction (in Fig. 4.27.B). After 28 days of osteogenic stimulation, the fraction of CD90⁻ cells was found to be approx. 50% (in Fig. 4.27.C). This phenomenon was not observed in the control cultures (in Fig. 4.27.D-F). In addition, the multicolor flow cytometric experiment permitted the demonstration that the subset of CD90⁻ cells maintained the CD73 expression (in Fig. 4.27.C).

Interestingly, the rising of CD90 negative cells within the population coincided with an overall decrease of cell growth in the osteogenic culture compared to the control culture. This fact is illustrated in Fig. 4.27. The percentages of CD90⁻ cells in the control and osteogenic cultures are plotted against time. Cell growth is given by the cumulative number of population doublings assayed at every cell passage. After 16 days, osteogenic stimulated cells exhibited significantly lower proliferation than the control culture. The proliferation diminished further with increasing numbers of CD90⁻ cells over the last 12 days of the experiment.
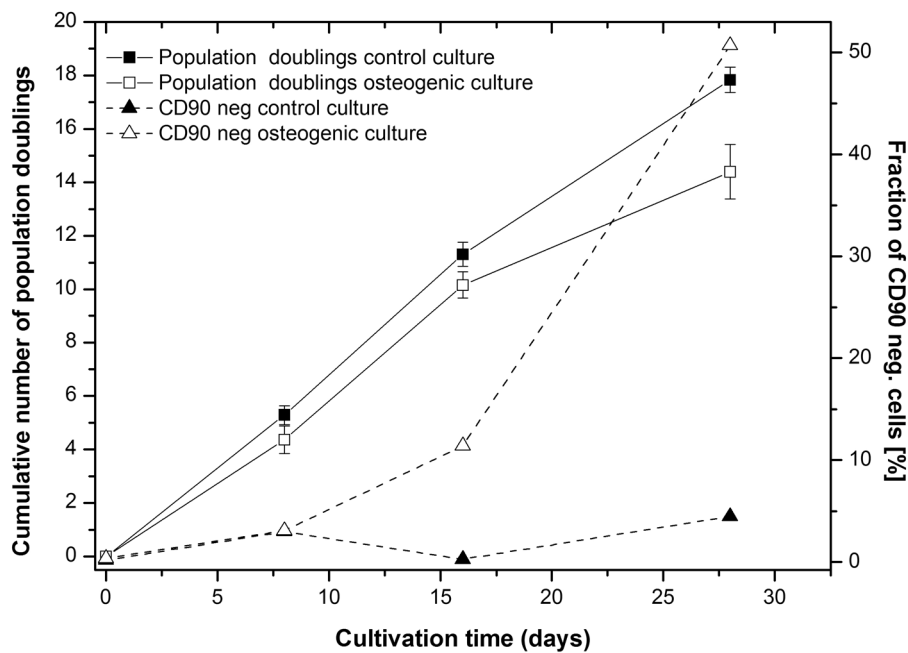
Fig. 4.28: CD90 expression and proliferation of UC-MSC cultures under osteogenic and control conditions.

A decrease of proliferation is a cellular feature of cell differentiation. It is generally acknowledged that differentiating MSCs progress through several maturation stages, characterized by a reduction of proliferation accompanied by a down-regulation of some cellular proteins to the benefit of tissue-specific markers [76, 236]. The experiment demonstrated that a subset of cells loses CD90 expression under osteogenic conditions, which coincides with

a decrease of proliferation. Consequently, the overall decrease of cell growth over the 28 days of induction may be reasonably explained by the accumulation of low proliferating CD90⁻ cells. As this phenomenon was not observed in the control culture, the decrease of CD90 expression was hypothesized to be an osteogenic feature. In order to verify this hypothesis, the subset of CD90⁻ cells was isolated and further characterized.

Flow cytometric cell sorting and characterization of the CD90⁻ cell population

The selection of the CD90⁻ sub-population was performed using flow cytometric cell sorting (termed in the following as FACS). After 22 days of osteogenic induction in sub-confluent cultures, UC-MSCs were harvested, stained for CD90 expression and finally sorted. A detailed procedure is presented in appendices 6.2.14. Following cell sorting, the cells were collected and mRNA isolation was performed (see 6.2.15). Expression of the osteogenic markers RUNX2, alkaline phosphatase (AP), osteocalcin (OCN) and osteopontin (OPN) was investigated on the transcriptional level via RT-PCR. A fraction of the sorted cells was further cultivated for another 4 days and stained for AP expression.

Fig. 4.29 shows the populations isolated by FACS. Re-analysis of the sorted fractions confirmed the success of the procedure. A purity superior to 99% for each fraction was obtained.
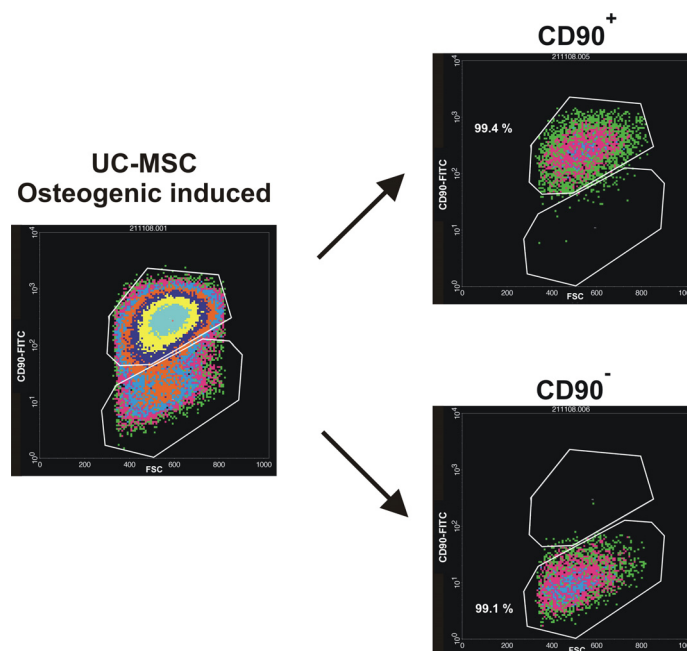
Fig. 4.29: Flow cytometric cell sorting of CD90⁻ and CD90⁺ cells from a UC-MSC culture maintained under osteogenic conditions in sub-confluent cultures (day 22).

The expression of the osteogenic markers by CD90⁻ cells was compared to the marker expression of the CD90⁺ cells. For this purpose, the transcription of each gene was analyzed by RT-PCR, quantified using densitometry and normalized on the expression level of the house keeping gene *GAPDH* (see 6.2.15). This approach allows a semi quantitative comparison of the osteogenic marker expression of the two populations.

Fig. 4.30 presents the results of the analysis. Interestingly, both populations expressed the osteogenic markers. However, a higher expression of all investigated genes was measured in the CD90⁻ cell population compared to CD90⁺ cells.
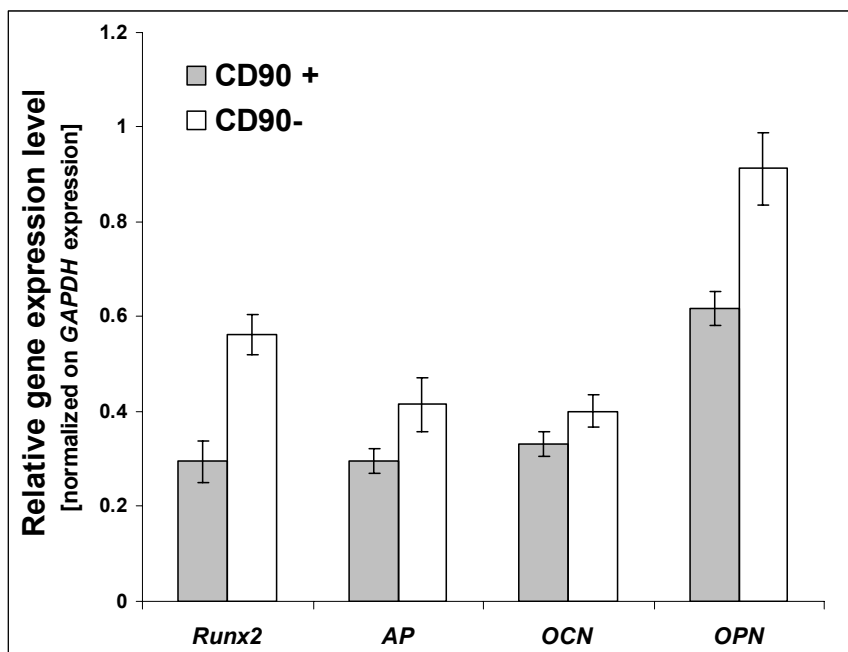
Fig. 4.30: Transcription level of osteogenic markers measured in the CD90⁻ and CD90⁺ cell populations. *Runx2*: transcription factor RUNX2. *AP*: alkaline phosphatase; *OCN*: osteocalcin; *OPN*: osteopontin. The expression level of each gene was quantified by densitometry on agarose gel and normalized on the *GAPDH* expression of each population (n=3).

In addition, AP staining of the sorted cultures revealed that numerous CD90⁻ cells indeed exhibited AP activity, confirming thus the expression of this marker on the functional level. This fact is illustrated in Fig. 4.31.A-B. In contrast, very few AP expressing cells could be observed in the CD90⁺ cultures (Fig. 4.31.C-D).
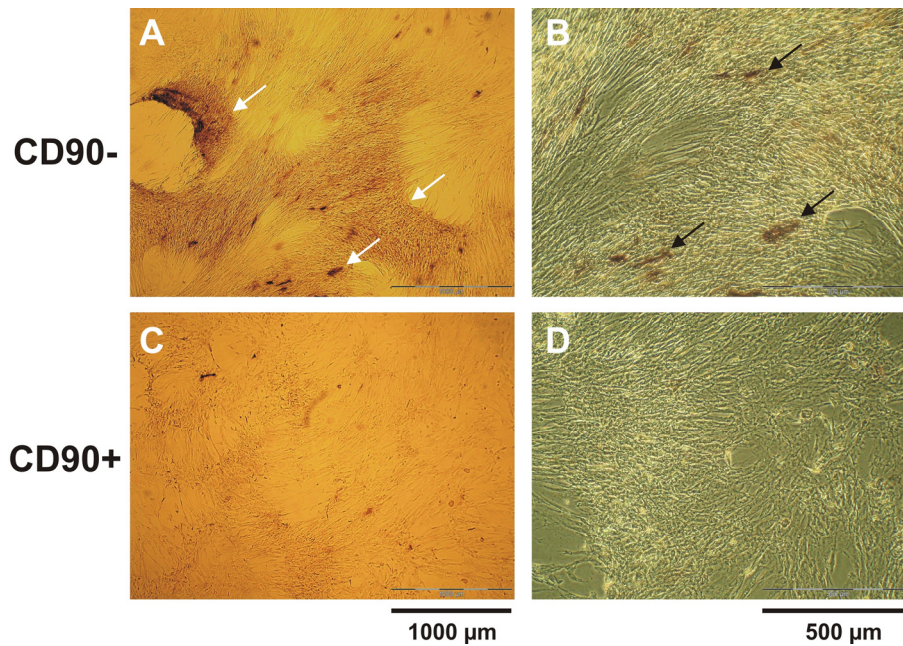
Fig. 4.31: Alkaline phosphatase staining of sorted CD90⁻ and CD90⁺ cells (22 days of osteogenic induction, 4 days after sorting). A and C: bright field pictures (40 x magnification; the pictures represent approx. 10% of the total culture surface), white arrows indicate AP positive area of the culture, B and D: phase contrast pictures (100 x magnification), black arrows indicate AP positive cells.

The experiment showed that $CD90^-$ cells expressed a higher level of osteogenic marker transcripts than $CD90^+$ cells. AP expression could be observed on the functional level, as some cells in culture exhibited AP activity. The results suggest that the subset of $CD90^-$ cells is in a more advanced state of differentiation than $CD90^+$ cells and support the hypothesis that the observed decrease of CD90 expression is an osteogenic feature. This interesting phenomenon deserves further investigations. For instance, a confirmation of the transcriptional analysis using quantitative RT-PCR as well as the detection of the osteogenic marker expression on the protein level, using immunocytochemistry for example, would resolutely confirm the hypothesis.

The induction of UC-MSCs in sub-confluent cultures revealed that the cells respond to the osteogenic stimulation by a reduced proliferation and a down regulation of the surface antigen CD90. Using flow cytometry, the fraction of induced cells in the culture could be monitored. In the performed experiment, approx. 50 % of differentiating cells were measured after 28 days of induction.

The function of CD90 and its regulation among the osteogenic lineage has not been clarified yet. However, an early report from Chen *et al.* in 1999 describes the CD90 expression by

osteoblastic cell lines from several species[237]. According to this study, early osteoblast progenitors lack the CD90 expression but in contrast late progenitors and mature osteoblasts express the antigen. Consequently, the results of Chen *et al.* suggest that the loss of CD90 is a transition state of cells maturating among the osteogenic lineage. This hypothesis was evaluated in the context of UC-MSCs, where the decrease of CD90 expression may indicate the transition of undifferentiated MSC into early osteogenic committed progenitors.

Regulation of CD90 expression over long-term osteogenic induction

During this experiment the cell response was observed over 40 days of osteogenic stimulation. In addition, CD90 expression was measured in relation to the expression of the osteogenic markers AP and the transcription factor RUNX2 on the protein level. In particular, RUNX2 expression was of high interest, as the expression of this transcription factor is a key element of osteogenesis, triggering the transcription of osteoblast-specific genes and inducing mineralization in cultures [238-240]

In this experiment, AP expression was monitored by performing staining of the cultures and by determination of the specific enzyme activity of the cells (see 6.2.13). Nuclear content of Runx2 was assayed by flow cytometry using an intra cellular staining procedure. For this purpose, a primary mouse antibody specific for the human protein RUNX2 and a secondary PE-labeled anti-mouse antibody were used (see 6.2.7).

Fig. 4.32 presents the obtained results. The fraction of CD90$^-$ cells over the entire cultivation time is presented in comparison to cell proliferation (in A), to the specific AP activity of the cell population (in B) and to Runx2 expression (in C). The results obtained for the control culture (non-induced UC-MSCs cultivated in parallel) are also displayed.

During this experiment a rapid decrease of CD90 surface expression was observed under osteogenic condition after 7 days (22 % CD90$^-$ cells), reaching approx. 33% after 22 days of induction (Fig. 4.32.A). Also, a significant decrease of proliferation was measured after 14 days (Fig. 4.32.A), confirming the results previously described. However, after 22 days of induction the fraction of CD90$^-$ cells decreases, so that only 16% CD90$^-$ cells were detected at the end of the experiment (40 days). The results are highly interesting and are in line with the hypothesis that CD90 down-regulation is a transitional state of differentiation.
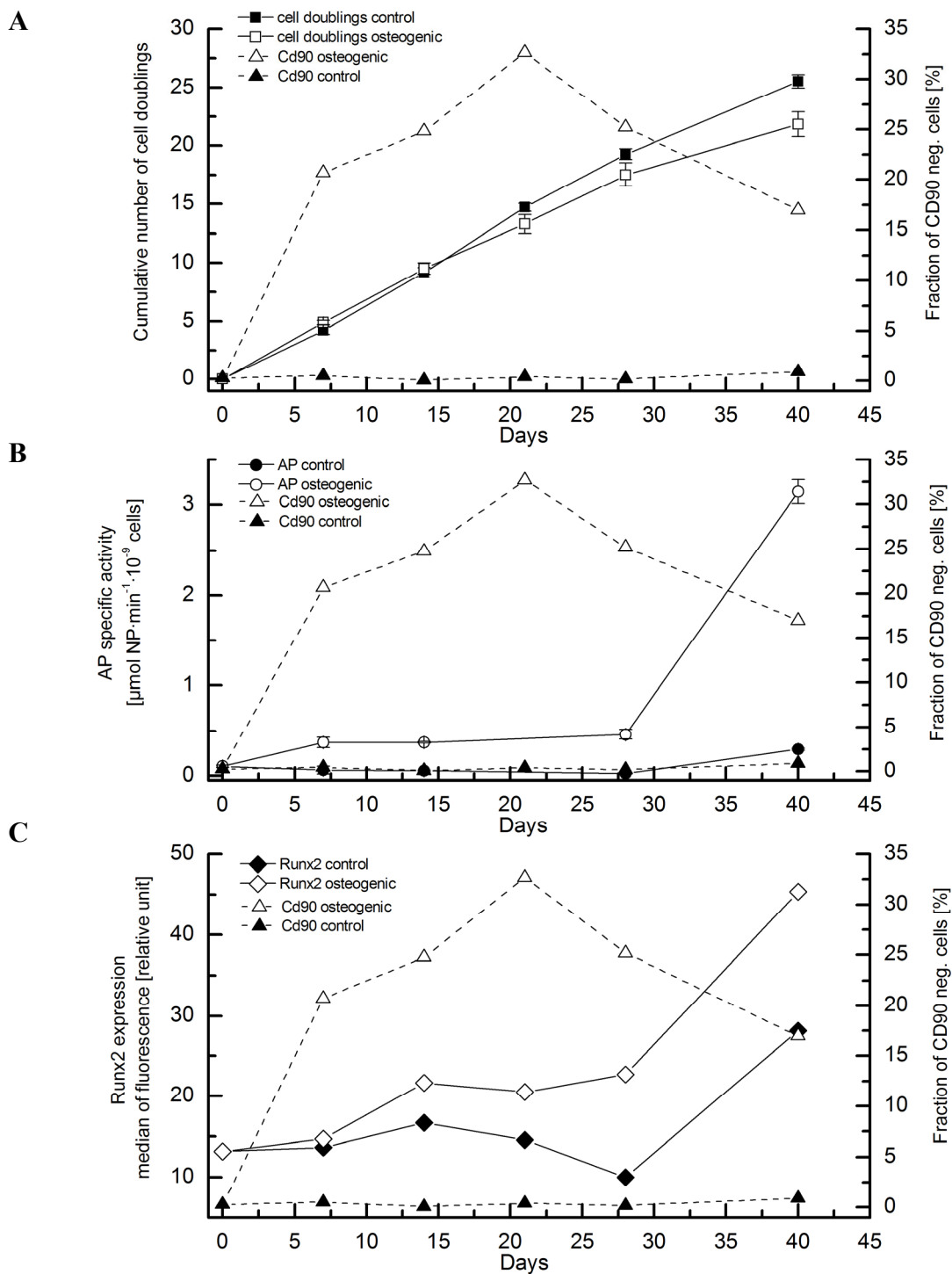
Fig. 4.32: CD90 expression of UC-MSCs during long-term osteogenic induction. In A: CD90 expression and cell growth; in B: CD90 expression and AP specific activity; in C: CD90 expression and RUNX2 intracellular content.

Interestingly, induced UC-MSCs exhibited a significantly higher AP specific activity compared to the control culture over the entire time frame (Fig. 4.32.B). The specific activity increased during the first 7 days of induction and remained nearly constant until 28 days. Staining of the cultures confirmed the presence of AP expressing cells among the population

(Fig. 4.33.A and B). Over the last 12 days of the experiment, induced UC-MSCs markedly enhanced their AP expression as demonstrated by the measured specific enzyme activity (Fig. 4.32.B) and the AP-staining of the culture on day 40 (Fig. 4.33.C). A slight increase in AP expression was also measured in the control culture during this time (Fig. 4.32.B).
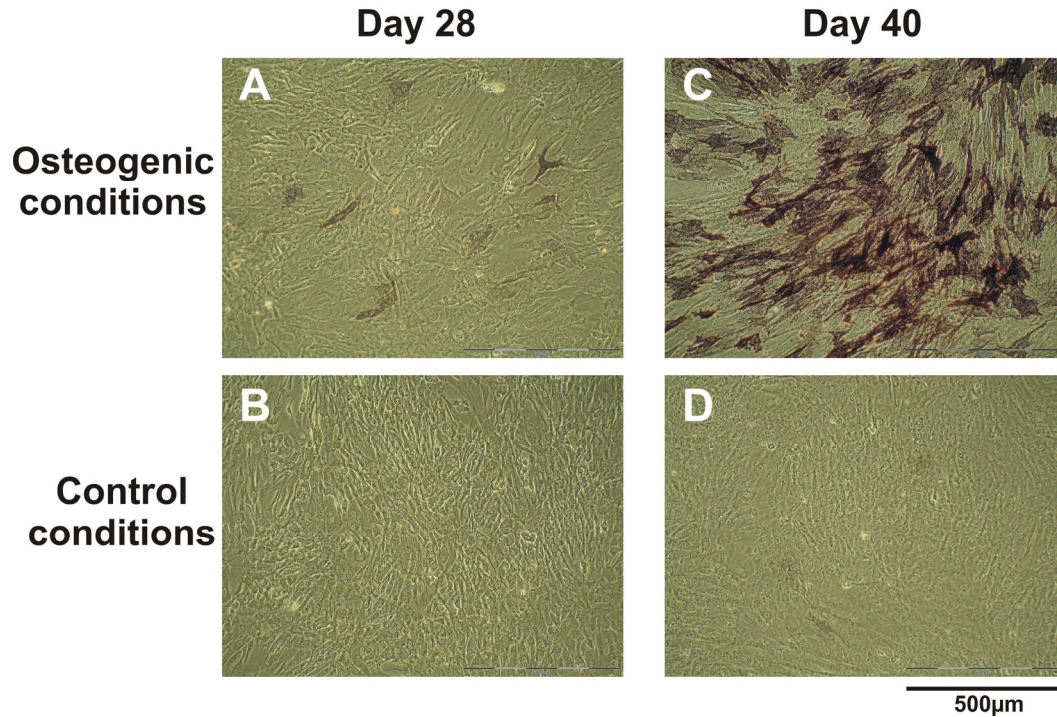
Fig. 4.33: AP expression of osteogenic induced and control cultures (100 x magnification).

Flow cytometric analysis of the RUNX2 cellular content did not reveal a clear sub-population of UC-MSCs expressing the osteogenic transcription factor, but indicated an overall increase of the intracellular content during osteogenic induction. This fact is illustrated in Fig. 4.34. The intracellular RUNX2 distribution of induced UC-MSC is presented at day 0, day 28 and day 40 of the experiment. A shift of intracellular fluorescence indicating an increase of RUNX2 expression could be observed during osteogenic induction. This enhanced expression was quantified using the median of the fluorescence distribution (see Fig. 4.34) and plotted against time in Fig. 4.32.C. The measured medians for the UC-MSCs in control conditions are also displayed.
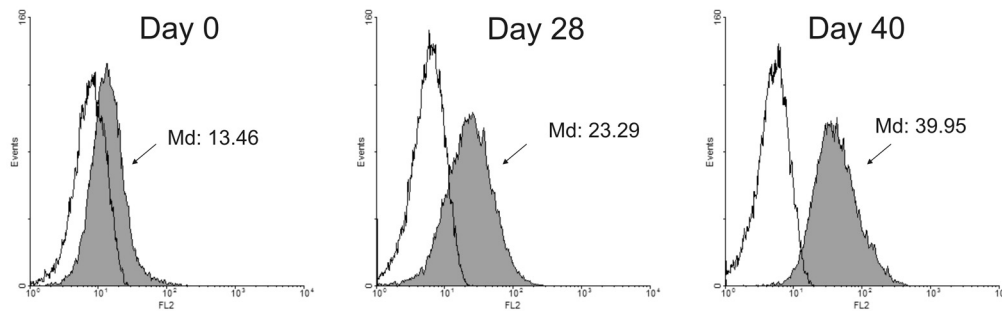
Fig. 4.34: Intracellular RUNX2 content of osteogenic induced UC-MSCs assayed by flow cytometry (filled histogram). Specificity of the staining procedure is demonstrated by the staining of the cells using solely the secondary PE-labeled antibody (unfilled histogram).

Induced UC-MSCs exhibited a significantly higher intracellular RUNX2 content than non-induced cells over the entire differentiation experiment. Interestingly, the time course of RUNX2 expression was found similar to the measured specific AP activity of the cells. Thus, the expression increased during the first 14 days of induction and remained nearly constant until 28 days. During the last 12 days of osteogenic stimulation, the intracellular content raised in parallel to the specific AP activity. However, during this time frame the control culture exhibited also an increased RUNX2 expression, suggesting that the long-term cultivation of the cells may also influence the expression of the transcription factor.

The results of the experiments performed here confirmed the CD90 down-regulation and a decreased cell proliferation in response to the osteogenic conditions. The rapid appearance of CD90$^-$ cells in the cultures during the first 14 days of the experiments may explain the slight increased of AP and RUNX2 expression, as a higher AP and RUNX2 expression was observed on the transcriptional level in sorted CD90$^-$ compared to CD90$^+$ cells. However, the loss of CD90 expression does not seem to be an end point of the differentiation, as after 21 days of induction the fraction of CD90$^-$ cells diminished in culture. The data suggest that the loss of CD90$^-$ cells is a transition step among the osteogenic lineage. This hypothesis is supported by the tremendous increase of AP and RUNX2 expression occurring once the fraction of CD90$^-$ cells decreases after 28 days of induction, suggesting that a new maturation stage is attained.

The experiment raises the question of the function and the role of CD90 during the osteogenic differentiation. CD90 down regulation, together with a reduced proliferation, were the first cellular features observed during the osteogenic induction. Because our experiments were

performed in sub-confluent cultures, some late osteogenic features such as extracellular matrix protein production and matrix maturation are not triggered. In this context, the observed CD90 down regulation may be proposed as an early osteogenic marker.

The results are in line with the work of Chen *et al.* reporting that skeletal osteogenic progenitors lack the expression of CD90, but in contrast the antigen was measured on cells representing more advanced stages of the osteogenic lineage (late precursors and mature osteoblasts)[237]. Thus, we postulate here that undifferentiated UC-MSCs exhibiting CD90 expression may first differentiate to early osteogenic committed progenitors loosing CD90 expression. With a further progression among the osteogenic lineage the expression of the surface antigen may be up-regulated anew, which would explain the diminution of CD90⁻ cells after 21 days of induction. The reduction of the CD90⁻ fraction in the culture seems to coincide with the increase of AP and RUNX2 expression observed during the last 12 days of the induction. This phenomenon can be explained by the accumulation of cells expressing CD90, RUNX2 and AP, which may correspond to the phenotype of late osteogenic precursor or osteoblast-like cells.

4.5.3 Conclusion

During this work, the differentiation of UC-MSCs into functional osteoblasts could not be demonstrated in post-confluent cultures *in vitro*. Post-confluent cultures could not be maintained and mineral deposits in the extra cellular matrix of UC-MSCs were not observed.

However, in sub-confluent cultures a response to the osteogenic stimulation illustrated by a reduced cell proliferation and by a CD90 down-regulation could be observed. Evidence was provided that the observed CD90 loss of expression is an osteogenesis-associated feature. In addition, the CD90 down regulation was found to be a transition state leading, after 40 days of induction, to a cell population predominantly expressing the osteogenic transcription factor RUNX2 and the enzyme alkaline phosphatase. These experiments demonstrated that the cells can be at least induced into the osteogenic lineage. It is however uncertain which degree of maturation was attained during the sub-confluent culture experiments. The capacity of these cells to form mineralized extra cellular matrix in post-confluent cultures remains to be attested.

From a technological point of view the time frame necessary to obtain an osteogenic response from UC-MSC should be critically discussed. Giving credit to the fact that after 40 days of sub-confluent induction cells exhibiting a phenotype similar to osteoblasts (CD90^{+}; AP^{+} and RUNX^{+}) are obtained, the differentiation time necessary to induce these cells is rather long. Long-term differentiation experiments may increase the risk of epigenetic damages of the cells and may be a major limitation in terms of cell engineering. In this context, other approaches should also be investigated for a more rapid induction of UC-MSC into the osteogenic lineage. The use of specific cytokines such as bone morphogenic proteins (BMPs), mechanical strain or specific scaffolds using 3D cultivation systems, which have been successfully applied for the differentiation of MSCs from other sources [182], may be more efficient in this regard.

The results of this study suggest a rather limited osteogenic potential for the isolated UC-MSCs, at least using standard differentiation conditions. This finding is not in line with numerous published reports. The osteogenic potential of MSC isolated from human umbilical cord tissue has been reported in several studies (reviewed in Section 2.2). However, a growing body of evidence suggests that the differentiation potential of UC-derived MSCs depends on their location in the UC-tissues. For instance Suzdal'tseva *et al.* reported that only a few cells isolated from the cord vein subendothelial tissue were able to differentiate to osteoblasts [136]. In contrast, cells isolated from perivascular tissues of the umbilical vein showed a high osteogenic potential with spontaneous formation of bone nodules [83], which was evaluated even higher than the potential of bone marrow MSCs in a comparative study [90]. Ishige *et al.* compared in a recent study the osteogenic potential of MSCs isolated from the umbilical vein, arteries and from the connective tissue surrounding the blood vessels (Wharton's jelly) and found a low potential for Wharton's jelly cells[241]. The hypothesis of a location-dependent differentiation potential of UC-derived stromal cells is also supported by the fact that a gradient of cell maturity was observed within the UC tissues [242]. According to the cytoskeletal complexity, the most immature cells are located in subamniotic and intervascular regions, whereas cells of perivascular regions may represent a more differentiated state [242, 243]. Thus, MSC derived from the perivascular tissue of the umbilical cord may be more committed to osteogenic differentiation, while Wharton's jelly or subamniotic cells would be more primitive and not yet committed to osteogenic differentiation.

The cells investigated in this work are isolated from the whole umbilical cord (see 4.1) and may be issued from every compartment of the cord. A high proportion of Wharton's jelly cells may explain the low osteogenic potential of the isolated cells and the extended induction time necessary to observe an osteogenic phenotype. On the other hand, a subset of perivascular UC-MSC may explain the osteogenic features spontaneously observed in cultures, such as the formation of bone nodule-like colonies (see 4.5.1).

4.6   Summary and perspectives

In this work, a reproducible and efficient procedure for the isolation of MSC from human umbilical cord tissue under xeno-free conditions was described. It was demonstrated that a large number of cells ($> 21 \cdot 10^6$ cells in the presented experimental set up) exhibiting a homogenous MSC phenotype could be isolated using a simple explant approach. The umbilical cord could be easily processed *ex vivo* and the development of controlled conditions for the isolation, i.e. GMP procedure, is conceivable. The overall procedure was performed within maximum three weeks. The use of specific chemokines, such as HGF or SDF-1, may allow accelerating the migration of MSCs out of the tissue and thus reduce the duration of the isolation procedure. The isolation under xeno-free conditions, i.e. using HS, may have an impact on the phenotype of the isolated cells, as for instance no expression of some HLA-I antigens could be measured. The lack of HLA-I antigens expression suggested immuno-privileged properties for the isolated cells, which may be highly interesting in the context of allogenic transplantation. Experiments using UC-MSCs in co-culture with human peripheral blood cells, may confirm this hypothesis.

The isolated cells exhibited a high proliferation potential under xeno-free conditions using HS. This feature is particularly interesting in terms of cell engineering. Compared to MSCs derived from other sources, clinical doses could be obtained more rapidly from UC-MSCs. Thus, no prolonged expansion will be required, thereby reducing the risk of possible damages occurring during the *ex vivo* expansion process. The generation of clinical grade MSCs will most likely be performed in disposable reactors. The monitoring of the cultures will be essential for controlling cell quality and the development of adequate *in-situ* sensors for the monitoring of the cultures will be of great interest [244]. In this work, it was demonstrated that

morphological features of UC-MSCs such as cell size or nucleus to cytoplasm ratios indicate cell aging in cultures. The use of this parameter for the non-invasive monitoring of the expansion process could be conceivable.

In the context of the delivery of undifferentiated MSC to a patient, an increasing number of publications indicate that transplanted MSC may not differentiate *in vivo*, but more likely migrate to the defect tissues and induce repair by so called parakrine effects, i.e. the cells express a pool of cytokines that stimulate the repair of the damaged tissue [85, 101, 151-153]. Thus, it may be of high interest to analyze the profile of cytokines expressed by the isolated UC-MSCs. Flow cytometric bead-based technologies are now available for the analysis of multiple soluble analytes such as cytokines [245, 246]. These so-called multiplex assays may be advantageous to specify the cytokine expression profile of UC-MSCs before the delivery to a patient.

Eventually, in the perspective of tissue engineering applications, the osteogenic potential of the cells was evaluated in differentiation experiments. The isolated cells could not be induced to a functional osteogenic phenotype, but responded at least to osteogenic stimulation, as illustrated by a reduced proliferation, by a down-regulation of the surface antigen CD90 and by the expression of typical cellular osteogenic markers such as AP and RUNX2. These results contrasted with several reports claiming a high osteogenic potential for UC-MSCs, in particular for cells derived from the perivascular tissue. However, a growing body of evidences suggests that the differentiation potential of the isolated MSC populations is dependent on their location in the UC-tissues. In this context, the question should be addressed, whether the applied isolation procedure is efficient for the isolation of osteogenic committed cell populations. The extended time frame necessary to obtain an osteogenic response suggests that the UC-MSCs isolated under the described conditions may have a limited potential for bone tissue engineering. Nevertheless, approaches involving the use of newly developed scaffolds, mechanical strain or 3D bioreactors for osteogenic tissue generation, which were successfully applied with MSCs from other sources [182], should be investigated for a more rapid osteogenic induction of the isolated cells.

Finally, it should be noted, that the differentiation of the cells to functional adipocytes and chondrocytes could be demonstrated by co-workers. Therefore, the isolated UC-MSC may be more committed for these differentiation lineages.

5 References

1. Bach, F.H., Albertini, R.J., Joo, P., Anderson, J.L. & Bortin, M.M. Bone-marrow transplantation in a patient with the Wiskott-Aldrich syndrome. *Lancet* **2**, 1364-1366 (1968).

2. Gatti, R.A., Meuwissen, H.J., Allen, H.D., Hong, R. & Good, R.A. Immunological reconstitution of sex-linked lymphopenic immunological deficiency. *Lancet* **2**, 1366-1369 (1968).

3. Thomson, J.A. et al. Embryonic stem cell lines derived from human blastocysts. *Science* **282**, 1145-1147 (1998).

4. Poulsom, R., Alison, M.R., Forbes, S.J. & Wright, N.A. Adult stem cell plasticity. *J Pathol* **197**, 441-456 (2002).

5. Zhang, C.C. et al. Angiopoietin-like proteins stimulate ex vivo expansion of hematopoietic stem cells. *Nat Med* **12**, 240-245 (2006).

6. Smith, A.G. et al. Inhibition of Pluripotential Embryonic Stem-Cell Differentiation by Purified Polypeptides. *Nature* **336**, 688-690 (1988).

7. Ying, Q.L., Nichols, J., Chambers, I. & Smith, A. BMP induction of Id proteins suppresses differentiation and sustains embryonic stem cell self-renewal in collaboration with STAT3. *Cell* **115**, 281-292 (2003).

8. Richards, S., Leavesley, D., Topping, G. & Upton, Z. Development of defined media for the serum-free expansion of primary keratinocytes and human embryonic stem cells. *Tissue Eng Pt C-Meth* **14**, 221-232 (2008).

9. Xu, C.H. et al. Basic fibroblast growth factor supports undifferentiated human embryonic stem cell growth without conditioned medium. *Stem Cells* **23**, 315-323 (2005).

10. Amit, M., Shariki, C., Margulets, V. & Itskovitz-Eldor, J. Feeder layer- and serum-free culture of human embryonic stem cells. *Biol Reprod* **70**, 837-845 (2004).

11. Xu, C.H. et al. Feeder-free growth of undifferentiated human embryonic stem cells. *Nature Biotechnology* **19**, 971-974 (2001).

12. Amit, M. Feeder-layer free culture system for human embryonic stem cells. *Methods Mol Biol* **407**, 11-20 (2007).

13. Parson, A.B. Stem cell biotech: seeking a piece of the action. *Cell* **132**, 511-513 (2008).

14. Takahashi, K. et al. Induction of pluripotent stem cells from adult human fibroblasts by defined factors. *Cell* **131**, 861-872 (2007).

15. Niebruegge, S. et al. Cardiomyocyte Production in Mass Suspension Culture: Embryonic Stem Cells as a Source for Great Amounts of Functional Cardiomyocytes. *Tissue Engineering Part A* **14**, 1591-1601 (2008).

16. Schroeder, M. et al. Differentiation and lineage selection of mouse embryonic stem cells in a stirred bench scale bioreactor with automated process control. *Biotechnology and Bioengineering* **92**, 920-933 (2005).

17. Friedenstein, A.J., Chailakhjan, R.K. & Lalykina, K.S. The development of fibroblast colonies in monolayer cultures of guinea-pig bone marrow and spleen cells. *Cell Tissue Kinet* **3**, 393-403 (1970).

18. Bajada, S., Mazakova, I., Richardson, J.B. & Ashammakhi, N. Updates on stem cells and their applications in regenerative medicine. *J Tissue Eng Regen Med* **2**, 169-183 (2008).

19. Castro-Malaspina, H. et al. Characterization of human bone marrow fibroblast colony-forming cells (CFU-F) and their progeny. *Blood* **56**, 289-301 (1980).

20. Kogler, G. et al. A new human somatic stem cell from placental cord blood with intrinsic pluripotent differentiation potential. *J Exp Med* **200**, 123-135 (2004).

References

21.   Sensebe, L. Clinical grade production of mesenchymal stem cells. *Biomed Mater Eng* **18**, S3-10 (2008).

22.   Bieback, K., Kern, S., Kluter, H. & Eichler, H. Critical parameters for the isolation of mesenchymal stem cells from umbilical cord blood. *Stem Cells* **22**, 625-634 (2004).

23.   Wexler, S.A. et al. Adult bone marrow is a rich source of human mesenchymal 'stem' cells but umbilical cord and mobilized adult blood are not. *Br J Haematol* **121**, 368-374 (2003).

24.   Baldi, L., Hacker, D.L., Adam, M. & Wurm, F.M. Recombinant protein production by large-scale transient gene expression in mammalian cells: state of the art and future perspectives. *Biotechnology Letters* **29**, 677-684 (2007).

25.   Piechaczek, C., Fetzer, C., Baiker, A., Bode, J. & Lipps, H.J. A vector based on the SV40 origin of replication and chromosomal S/MARs replicates episomally in CHO cells. *Nucleic Acids Research* **27**, 426-428 (1999).

26.   Chen, C., Smye, S.W., Robinson, M.P. & Evans, J.A. Membrane electroporation theories: a review. *Medical & Biological Engineering & Computing* **44**, 5-14 (2006).

27.   Zhang, Y. & Yu, L.C. Microinjection as a tool of mechanical delivery. *Current Opinion in Biotechnology* **19**, 506-510 (2008).

28.   Klein, T.M., Arentzen, R., Lewis, P.A. & Fitzpatrick-McElligott, S. Transformation of microbes, plants and animals by particle bombardment. *Biotechnology (N Y)* **10**, 286-291 (1992).

29.   Miller, D.L., Pislaru, S.V. & Greenleaf, J.E. Sonoporation: mechanical DNA delivery by ultrasonic cavitation. *Somat Cell Mol Genet* **27**, 115-134 (2002).

30.   Schenborn, E.T. & Goiffon, V. Calcium phosphate transfection of mammalian cultured cells. *Methods Mol Biol* **130**, 135-145 (2000).

31.   Schenborn, E.T. & Goiffon, V. DEAE-dextran transfection of mammalian cultured cells. *Methods Mol Biol* **130**, 147-153 (2000).

32.   Zuhorn, I.S. & Hoekstra, D. On the mechanism of cationic amphiphile-mediated transfection. To fuse or not to fuse: Is that the question? *Journal of Membrane Biology* **189**, 167-179 (2002).

33.   Schwartz, J.J. & Zhang, S.G. Peptide-mediated cellular delivery. *Current Opinion in Molecular Therapeutics* **2**, 162-167 (2000).

34.   Dufes, C., Uchegbu, I.F. & Schatzlein, A.G. Dendrimers in gene delivery. *Adv Drug Deliv Rev* **57**, 2177-2202 (2005).

35.   De Smedt, S.C., Demeester, J. & Hennink, W.E. Cationic polymer based gene delivery systems. *Pharm Res* **17**, 113-126 (2000).

36.   Grant, S.L., Douglas, A.M., Goss, G.A. & Begley, C.G. Oncostatin M and leukemia inhibitory factor regulate the growth of normal human breast epithelial cells. *Growth Factors* **19**, 153-162 (2001).

37.   Daly, T.M. Overview of adeno-associated viral vectors. *Methods Mol Biol* **246**, 157-165 (2004).

38.   Karlsson, G.B. & Liljestrom, P. Delivery and expression of heterologous genes in mammalian cells using self-replicating alphavirus vectors. *Methods Mol Biol* **246**, 543-557 (2004).

39.   Merrihew, R.V., Kost, T.A. & Condreay, J.P. Baculovirus-mediated gene delivery into mammalian cells. *Methods Mol Biol* **246**, 355-365 (2004).

40.   Goins, W.F. et al. Delivery using herpes simplex virus: an overview. *Methods Mol Biol* **246**, 257-299 (2004).

41.   Somia, N. Gene transfer by retroviral vectors: an overview. *Methods Mol Biol* **246**, 463-490 (2004).

42.   Gordon, K. & Ruddle, F.H. Gene transfer into mouse embryos. *Dev Biol (N Y 1985)* **4**, 1-36 (1986).

References

43.   Mahvi, D.M., Sheehy, M.J. & Yang, N.S. DNA cancer vaccines: A gene gun approach. *Immunology and Cell Biology* **75**, 456-460 (1997).

44.   Taylor, N.J. & Fauquet, C.M. Microparticle bombardment as a tool in plant science and agricultural biotechnology. *DNA and Cell Biology* **21**, 963-977 (2002).

45.   Mehier-Humbert, S., Bettinger, T., Yan, F. & Guy, R.H. Ultrasound-mediated gene delivery: kinetics of plasmid internalization and gene expression. *J Control Release* **104**, 203-211 (2005).

46.   Chenuet, S. et al. Calcium Phosphate Transfection Generates Mammalian Recombinant Cell Lines With Higher Specific Productivity Than Polyfection. *Biotechnology and Bioengineering* **101**, 937-945 (2008).

47.   Parker, G.C. et al. Stem cells: shibboleths of development, part II: Toward a functional definition. *Stem Cells Dev* **14**, 463-469 (2005).

48.   Wagner, E., Ogris, M. & Zauner, W. Polylysine-based transfection systems utilizing receptor-mediated delivery. *Adv Drug Deliv Rev* **30**, 97-113 (1998).

49.   Karak, N. & Maiti, S. Dendritic polymers: A class of novel material. *Journal of Polymer Materials* **14**, 105-& (1997).

50.   Boussif, O. et al. A versatile vector for gene and oligonucleotide transfer into cells in culture and in vivo: polyethylenimine. *Proc Natl Acad Sci U S A* **92**, 7297-7301 (1995).

51.   Diebold, S.S., Kursa, P., Wagner, E., Cotten, M. & Zenke, M. Mannose polyethylenimine conjugates for targeted DNA delivery into dendritic cells. *Journal of Biological Chemistry* **274**, 19087-19094 (1999).

52.   Ogris, M., Brunner, S., Schuller, S., Kircheis, R. & Wagner, E. PEGylated DNA/transferrin-PEI complexes: reduced interaction with blood components, extended circulation in blood and potential for systemic gene delivery. *Gene Ther* **6**, 595-605 (1999).

53.   Boussif, O., Zanta, M.A. & Behr, J.P. Optimized galenics improve in vitro gene transfer with cationic molecules up to 1000-fold. *Gene Therapy* **3**, 1074-1080 (1996).

54.   Kichler, A., Leborgne, C., Coeytaux, E. & Danos, O. Polyethylenimine-mediated gene delivery: a mechanistic study. *J Gene Med* **3**, 135-144 (2001).

55.   Won, Y.Y., Sharma, R. & Konieczny, S.F. Missing pieces in understanding the intracellular trafficking of polycation/DNA complexes. *J Control Release* **139**, 88-93 (2009).

56.   Holmes, A.R., Dohrman, A.F., Ellison, A.R., Goncz, K.K. & Gruenert, D.C. Intracellular compartmentalization of DNA fragments in cultured airway epithelial cells mediated by cationic lipids. *Pharm Res* **16**, 1020-1025 (1999).

57.   Oh, Y.K. et al. Polyethylenimine-mediated cellular uptake, nucleus trafficking and expression of cytokine plasmid DNA. *Gene Ther* **9**, 1627-1632 (2002).

58.   Branden, L.J., Mohamed, A.J. & Smith, C.I. A peptide nucleic acid-nuclear localization signal fusion that mediates nuclear transport of DNA. *Nat Biotechnol* **17**, 784-787 (1999).

59.   Byrnes, C.K., Nass, P.H., Duncan, M.D. & Harmon, J.W. A nuclear targeting peptide, M9, improves transfection efficiency in fibroblasts. *J Surg Res* **108**, 85-90 (2002).

60.   Norton, P.A. & Pachuk, C.J. Methods for DNA introduction into mammalian cells, Vol. 38, Edn. Makrides, S. C. (Elsevier Science BV, Amsterdam; 2003).

61.   Barnes, L.M. & Dickson, A.J. Mammalian cell factories for efficient and stable protein expression. *Curr Opin Biotechnol* **17**, 381-386 (2006).

62.   Bode, J. et al. The transgeneticist's toolbox: Novel methods for the targeted modification of eukaryotic genomes. *Biological Chemistry* **381**, 801-813 (2000).

63.   Huang, Y. et al. An efficient and targeted gene integration system for high-level antibody expression. *J Immunol Methods* **322**, 28-39 (2007).

64.   Wilson, T.J. & Kola, I. The LoxP/CRE system and genome modification. *Methods Mol Biol* **158**, 83-94 (2001).

65.   Barnes, L.M., Bentley, C.M. & Dickson, A.J. Stability of protein production from recombinant mammalian cells. *Biotechnol Bioeng* **81**, 631-639 (2003).

66.   Lodish, H. et al. Molecular cell biology, Vol. Fourth Edition. (W. H. Freeman and Company, New York; 2000).

67.   Lewis, P., Hensel, M. & Emerman, M. Human immunodeficiency virus infection of cells arrested in the cell cycle. *Embo J* **11**, 3053-3058 (1992).

68.   Buchschacher, G.L. & Wong-Staal, F. Development of lentiviral vectors for gene therapy for human diseases. *Blood* **95**, 2499-2504 (2000).

69.   Escors, D. & Breckpot, K. Lentiviral Vectors in Gene Therapy: Their Current Status and Future Potential. *Arch Immunol Ther Exp (Warsz)* (2010).

70.   Mitchell, R.S. et al. Retroviral DNA integration: ASLV, HIV, and MLV show distinct target site preferences. *Plos Biology* **2**, 1127-1137 (2004).

71.   Schambach, A. et al. Lentiviral vectors pseudotyped with murine ecotropic envelope: increased biosafety and convenience in preclinical research. *Exp Hematol* **34**, 588-592 (2006).

72.   Schambach, A. et al. Equal potency of gammaretroviral and lentiviral SIN vectors for expression of O6-methylguanine-DNA methyltransferase in hematopoietic cells. *Mol Ther* **13**, 391-400 (2006).

73.   Bartz, S.R. & Vodicka, M.A. Production of high-titer human immunodeficiency virus type 1 pseudotyped with vesicular stomatitis virus glycoprotein. *Methods-a Companion to Methods in Enzymology* **12**, 337-342 (1997).

74.   Barry, S.C. et al. Lentivirus vectors encoding both central polypurine tract and posttranscriptional regulatory element provide enhanced transduction and transgene expression. *Human Gene Therapy* **12**, 1103-1108 (2001).

75.   Martinez, C., Hofmann, T.J., Marino, R., Dominici, M. & Horwitz, E.M. Human bone marrow mesenchymal stromal cells express the neural ganglioside GD2: a novel surface marker for the identification of MSCs. *Blood* **109**, 4245-4248 (2007).

76.   Malaval, L., Gupta, A.K. & Aubin, J.E. Leukemia inhibitory factor inhibits osteogenic differentiation in rat calvaria cell cultures. *Endocrinology* **136**, 1411-1418 (1995).

77.   Chen, X.F. et al. Prevascularization of a Fibrin-Based Tissue Construct Accelerates the Formation of Functional Anastomosis with Host Vasculature. *Tissue Engineering Part A* **15**, 1363-1371 (2009).

78.   Jaatinen, T. & Laine, J. Isolation of hematopoietic stem cells from human cord blood. *Curr Protoc Stem Cell Biol* **Chapter 2**, Unit 2A 2 (2007).

79.   Erices, A., Conget, P. & Minguell, J.J. Mesenchymal progenitor cells in human umbilical cord blood. *British Journal of Haematology* **109**, 235-242 (2000).

80.   Romanov, Y.A., Svintsitskaya, V.A. & Smirnov, V.N. Searching for alternative sources of postnatal human mesenchymal stem cells: candidate MSC-like cells from umbilical cord. *Stem Cells* **21**, 105-110 (2003).

81.   Fu, Y.S., Shih, Y.T., Cheng, Y.C. & Min, M.Y. Transformation of human umbilical mesenchymal cells into neurons in vitro. *J Biomed Sci* **11**, 652-660 (2004).

82.   Mitchell, K.E. et al. Matrix cells from Wharton's jelly form neurons and glia. *Stem Cells* **21**, 50-60 (2003).

83.   Sarugaser, R., Lickorish, D., Baksh, D., Hosseini, M.M. & Davies, J.E. Human umbilical cord perivascular (HUCPV) cells: a source of mesenchymal progenitors. *Stem Cells* **23**, 220-229 (2005).

84.   Karahuseyinoglu, S. et al. Biology of stem cells in human umbilical cord stroma: in situ and in vitro surveys. *Stem Cells* **25**, 319-331 (2007).

References

85. Weiss, M.L. et al. Human umbilical cord matrix stem cells: preliminary characterization and effect of transplantation in a rodent model of Parkinson's disease. *Stem Cells* **24**, 781-792 (2006).

86. La Rocca, G. et al. Isolation and characterization of Oct-4+/HLA-G+ mesenchymal stem cells from human umbilical cord matrix: differentiation potential and detection of new markers. *Histochem Cell Biol* **131**, 267-282 (2009).

87. Lu, L.L. et al. Isolation and characterization of human umbilical cord mesenchymal stem cells with hematopoiesis-supportive function and other potentials. *Haematologica* **91**, 1017-1026 (2006).

88. Kadner, A. et al. Human umbilical cord cells for cardiovascular tissue engineering: a comparative study. *Eur J Cardiothorac Surg* **25**, 635-641 (2004).

89. Majore, I., Moretti, P., Hass, R. & Kasper, C. Identification of subpopulations in mesenchymal stem cell-like cultures from human umbilical cord. *Cell Commun Signal* **7**, 6 (2009).

90. Baksh, D., Yao, R. & Tuan, R.S. Comparison of proliferative and multilineage differentiation potential of human mesenchymal stem cells derived from umbilical cord and bone marrow. *Stem Cells* **25**, 1384-1392 (2007).

91. Covas, D.T., Siufi, J.L., Silva, A.R. & Orellana, M.D. Isolation and culture of umbilical vein mesenchymal stem cells. *Braz J Med Biol Res* **36**, 1179-1183 (2003).

92. Panepucci, R.A. et al. Comparison of gene expression of umbilical cord vein and bone marrow-derived mesenchymal stem cells. *Stem Cells* **22**, 1263-1278 (2004).

93. Horwitz, E.M. et al. Clarification of the nomenclature for MSC: The International Society for Cellular Therapy position statement. *Cytotherapy* **7**, 393-395 (2005).

94. Dominici, M. et al. Minimal criteria for defining multipotent mesenchymal stromal cells. The International Society for Cellular Therapy position statement. *Cytotherapy* **8**, 315-317 (2006).

95. Goodwin, H.S. et al. Multilineage differentiation activity by cells isolated from umbilical cord blood: expression of bone, fat, and neural markers. *Biol Blood Marrow Transplant* **7**, 581-588 (2001).

96. Wang, J.F. et al. Mesenchymal stem/progenitor cells in human umbilical cord blood as support for ex vivo expansion of CD34(+) hematopoietic stem cells and for chondrogenic differentiation. *Haematologica* **89**, 837-844 (2004).

97. Chen, M.Y., Lie, P.C., Li, Z.L. & Wei, X. Endothelial differentiation of Wharton's jelly-derived mesenchymal stem cells in comparison with bone marrow-derived mesenchymal stem cells. *Exp Hematol* **37**, 629-640 (2009).

98. Wu, L.F., Wang, N.N., Liu, Y.S. & Wei, X. Differentiation of Wharton's Jelly Primitive Stromal Cells into Insulin-Producing Cells in Comparison with Bone Marrow Mesenchymal Stem Cells. *Tissue Eng Part A* (2009).

99. Jo, C.H. et al. Fetal mesenchymal stem cells derived from human umbilical cord sustain primitive characteristics during extensive expansion. *Cell Tissue Res* **334**, 423-433 (2008).

100. Conconi, M.T. et al. CD105(+) cells from Wharton's jelly show in vitro and in vivo myogenic differentiative potential. *Int J Mol Med* **18**, 1089-1096 (2006).

101. Lund, R.D. et al. Cells isolated from umbilical cord tissue rescue photoreceptors and visual functions in a rodent model of retinal disease. *Stem Cells* **25**, 602-611 (2007).

102. Fan, X., Liu, T., Liu, Y., Ma, X. & Cui, Z. Optimization of primary culture condition for mesenchymal stem cells derived from umbilical cord blood with factorial design. *Biotechnol Prog* **25**, 499-507 (2009).

103. Lechner, V., Hocht, B., Ulrichs, K., Thiede, A. & Meyer, T. [Obtaining of mesenchymal progenitor cells from the human umbilical cord]. *Zentralbl Chir* **132**, 358-364 (2007).

References

104. Lupatov, A.Y. et al. Cytofluorometric analysis of phenotypes of human bone marrow and umbilical fibroblast-like cells. *Bull Exp Biol Med* **142**, 521-526 (2006).

105. Walenda, T. et al. Co-Culture with Mesenchymal Stromal Cells Increases Proliferation and Maintenance of Hematopoietic Progenitor Cells. *J Cell Mol Med* (2009).

106. Wu, K.H. et al. In vitro and in vivo differentiation of human umbilical cord derived stem cells into endothelial cells. *J Cell Biochem* **100**, 608-616 (2007).

107. Yan, Y. et al. Mesenchymal stem cells from human umbilical cords ameliorate mouse hepatic injury in vivo. *Liver Int* **29**, 356-365 (2009).

108. Yu, Y. et al. [Differentiation of human umbilical cord blood-derived mesenchymal stem cells into chondroblast and osteoblasts]. *Sheng Wu Yi Xue Gong Cheng Xue Za Zhi* **25**, 1385-1389 (2008).

109. Liu, X.D., Liu, B., Li, X.S. & Mao, N. [Isolation and identification of mesenchymal stem cells from perfusion of human umbilical cord vein]. *Zhongguo Shi Yan Xue Ye Xue Za Zhi* **15**, 1019-1022 (2007).

110. Diao, Y., Ma, Q., Cui, F. & Zhong, Y. Human umbilical cord mesenchymal stem cells: Osteogenesis in vivo as seed cells for bone tissue engineering. *J Biomed Mater Res A* (2008).

111. Bakhshi, T. et al. Mesenchymal stem cells from the Wharton's jelly of umbilical cord segments provide stromal support for the maintenance of cord blood hematopoietic stem cells during long-term ex vivo culture. *Transfusion* **48**, 2638-2644 (2008).

112. Hou, T. et al. Umbilical Cord Wharton's Jelly: A New Potential Cell Source of Mesenchymal Stromal Cells for Bone Tissue Engineering. *Tissue Eng Part A* (2009).

113. Kadivar, M. et al. In vitro cardiomyogenic potential of human umbilical vein-derived mesenchymal stem cells. *Biochem Biophys Res Commun* **340**, 639-647 (2006).

114. Kestendjieva, S. et al. Characterization of mesenchymal stem cells isolated from the human umbilical cord. *Cell Biol Int* **32**, 724-732 (2008).

115. Qiao, C. et al. Human mesenchymal stem cells isolated from the umbilical cord. *Cell Biol Int* **32**, 8-15 (2008).

116. Wang, H.S. et al. Mesenchymal stem cells in the Wharton's jelly of the human umbilical cord. *Stem Cells* **22**, 1330-1337 (2004).

117. Kadam, S.S., Tiwari, S. & Bhonde, R.R. Simultaneous isolation of vascular endothelial cells and mesenchymal stem cells from the human umbilical cord. *In Vitro Cell Dev Biol Anim* **45**, 23-27 (2009).

118. Fu, Y.S. et al. Conversion of human umbilical cord mesenchymal stem cells in Wharton's jelly to dopaminergic neurons in vitro: potential therapeutic application for Parkinsonism. *Stem Cells* **24**, 115-124 (2006).

119. Martin-Rendon, E. et al. 5-Azacytidine-treated human mesenchymal stem/progenitor cells derived from umbilical cord, cord blood and bone marrow do not generate cardiomyocytes in vitro at high frequencies. *Vox Sang* **95**, 137-148 (2008).

120. Lu, L.L. et al. [Comparative characterization of mesenchymal stem cells from human umbilical cord tissue and bone marrow]. *Zhongguo Shi Yan Xue Ye Xue Za Zhi* **16**, 140-146 (2008).

121. Covas, D.T. et al. Multipotent mesenchymal stromal cells obtained from diverse human tissues share functional properties and gene-expression profile with CD146+ perivascular cells and fibroblasts. *Exp Hematol* **36**, 642-654 (2008).

122. Magin, A.S. et al. Primary Cells As Feeder Cells For Coculture Expansion Of Human Hematopoietic Stem Cells From Umbilical Cord Blood A Comparative Study. *Stem Cells Dev* (2008).

123. Kermani, A.J., Fathi, F. & Mowla, S.J. Characterization and genetic manipulation of human umbilical cord vein mesenchymal stem cells: potential application in cell-based gene therapy. *Rejuvenation Res* **11**, 379-386 (2008).

124. Xu, J. et al. Neural ganglioside GD2 identifies a subpopulation of mesenchymal stem cells in umbilical cord. *Cell Physiol Biochem* **23**, 415-424 (2009).

125. Zhang, Z.Y. et al. Superior osteogenic capacity for bone tissue engineering of fetal compared with perinatal and adult mesenchymal stem cells. *Stem Cells* **27**, 126-137 (2009).

126. Weiss, M.L. et al. Immune properties of human umbilical cord Wharton's jelly-derived cells. *Stem Cells* **26**, 2865-2874 (2008).

127. Carlin, R., Davis, D., Weiss, M., Schultz, B. & Troyer, D. Expression of early transcription factors Oct-4, Sox-2 and Nanog by porcine umbilical cord (PUC) matrix cells. *Reprod Biol Endocrinol* **4**, 8 (2006).

128. Hiroyama, T. et al. Human umbilical cord-derived cells can often serve as feeder cells to maintain primate embryonic stem cells in a state capable of producing hematopoietic cells. *Cell Biol Int* **32**, 1-7 (2008).

129. Weiss, M.L. & Troyer, D.L. Stem cells in the umbilical cord. *Stem Cell Rev* **2**, 155-162 (2006).

130. Buhring, H.J. et al. Novel markers for the prospective isolation of human MSC. *Ann N Y Acad Sci* **1106**, 262-271 (2007).

131. Battula, V.L. et al. Isolation of functionally distinct mesenchymal stem cell subsets using antibodies against CD56, CD271, and mesenchymal stem cell antigen-1. *Haematologica* **94**, 173-184 (2009).

132. Gang, E.J., Bosnakovski, D., Figueiredo, C.A., Visser, J.W. & Perlingeiro, R.C. SSEA-4 identifies mesenchymal stem cells from bone marrow. *Blood* **109**, 1743-1751 (2007).

133. Karahuseyinoglu, S., Kocaefe, C., Balci, D., Erdemli, E. & Can, A. Functional structure of adipocytes differentiated from human umbilical cord stroma-derived stem cells. *Stem Cells* **26**, 682-691 (2008).

134. Ciavarella, S., Dammacco, F., De Matteo, M., Loverro, G. & Silvestris, F. Umbilical cord mesenchymal stem cells: role of regulatory genes in their differentiation to osteoblasts. *Stem Cells Dev* (2009).

135. Sudo, K. et al. Mesenchymal progenitors able to differentiate into osteogenic, chondrogenic, and/or adipogenic cells in vitro are present in most primary fibroblast-like cell populations. *Stem Cells* **25**, 1610-1617 (2007).

136. Suzdal'tseva, Y.G., Burunova, V.V., Vakhrushev, I.V., Yarygin, V.N. & Yarygin, K.N. Capability of human mesenchymal cells isolated from different sources to differentiation into tissues of mesodermal origin. *Bull Exp Biol Med* **143**, 114-121 (2007).

137. Tian, X., Fu, R.Y., Chen, Y. & Yuan, L.X. [Isolation of multipotent mesenchymal stem cells from the tissue of umbilical cord for osteoblasts and adipocytes differentiation]. *Sichuan Da Xue Xue Bao Yi Xue Ban* **39**, 26-29 (2008).

138. Bailey, M.M., Wang, L., Bode, C.J., Mitchell, K.E. & Detamore, M.S. A comparison of human umbilical cord matrix stem cells and temporomandibular joint condylar chondrocytes for tissue engineering temporomandibular joint condylar cartilage. *Tissue Eng* **13**, 2003-2010 (2007).

139. Passeri, S. et al. Isolation and expansion of equine umbilical cord-derived matrix cells (EUCMCs). *Cell Biol Int* **33**, 100-105 (2009).

140. Honsawek, S., Dhitiseith, D. & Phupong, V. Effects of demineralized bone matrix on proliferation and osteogenic differentiation of mesenchymal stem cells from human umbilical cord. *J Med Assoc Thai* **89 Suppl 3**, S189-195 (2006).

141. Pereira, W.C., Khushnooma, I., Madkaikar, M. & Ghosh, K. Reproducible methodology for the isolation of mesenchymal stem cells from human umbilical cord

and its potential for cardiomyocyte generation. *J Tissue Eng Regen Med* **2**, 394-399 (2008).

142. Ma, L. et al. Human umbilical cord Wharton's Jelly-derived mesenchymal stem cells differentiation into nerve-like cells. *Chin Med J (Engl)* **118**, 1987-1993 (2005).

143. Ma, L. et al. [Biological characteristics of human umbilical cord-derived mesenchymal stem cells and their differentiation into neurocyte-like cells]. *Zhonghua Er Ke Za Zhi* **44**, 513-517 (2006).

144. Chou, S.C., Ko, T.L., Fu, Y.Y., Wang, H.W. & Fu, Y.S. Identification of genetic networks during mesenchymal stem cell transformation into neurons. *Chin J Physiol* **51**, 230-246 (2008).

145. Chao, K.C., Chao, K.F., Fu, Y.S. & Liu, S.H. Islet-like clusters derived from mesenchymal stem cells in Wharton's Jelly of the human umbilical cord for transplantation to control type 1 diabetes. *PLoS ONE* **3**, e1451 (2008).

146. Campard, D., Lysy, P.A., Najimi, M. & Sokal, E.M. Native umbilical cord matrix stem cells express hepatic markers and differentiate into hepatocyte-like cells. *Gastroenterology* **134**, 833-848 (2008).

147. Ennis, J., Gotherstrom, C., Le Blanc, K. & Davies, J.E. In vitro immunologic properties of human umbilical cord perivascular cells. *Cytotherapy* **10**, 174-181 (2008).

148. Yoo, K.H. et al. Comparison of immunomodulatory properties of mesenchymal stem cells derived from adult human tissues. *Cell Immunol* (2009).

149. Le Blanc, K. et al. Treatment of severe acute graft-versus-host disease with third party haploidentical mesenchymal stem cells. *Lancet* **363**, 1439-1441 (2004).

150. Ringden, O. et al. Mesenchymal stem cells for treatment of therapy-resistant graft-versus-host disease. *Transplantation* **81**, 1390-1397 (2006).

151. Yang, C.C. et al. Transplantation of human umbilical mesenchymal stem cells from Wharton's jelly after complete transection of the rat spinal cord. *PLoS ONE* **3**, e3336 (2008).

152. Liao, W. et al. Therapeutic effect of human umbilical cord multipotent mesenchymal stromal cells in a rat model of stroke. *Transplantation* **87**, 350-359 (2009).

153. Koh, S.H. et al. Implantation of human umbilical cord-derived mesenchymal stem cells as a neuroprotective therapy for ischemic stroke in rats. *Brain Res* **1229**, 233-248 (2008).

154. Breymann, C., Schmidt, D. & Hoerstrup, S.P. Umbilical cord cells as a source of cardiovascular tissue engineering. *Stem Cell Rev* **2**, 87-92 (2006).

155. Hoerstrup, S.P. et al. Living, autologous pulmonary artery conduits tissue engineered from human umbilical cord cells. *Ann Thorac Surg* **74**, 46-52; discussion 52 (2002).

156. Schmidt, D. et al. Engineering of biologically active living heart valve leaflets using human umbilical cord-derived progenitor cells. *Tissue Eng* **12**, 3223-3232 (2006).

157. Schmidt, D. et al. Living patches engineered from human umbilical cord derived fibroblasts and endothelial progenitor cells. *Eur J Cardiothorac Surg* **27**, 795-800 (2005).

158. Naldini, L., Blomer, U., Gage, F.H., Trono, D. & Verma, I.M. Efficient transfer, integration, and sustained long-term expression of the transgene in adult rat brains injected with a lentiviral vector. *Proc Natl Acad Sci U S A* **93**, 11382-11388 (1996).

159. Dillon, N. Heterochromatin structure and function. *Biology of the Cell* **96**, 631-637 (2004).

160. Kwaks, T.H.J. & Otte, A.P. Employing epigenetics to augment the expression of therapeutic proteins in mammalian cells. *Trends in Biotechnology* **24**, 137-142 (2006).

161. Kim, I. et al. Molecular cloning, expression, and characterization of angiopoietin-related protein - Angiopoietin-related protein induces endothelial cell sprouting. *Journal of Biological Chemistry* **274**, 26523-26528 (1999).

162. Kim, I. et al. Molecular cloning and characterization of a novel angiopoietin family protein, angiopoietin-3. *FEBS Lett* **443**, 353-356 (1999).

163. Kim, I. et al. Angiopoietin-1 induces endothelial cell sprouting through the activation of focal adhesion kinase and plasmin secretion. *Circ Res* **86**, 952-959 (2000).

164. Morisada, T., Kubota, Y., Urano, T., Suda, T. & Oike, Y. Angiopoietins and angiopoietin-like proteins in angiogenesis. *Endothelium-Journal of Endothelial Cell Research* **13**, 71-79 (2006).

165. Chao, N.J., Emerson, S.G. & Weinberg, K.I. Stem cell transplantation (cord blood transplants). *Hematology Am Soc Hematol Educ Program*, 354-371 (2004).

166. Kelly, S.S., Sola, C.B., de Lima, M. & Shpall, E. Ex vivo expansion of cord blood. *Bone Marrow Transplant* **44**, 673-681 (2009).

167. Kenthirapalan, S. Konstruktion von Säugerzelllinien zur Produktion von glykosilierten Proteinen an den Beispielen Angiopoietin-like protein 1 und 2, Bachelor Thesis, Gottfried Wilhelm Leibniz Universität Hannover. (2008).

168. Dhanabal, M., Jeffers, M., LaRochelle, W.J. & Lichenstein, H.S. Angioarrestin: a unique angiopoietin-related protein with anti-angiogenic properties. *Biochem Biophys Res Commun* **333**, 308-315 (2005).

169. Knappskog, S. et al. The level of synthesis and secretion of Gaussia princeps luciferase in transfected CHO cells is heavily dependent on the choice of signal peptide. *J Biotechnol* **128**, 705-715 (2007).

170. Plisov, S.Y. et al. TGF beta 2, LIF and FGF2 cooperate to induce nephrogenesis. *Development* **128**, 1045-1057 (2001).

171. Oskowitz, A.Z. et al. Human multipotent stromal cells from bone marrow and microRNA: regulation of differentiation and leukemia inhibitory factor expression. *Proc Natl Acad Sci U S A* **105**, 18372-18377 (2008).

172. Stewart, C.L. et al. Blastocyst implantation depends on maternal expression of leukaemia inhibitory factor. *Nature* **359**, 76-79 (1992).

173. Moon, C. et al. Leukemia inhibitory factor inhibits neuronal terminal differentiation through STAT3 activation. *Proc Natl Acad Sci U S A* **99**, 9015-9020 (2002).

174. Kurek, J. AM424: history of a novel drug candidate. *Clin Exp Pharmacol Physiol* **27**, 553-557 (2000).

175. Davis, I.D. et al. A randomized, double-blinded, placebo-controlled phase II trial of recombinant human leukemia inhibitory factor (rhuLIF, emfilermin, AM424) to prevent chemotherapy-induced peripheral neuropathy. *Clin Cancer Res* **11**, 1890-1898 (2005).

176. Gearing, D.P. et al. Production of Leukemia Inhibitory Factor in Escherichia-Coli by a Novel Procedure and Its Use in Maintaining Embryonic Stem-Cells in Culture. *Bio-Technol* **7**, 1157-1161 (1989).

177. Schmelzer, C.H. et al. Glycosylation Pattern and Disulfide Assignments of Recombinant Human Differentiation-Stimulating Factor. *Archives of Biochemistry and Biophysics* **302**, 484-489 (1993).

178. Geisse, S., Gram, H., Kleuser, B. & Kocher, H.P. Eukaryotic expression systems: A comparison. *Protein Expression and Purification* **8**, 271-282 (1996).

179. Tomala, M. laufende Dissertation, Gottfried Wilhelm Leibniz Universität Hannover.

180. Bahnemann, J. Produktion von rekombinanten Zytokinen in CHO-Zellkulturen am Beispiel des human leukemia inhibitory factor, Master Thesis, Gottfried Wilhelm Leibniz Universität Hannover. (2009).

181. FDA To Manufacturers of Biological Products: Recommendations Regarding Bovine Spongiform Encephalopathy (BSE), 2010 via http://www.fda.gov/BiologicsBloodVaccines/SafetyAvailability/ucm105877.htm.

182. van Griensven, M. et al. Mechanical Strain Using 2D and 3D Bioreactors Induces Osteogenesis: Implications for Bone Tissue Engineering. *Adv Biochem Eng Biotechnol* **112**, 95-123 (2009).

183. Hatlapatka, T. laufende Dissertation, Gottfried Wilhelm Leibniz Universität Hannover.

184. Moretti, P. et al. Mesenchymal Stromal Cells Derived from Human Umbilical Cord Tissues: Primitive Cells with Potential for Clinical and Tissue Engineering Applications. *Adv Biochem Eng Biotechnol* (2009).

185. Woodfin, A., Voisin, M.B. & Nourshargh, S. PECAM-1: a multi-functional molecule in inflammation and vascular biology. *Arterioscler Thromb Vasc Biol* **27**, 2514-2523 (2007).

186. Ponte, A.L. et al. The in vitro migration capacity of human bone marrow mesenchymal stem cells: comparison of chemokine and growth factor chemotactic activities. *Stem Cells* **25**, 1737-1745 (2007).

187. Son, B.R. et al. Migration of bone marrow and cord blood mesenchymal stem cells in vitro is regulated by stromal-derived factor-1-CXCR4 and hepatocyte growth factor-c-met axes and involves matrix metalloproteinases. *Stem Cells* **24**, 1254-1264 (2006).

188. Raio, L. et al. Hyaluronan content of Wharton's jelly in healthy and Down syndrome fetuses. *Matrix Biol* **24**, 166-174 (2005).

189. Desharnais, P., Dupere-Minier, G., Hamelin, C., Devine, P. & Bernier, J. Involvement of CD45 in DNA fragmentation in apoptosis induced by mitochondrial perturbing agents. *Apoptosis* **13**, 197-212 (2008).

190. Resta, R. et al. Glycosyl phosphatidylinositol membrane anchor is not required for T cell activation through CD73. *J Immunol* **153**, 1046-1053 (1994).

191. Higa, K., Shimmura, S., Shimazaki, J. & Tsubota, K. Hyaluronic acid-CD44 interaction mediates the adhesion of lymphocytes by amniotic membrane stroma. *Cornea* **24**, 206-212 (2005).

192. Sweeney, E. et al. Quantitative multiplexed quantum dot immunohistochemistry. *Biochem Biophys Res Commun* **374**, 181-186 (2008).

193. Donnenberg, A.D. & Donnenberg, V.S. Rare-event analysis in flow cytometry. *Clin Lab Med* **27**, 627-652, viii (2007).

194. Charles A Janeway, Paul Travers, Mark Walport & Shlomchik, M.J. Immunobiology : the immune system in health and disease Edn. 5th. (Garland Publishing, New York; 2001).

195. Thellin, O., Coumans, B., Zorzi, W., Igout, A. & Heinen, E. Tolerance to the foeto-placental 'graft': ten ways to support a child for nine months. *Curr Opin Immunol* **12**, 731-737 (2000).

196. Gilbert, S.F. Developmental Biology, Edn. 6th (Sinauer Associ- ates, Inc, Sunderland, MA, USA.; 2000).

197. Thellin, O. & Heinen, E. Pregnancy and the immune system: between tolerance and rejection. *Toxicology* **185**, 179-184 (2003).

198. Hammer, A., Hutter, H. & Dohr, G. HLA class I expression on the materno-fetal interface. *Am J Reprod Immunol* **38**, 150-157 (1997).

199. King, A. et al. Evidence for the expression of HLAA-C class I mRNA and protein by human first trimester trophoblast. *J Immunol* **156**, 2068-2076 (1996).

200. Kovats, S. et al. A class I antigen, HLA-G, expressed in human trophoblasts. *Science* **248**, 220-223 (1990).

References

201. Cheng, L., Hammond, H., Ye, Z., Zhan, X. & Dravid, G. Human adult marrow cells support prolonged expansion of human embryonic stem cells in culture. *Stem Cells* **21**, 131-142 (2003).

202. Hutter, H. et al. Expression of HLA class I molecules in human first trimester and term placenta trophoblast. *Cell Tissue Res* **286**, 439-447 (1996).

203. Proll, J., Blaschitz, A., Hutter, H. & Dohr, G. First trimester human endovascular trophoblast cells express both HLA-C and HLA-G. *Am J Reprod Immunol* **42**, 30-36 (1999).

204. Moreau, P. et al. Molecular and immunologic aspects of the nonclassical HLA class I antigen HLA-G: evidence for an important role in the maternal tolerance of the fetal allograft. *Am J Reprod Immunol* **40**, 136-144 (1998).

205. Banfalvi, G. Cell cycle synchronization of animal cells and nuclei by centrifugal elutriation. *Nat Protoc* **3**, 663-673 (2008).

206. Baserga, R. Growth in size and cell DNA replication. *Exp Cell Res* **151**, 1-5 (1984).

207. Brockhoff, G. in Zelluläre Diagnostik: Grundlagen, Methoden und klinische Anwendungen der Durchflusszytometrie, Vol. 1, Edn. Karger. (eds. U. Sack, A. Tárnok & G. Rothe) 604-646 (Karger, Basel; 2007).

208. Ohtani, N., Mann, D.J. & Hara, E. Cellular senescence: its role in tumor suppression and aging. *Cancer Sci* **100**, 792-797 (2009).

209. Itahana, K., Campisi, J. & Dimri, G.P. Methods to detect biomarkers of cellular senescence: the senescence-associated beta-galactosidase assay. *Methods Mol Biol* **371**, 21-31 (2007).

210. Forsyth, N.R. et al. Spontaneous immortalization of clinically normal colon-derived fibroblasts from a familial adenomatous polyposis patient. *Neoplasia* **6**, 258-265 (2004).

211. Troyer, D.L. & Weiss, M.L. Wharton's jelly-derived cells are a primitive stromal cell population. *Stem Cells* **26**, 591-599 (2008).

212. Bieback, K. et al. Human alternatives to fetal bovine serum for the expansion of mesenchymal stromal cells from bone marrow. *Stem Cells* **27**, 2331-2341 (2009).

213. Hovatta, O. et al. A culture system using human foreskin fibroblasts as feeder cells allows production of human embryonic stem cells. *Hum Reprod* **18**, 1404-1409 (2003).

214. Choo, A., Padmanabhan, J., Chin, A., Fong, W.J. & Oh, S.K. Immortalized feeders for the scale-up of human embryonic stem cells in feeder and feeder-free conditions. *J Biotechnol* **122**, 130-141 (2006).

215. Nie, Y., Bergendahl, V., Hei, D.J., Jones, J.M. & Palecek, S.P. Scalable culture and cryopreservation of human embryonic stem cells on microcarriers. *Biotechnol Prog* **25**, 20-31 (2009).

216. Suva, D. et al. Non-hematopoietic human bone marrow contains long-lasting, pluripotential mesenchymal stem cells. *J Cell Physiol* **198**, 110-118 (2004).

217. de Girolamo, L., Sartori, M.F., Albisetti, W. & Brini, A.T. Osteogenic differentiation of human adipose-derived stem cells: comparison of two different inductive media. *J Tissue Eng Regen Med* **1**, 154-157 (2007).

218. Izadpanah, R. et al. Long-term in vitro expansion alters the biology of adult mesenchymal stem cells. *Cancer Res* **68**, 4229-4238 (2008).

219. Braun, K. et al. High-resolution flow cytometry: a suitable tool for monitoring aneuploid prostate cancer cells after TMZ and TMZ-BioShuttle treatment. *Int J Med Sci* **6**, 338-347 (2009).

220. Tokar, E.J., Diwan, B.A. & Waalkes, M.P. Arsenic Exposure Transforms Human Epithelial Stem/Progenitor Cells into a Cancer Stem-like Phenotype. *Environ Health Perspect* **118**, 108-115 (2010).

References

221. Liu, H.S., Biing, J.T., Yang, Y.F. & Chao, C.F. Establishment and characterization of the transfectable golden hamster embryo fibroblast cell line. *Proc Natl Sci Counc Repub China B* **18**, 1-11 (1994).

222. Ke, X.S. et al. Epithelial to mesenchymal transition of a primary prostate cell line with switches of cell adhesion modules but without malignant transformation. *PLoS One* **3**, e3368 (2008).

223. von Bonin, M. et al. Treatment of refractory acute GVHD with third-party MSC expanded in platelet lysate-containing medium. *Bone Marrow Transplant* **43**, 245-251 (2009).

224. Le Blanc, K. et al. Mesenchymal stem cells for treatment of steroid-resistant, severe, acute graft-versus-host disease: a phase II study. *Lancet* **371**, 1579-1586 (2008).

225. Koc, O.N. et al. Rapid hematopoietic recovery after coinfusion of autologous-blood stem cells and culture-expanded marrow mesenchymal stem cells in advanced breast cancer patients receiving high-dose chemotherapy. *J Clin Oncol* **18**, 307-316 (2000).

226. Horwitz, E.M. et al. Isolated allogeneic bone marrow-derived mesenchymal cells engraft and stimulate growth in children with osteogenesis imperfecta: Implications for cell therapy of bone. *Proc Natl Acad Sci U S A* **99**, 8932-8937 (2002).

227. Saito, S. et al. Isolation of embryonic stem-like cells from equine blastocysts and their differentiation in vitro. *FEBS Lett* **531**, 389-396 (2002).

228. Carter, W.G. & Wayner, E.A. Characterization of the class III collagen receptor, a phosphorylated, transmembrane glycoprotein expressed in nucleated human cells. *J Biol Chem* **263**, 4193-4201 (1988).

229. Cichy, J. & Pure, E. The liberation of CD44. *J Cell Biol* **161**, 839-843 (2003).

230. Peola, S. et al. Selective induction of CD73 expression in human lymphocytes by CD38 ligation: a novel pathway linking signal transducers with ecto-enzyme activities. *J Immunol* **157**, 4354-4362 (1996).

231. Nishimura, H. et al. Exogenous Thy-1.1 expression as a marker for thymocyte maturation in transgenic mice. *Thymus* **19**, 35-44 (1992).

232. Hueber, A.O. et al. Thymocytes in Thy-1-/- mice show augmented TCR signaling and impaired differentiation. *Curr Biol* **7**, 705-708 (1997).

233. Delorme, B. et al. Specific plasma membrane protein phenotype of culture-amplified and native human bone marrow mesenchymal stem cells. *Blood* **111**, 2631-2635 (2008).

234. Campioni, D., Lanza, F., Moretti, S., Ferrari, L. & Cuneo, A. Loss of Thy-1 (CD90) antigen expression on mesenchymal stromal cells from hematologic malignancies is induced by in vitro angiogenic stimuli and is associated with peculiar functional and phenotypic characteristics. *Cytotherapy* **10**, 69-82 (2008).

235. Jin, H.J. et al. Down-regulation of CD105 is associated with multi-lineage differentiation in human umbilical cord blood-derived mesenchymal stem cells. *Biochem Biophys Res Commun* **381**, 676-681 (2009).

236. Baksh, D., Song, L. & Tuan, R.S. Adult mesenchymal stem cells: characterization, differentiation, and application in cell and gene therapy. *J Cell Mol Med* **8**, 301-316 (2004).

237. Chen, X.D., Qian, H.Y., Neff, L., Satomura, K. & Horowitz, M.C. Thy-1 antigen expression by cells in the osteoblast lineage. *J Bone Miner Res* **14**, 362-375 (1999).

238. Byers, B.A., Pavlath, G.K., Murphy, T.J., Karsenty, G. & Garcia, A.J. Cell-type-dependent up-regulation of in vitro mineralization after overexpression of the osteoblast-specific transcription factor Runx2/Cbfal. *J Bone Miner Res* **17**, 1931-1944 (2002).

239. Ducy, P., Zhang, R., Geoffroy, V., Ridall, A.L. & Karsenty, G. Osf2/Cbfa1: a transcriptional activator of osteoblast differentiation. *Cell* **89**, 747-754 (1997).

240. Yang, S.Y. et al. In vitro and in vivo synergistic interactions between the Runx2/Cbfa1 transcription factor and bone morphogenetic protein-2 in stimulating osteoblast differentiation. *Journal of Bone and Mineral Research* **18**, 705-715 (2003).

241. Ishige, I. et al. Comparison of mesenchymal stem cells derived from arterial, venous, and Wharton's jelly explants of human umbilical cord. *Int J Hematol* **90**, 261-269 (2009).

242. Nanaev, A.K., Kohnen, G., Milovanov, A.P., Domogatsky, S.P. & Kaufmann, P. Stromal differentiation and architecture of the human umbilical cord. *Placenta* **18**, 53-64 (1997).

243. Kobayashi, K., Kubota, T. & Aso, T. Study on myofibroblast differentiation in the stromal cells of Wharton's jelly: expression and localization of alpha-smooth muscle actin. *Early Hum Dev* **51**, 223-233 (1998).

244. Glindkamp, A. et al. Sensors in Disposable Bioreactors Status and Trends. *Adv Biochem Eng Biotechnol* (2009).

245. Leng, S.X. et al. ELISA and multiplex technologies for cytokine measurement in inflammation and aging research. *Journals of Gerontology Series a-Biological Sciences and Medical Sciences* **63**, 879-884 (2008).

246. Morgan, E. et al. Cytometric bead array: a multiplexed assay platform with applications in various areas of biology. *Clinical Immunology* **110**, 252-266 (2004).

247. Kamnerdpetch, C., Weiss, M., Kasper, C. & Scheper, T. An improvement of potato pulp protein hydrolyzation process by the combination of protease enzyme systems. *Enzyme and Microbial Technology* **40**, 508-514 (2007).

248. Young, I.T. Proof without prejudice: use of the Kolmogorov-Smirnov test for the analysis of histograms from flow systems and other sources. *J Histochem Cytochem* **25**, 935-941 (1977).

6 Appendices

6.1 Materials

6.1.1 Disposable materials

Product	Company
BD BioCoat™ Collagen I 6-well Plates	BD Biosciences, Heidelberg
BD Falcon Cell Strainers, 70μm	BD Biosciences, Heidelberg
Centrifugal concentrators, Vivaspin6 and Vivaspin20, 10 kDa exclusion limit	Sartorius-Stedim Biotech GmbH, Göttingen
Centrifuge tubes, 15 and 50 mL	SARSTEDT AG, Nümbrecht
Cryo-tubes	SARSTEDT AG, Nümbrecht
CultiFlask 50 Tubes	Sartorius-Stedim Biotech GmbH, Göttingen
Erlenmeyer flasks, 125 ml, 250 ml,	VWR International GmbH, Darmstadt
Gloves	Semperguard, Semperit AG Holding, Vienna
Petridishes, 60- and 94 mm	Greiner Bio One, Frickenhausen
Pipettes 1, 2, 5 ,10, 25 und 50 ml,	Sarstedt AG & Co, Nümbrecht
Pipette tips	Sarstedt AG & Co, Nümbrecht
PVDF Membranes	Bio-Rad, München
Reaction tubes, 1.5 and 2 mL	SARSTEDT AG, Nümbrecht
Steril filters, Minisart 0,2 μm	Sartorius-Stedim Biotech GmbH, Göttingen
T-Flasks, 25, 75 and 175 cm²	SARSTEDT AG, Nümbrecht
Well-plates (6-wells; 12-wells and 96-wells)	SARSTEDT AG, Nümbrecht

6.1.2 Antibodies

	Company	Antigen	Fluorophore	Reactivity	Isotype	Product #	[μg/μL]
Labeled antibodies							
	Invitrogen	HLA I	FITC	human	Mouse IgG2a	MHBC01	0.800
	BD	Oct3/4	PE	mouse/human	Mouse IgG1, κ	560186	0.013
	BD	SSEA-1	FITC	mouse/human	Mouse IgM, k	560127	0.006
	Miltenyi Biotec	CD31	FITC	human	Mouse IgG1	130-092-654	0.077
	BD	CD34	FITC	human	Mouse IgG1, k	555821	0.006
	BD	CD34	PE-Cy5	human		555823	0.006
	BD	CD 45	PE-Cy5	human		555484	0.002
	BD	CD 45	FITC	human	Mouse IgG1, k	555482	0.006
	BD	CD 44	PE	human	Mouse IgG1, k	550989	0.013
	BD	CD73	PE	human	Mouse IgG1, k	550257	0.006
	BD	CD 90	FITC	human	Mouse IgG1, k	555595	0.500
	Invitrogen	CD105	R-PE	human	Mouse IgG1	MHCD10504	0.100
	Miltenyi Biotec	CD271	PE	human	Mouse IgG1	130-091-885	/
	Miltenyi Biotec	MSCA-1	PE	human	Mouse IgG1	130-093-587	/
Primary antibodies							
	BD	GD2	/	human	Mouse IgG2a	554272	0.500
	Santa cruz biotec	Runx2	/	human	mouse IgG2b	sc-101145	0.100
	Santa cruz biotec	His6	/	/	Mouse IgG2b	sc-57598	0.100
	RD Systems	hLIF	/	human	Mouse IgG1	MAB2501	0.5
Secondary antibody							
	BD	mouse IG	PE	mouse	Goat Ig	550589	0.200
Isotype controls							

BD	FITC	Mouse IgM, k	553474	0.500
BD	PE	Mouse IgM, k	555584	0.050
BD	FITC	Mouse IgG2a, k	553456	0.500
BD	FITC	Mouse IgG1, k	555748	0.050
BD	PE	Mouse IgG1, k	555749	0.050
Invitrogen	FITC	Mouse IgG2a	MG2a01	0.100
Invitrogen	R-PE	Mouse IgG1	MG104	0.100
BD	PE-Cy5	Mouse IgG1, k	555750	0.006

6.1.3 Enzymes

Product	Company
HotOls DNA-Polymerase	Omni Life Science GmbH, Bremen
M-MLV-Reverse Transkriptas	Promega GmbH, Mannheim

6.1.4 **Primers**

Oligo dT-Primer 5' d(T)$_{18}$ 3', Fermentas, St. Leon-Rot
All specific primers were purchased from the company Firma Eurofins MWG Operon:

Name	Product size [bp]	5´ Forward	3´ Reverse	Annealing temperature [°C]
AP	267	gctgaacaggaacaacgtga	ccaccaaatgtgaagacgtg	51
CD31	157	gagtcctgctgacccttctg	tgagaggtggtgctgacatc	56.2
CD34	158	actcggtgcgtctctctagg	tggggtagcagtaccgttgt	56.2
CD44	142	ggctttcaatagcaccttgc	gttgtttgctgcacagatgg	53.8
CD45	116	ttcatgcagctagcaagtgg	agtcagccgtgtccctaaga	53.8
CD73	261	gctcttcaccaaggttcagc	agtggcccctttgctttaat	52
CD90	173	tcctcccagaacgtcacagt	aggcttcctgtctcctccat	56.2
CD105	205	tgccactggacacaggataa	ccttcgagacctggctagtg	53.8
GAPDH	419	gccacccagaagactgtggat	tggtccagggtttcttactcc	61.8
hLIF	211	tgccaatgccctctttattc	ggggttgaggatcttctggt	54
OCN	315	aggcgctacctgtatcaat	cagattcctcttctggagttt	48
OPN	330	ctaggcatcacctgtgccatacc	cagtgaccagttcatcagattcat	60
RUNX2	229	tcttcacaaatcctccccc	tggattaaaaggacttggtg	52

6.1.5 Kits

Product	Company
β-Galactosidase Staining Kit	Cell Signaling Technology, Danvers, USA
FITC Annexin V Apoptosis Detection Kit I	BD Biosciences, Heidelberg
RNeasy Plus Mini Kit	QIAGEN, Hilden
AP conjugate substrate Kit	Biorad, München

6.1.6 Chemicals

Reagenz	Company
Accutase	PAA Laboratories GmbH, Pasching
Acetic acid	Roth GmbH + Co. KG, Karlsruhe
Acrylamide	Carl Roth GmbH + Co KG, Karlsruhe
Alizarin Red S	Sigma Aldrich Chemie GmbH, München
Agarose	ABgene, Hamburg
Ampicillin	Fluka Chemie AG, Buchs
APS	Sigma Aldrich Chemie GmbH, München
BCIP/NBT tablets, SIGMA FAST	Sigma Aldrich Chemie GmbH, München
Bismethylenacrylamide	Carl Roth GmbH + Co KG, Karlsruhe
Bromphenol blue	Fluka Chemie AG, Buchs
BSA	Sigma Aldrich Chemie-GmbH, München
Calcium chloride	Merck KGaA, Darmstadt
Cell Dissociation Solution Non enzymatic	Sigma Aldrich Chemie GmbH, München
Coomassie PhastGel Blue R	Amersham Pharmacia, Uppsala, Schweden
DAPI	Sigma Aldrich Chemie-GmbH, München
Dexamethason	Sigma Aldrich Chemie-GmbH, München
DMSO	Merck KGaA, Darmstadt
dNTP's	Fermentas, St. Leon-Rot
EDTA	AppliChem GmbH, Darmstadt
Ethanol	Roth GmbH + Co. KG, Karlsruhe
Ethidium bromide	Sigma Aldrich Chemie-GmbH, München
FCS "standard quality"	PAA Laboratories GmbH, Pasching
FCS "gold quality"	PAA Laboratories GmbH, Pasching
FCS "heat inactivated"	PAA Laboratories GmbH, Pasching
FCS "pre-tested for amnion cells"	PAA Laboratories GmbH, Pasching
GeneRuler™ DNA Ladder Mix	Fermentas, St. Leon-Rot
Gentamicin	PAA Laboratories GmbH, Pasching
FCS, ES cell tested	HyClone, Thermo Fischer, Karlsruhe
Glycerol	Fluka Chemie AG, Buchs
Glycine	Sigma Aldrich Chemie GmbH, München
Hypoxanthine	Sigma Aldrich Chemie-GmbH, München
Imidazole	Sigma Aldrich Chemie GmbH, München
Isopropanol	Merck KGaA, Darmstadt
Calcium Dihydrogen Phosphate	Fluka Chemie AG, Buchs
L-Ascorbat-2-Phosphat	Sigma Aldrich Chemie-GmbH, München
L-Glutamine	PAA Laboratories GmbH, Pasching
LIF, ESGRO	Millipore GmbH, Schwalbach
Magnesium chloride	Merck KGaA, Darmstadt

β-Mercaptoethanol	Gibco, Karlsruhe
Methanol	Roth GmbH + Co. KG, Karlsruhe
Non-essential amino acid	Gibco, Karlsruhe
Potassium chloride	Merck KGaA, Darmstadt
Sodium chloride	Merck KGaA, Darmstadt
Sodium Pyruvate	Fluka Chemie AG, Buchs
Paraformaldehyde	Sigma Aldrich Chemie-GmbH, München
p-Nitrophenyl phosphate tablets, SIGMA FAST	Sigma Aldrich Chemie-GmbH, München
p-Nitrophenol	Fluka Chemie AG, Buchs
Penicillin / Streptomycin	PAA Laboratories GmbH, Pasching
Propidiumiodide	Sigma Aldrich Chemie-GmbH, München
RNAse free water	Qiagen, Hilden
RPMI 1640	PAA Laboratories GmbH, Pasching
Hydrochloric acid	Fluka Chemie AG, Buchs
Saponin	Sigma Aldrich Chemie-GmbH, München
SDS	Sigma Aldrich Chemie-GmbH, München
TEMED	Sigma Aldrich Chemie-GmbH, München
Tris Base	Sigma Aldrich Chemie-GmbH, München
Trypsin	Sigma Aldrich Chemie-GmbH, München
Thymidine	Sigma Aldrich Chemie-GmbH, München
Tween 20	Serva Elektrophoresis GmbH, Heidelberg

6.1.7 Equipment

Equipment	Company
AlphaEaseFC software, 3.2.3	Cell Biosciences, Inc., Santa Clara, USA
Autoclave, Systec V-150	Systec GmbH, Wettenberg
Cell sorter	
FACS Vantage SE	BD Biosciences, Heidelberg
Software Cell Quest Pro v3.5	BD Biosciences, Heidelberg
Argon Laser Enterprise II (488 nm)	Coherent, Santa Clara, USA
Filters:	
FL1: BP 515-545 nm	
FL1: 564-606 nm	
FL3: 665-685 nm	
Cell[B] Imaging Software	Olympus Corporation, Tokio, Japan
Centrifuge, Multifuge 3s	Heraeus Holding GmbH, Hanau
Clean bench	Technoflow 2F150-II GS, Integra Biosciences AG, Zürich, Switzerland
Electrophoresis system (Protein) Mini-PROTEAN	Bio-Rad, München
Electrophoresis system (DNA)	Thermo Fischer Scientific, Bonn
Electrophoretic transfer cell for western blot, Criterion Blotter	Bio-Rad, München
Fluorescence microscope, Olympus IX 50	Olympus Corporation, Tokio, Japan
FPLC, BioLogic Duo-Flow Systems	Bio-Rad, München

Freezing Containers, Nalgene® Cryo 1°C	Krackeler Scientific, Inc. NY, USA
Gel documentation, Gel IX Imager	Intas Science Imaging Instruments GmbH, Göttingen
Hemacytometer, Neubauer	Brand GmbH & Co KG, Wertheim
Flow cytometer	
Epics XL/MCL	Beckman Coulter, Krefeld
Filters:	
FL1: BP 505-545 nm	
FL2: BP 560-590 nm	
FL3: 660-690 nm	
Incubator, Heracell 240	Heraeus Holding GmbH, Hanau
Laboratory balance, MC 1	Sartorius-Stedim Biotech, Göttingen
Metal Chelate Membrane Adsorber (IDA75	Sartorius-Stedim Biotech, Göttingen
Microplate Reader 680,	Bio-Rad, München
Orbital shaker cell culture, DOS-10M Elmi Skyline	Elmi Ltd., Riga, Lettland
PCR-Thermocycler; Px2 Thermal Cycler	Thermo Electron Corporation, Waltham, USA
pH-Electrode, Checker®,	Hanna Instruments Ltd, Leighton Buzzard, UK
Pipettes, Research®	Eppendorf AG, Hamburg
Pipetting device, Pipetus®	Hirschmann Laborgeräte GmbH & Co KG, Eberstadt
Spectrophotometer, NanoDrop ND-1000	NanoDrop Technologies, Inc, Wilmington, DE, USA
Shaker (Gels or blot staining), MTS 4	IKA Werke GmbH, Staufen
Ultrapure Water System, Arium 611	Sartorius-Stedim Biotech GmbH, Göttingen
Ultrasonic bath, Bandelin Sonorex Super RK 510 H	BANDELIN electronic GmbH & Co. KG, Berlin
Ultrasonic homogenizer, Labsonic	Sartorius-Stedim Biotech GmbH, Göttingen
UV/Vis-Spectrophotometer, NanoDrop ND-1000	PEQLAB -Biotechnologie GmbH, Erlangen
WinMDI 2.8	Joseph Trotter
YSI 2700 Select analyzer	YSI Incorporated Life Sciences, Yellow Springs, US

6.1.8 Cell lines and primary cells

CHO cell line

The CHO[SFS] clone II cell line was obtained from the company CCS Cell Culture Service (Hamburg, Germany). The cell line is DHFR defective and thus, is glycine, thymidine and hypoxanthine dependent.

Jurkat cells

The human T cell leukemia Jurkat (ACC 282) was purchased from the DSMZ - Deutsche Sammlung von Mikroorganismen und Zellkulturen GmbH (Hamburg, Germany).

MSC from human adipose tissue

The MSCs (huF53 (N127)) isolated from human adipose tissue were kindly provided by Prof. Martijn van Griensven (Ludwig Boltzmann Institut für experimentelle und klinische Traumatologie, Vienna, Austria).

Isolated MSC from human umbilical cord tissue:

The use of the biological material has been approved by the Institutional Review Board, project #3037 in an extended permission on 17th June, 2006. The MSCs isolated within the framework of this thesis are summarized in the following table:

Name	Date of birth/isolation
HD140509	14.05.09/14.05.09
MK2407	24.07.08/24.07.08
NS010408	01.04.08/01.04.08
NS190109	19.01.09/19.01.09
NS110809	11.08.09/11.08.09
NS120809	11.08.09/12.08.09

Murine ES cell line Brachyury

The murine ES cell lines E14.1, isolated from the mouse line 129/Ola was kindly provided by Prof. Ulrich Martin (Department of Cardiac, Thoracic, Transplantation and Vascular Surgery, MHH).

6.1.9 Cell culture media

CHO cultivation medium

The serum free medium ProCHO 5 (Lonza, Verviers, Belgium) was supplemented with L-glutamine (4mM), hypoxanthine (100 μM), thymidine (10μM), glycine (333μM) and penicillin /streptavidin (100 U·mL^{-1} and 10 μg·mL^{-1} respectively).

Jurkat cultivation medium

RPMI 1640 was supplemented with 10 % FCS, L-glutamine (2mM), and penicillin/streptavidin (100 U·mL^{-1} and 10 μg·mL^{-1} respectively).

UC-MSC cultivation medium

Basal medium (αMEM) was supplemented with HS (final concentration 10%) and gentamicin (final concentration 50 μg·ml^{-1}). HS was obtained from the institute of transfusion medicine of the Hannover medical school and consisted of a pool of sera without regard to blood type or Rhesus factor. Before use the HS was centrifuged 10 minutes at maximal centrifugation speed. The clear supernatant was used for medium preparation.

Osteogenic differentiation medium

Cultivation medium was supplemented with the following osteogenic additives:

Substances	Final concentration
β-Glycerophosphat	5 mM
L-Ascorbat-2-Phosphat	0,2 mM
Dexamethason	100 nM

ES cells cultivation medium

The culture medium was composed of DMEM supplemented with 15 % fetal calf serum (HyClone), 0.2 mM L-glutamine, 0.1 mM β-mercaptoethanol, 0.1 mM non-essential amino acid stock and 1000 units / ml (10 ng / ml) leukemia inhibitory factor.

6.1.10 Buffers and reagents

Agarose gel electrophoresis

Name	Composition
Loading buffer	95% Formamide, 0.05 mM EDTA, je 0.025 % SDS, Bromphenol blue, Xylencyanol FF, Ethidiumbromide
TAE runnig buffer	40 mM Tris Base, 1 mM EDTA, pH 8

Bradford reagent

25 mg Coomassie Blue G-250, 12.5 mL 95 % Ethanol, 25 mL 85 % H_3PO_4, ad 250 mL ddH_2O

Cell culture solution

Name	Composition
Trypsin solution	0.2 % Trypsin, pH 7.5 in PBS, 0.02 % EDTA

Cell staining

Name	Composition
Alizarin red S reagens	1% Alizarin red S in 2% EtOH
Blocking solution	2 % FCS in PBS
DAPI solution	Dilution of the stock solution (500 μg/ml) 1:1000 in 1 x PBS.
FITC solution	12 mg FITC in 20 mL 50% EtOH
Fixation solution	4 % Paraformaldehyde in Permeabilisierungslösung bei 90°C im Wasserbad ca. 1 h lang lösen
Permeabilization solution	0.1 % Saponin in Blocking solution (filtered, 0.2)
Propidium iodide solution	50 μg/ml in 0,9 % NaCl
Von Kossa $AgNO_3$ solution	5 % $AgNO_3$ in ddH_2O
Von Kossa formaldehyde solution	5% NA_2CO_3 and 0.2% Formaldehyde in ddH_2O

FPLC and Vivawell 8-strips Metal Chelate (IMAC) buffers

Equilibration buffer	*Binding buffer*
100 mM NaAc	50 mM NaH_2PO_4
500 mM NaCl	500 mM NaCl
pH 4.5	pH 8

Co^{2+} solution	*Elution buffer*
100 mM NaAc	100 mM NaAc
500 mM NaCl	500 mM NaCl
100 mM Co^{2+}	250 mM Imidazol, pH 8

Phosphate Buffered Saline (PBS)

PBS: 140 mM NaCl, 27 mM KCl, 7.2 mM Na_2HPO_4, 14.7 mM KH_2PO_4; pH = 7.4

SDS-PAGE

Name	Composition
Acetic acid solution	5 % (v/v) CH_3COOH
Coomassie destain solution	30 % acetic acid, 10 % methanol, 70 % $_{dd}H_2O$
Coomassie stain solution	1 PhastGel Blue R tab in 80 ml $_{dd}H_2O$ + 120 ml methanol, filtrated
Farmers Reducer	10 mg $K_3[Fe(CN)_6]$ and $Na_2S_2O_3$ in 100 ml $_{dd}H_2O$
Formaldehyde solution	36.5 % (v/v) CH_2O
Sample buffer	20 mM Tris-HCl, 2 mM EDTA, 5 % SDS, (0.02 %) Bromphenolblau, 10% β-Mercaptoethano
Separation gel (12 %)	2.92 ml acrylamide (40 %), 1.56 ml Bisacrylamid (2 %), 2.8 ml 1.5 M Tris, 1 ml SDS (1%), 1.76 ml H_2O, 20 µl Temed and APS
Silver solution	0.1 % (w/v) $AgNO_3$
Sodium carbonate	2.5 % (w/v) Na_2CO_3
Stacking gel (6 %)	731 µl acrylamide (40 %), 390 µl bisacrylamide (2 %), 760 µl 1.5 M Tris, 0.3 ml SDS (1 %), 3.82 ml H_2O, 10 µl Temed and APS
TGS running buffer	25 mM Tris, 192 mM Glycin, 0.1 % SDS; pH 8.3

Western blot

Name	Composition
Blocking buffer	TBST + 2 % BSA
TBS buffer	25 mM Tris, 150 mM NaCl; pH 7.4
TBST (TBS + Tween20)	TBS + 0.05 % Tween 20
Transfer buffer	25 mM Tris, 192 mM Glycin; 10 % Ethanol; pH 8,3

6.2 Methods

6.2.1 Cell culture

CHO cultivation

CHO cells were routinely cultivated in 175 cm² mL containing 40mL supplemented ProCHO5 medium. The cells were passaged every 3-4 days by centrifugation (5min, 200 g) and resuspension of the pellet in fresh medium. Cell density was maintained between $4·10^5$ and $1.5·10^6$ cells·mL^{-1}.
For long-term cultivation experiments, the cells were cultivated in CultiFlask 50 Tubes containing 10 mL medium.
Batch cultures were performed in 250 mL Spinner flasks containing 100 mL cultivation medium.

Jurkat cultivation

Jurkat cells were routinely cultivated in T-Flasks (75 or 175 cm²) in supplemented cultivation medium. The cells were passaged every 3-4 days by centrifugation (5min, 200 g) and resuspension of the pellet in fresh medium. Cell density was maintained between $4·10^5$ and $1.5·10^6$ cells·mL^{-1}.

MSCs cultivation

MSCs were cultivated in 25, 75 or 175 cm² T-Flasks in cultivation medium. The cultures were started with a cell density of 500 or 4000 cells/cm². The cells were passaged when the cultures were evaluated to be 80%–90% confluent by phase contrast microscopy. For this purpose, the cultures were washed once with pre-warmed PBS (37°C) and treated with accutase (5 min at 37°C). After centrifugation (5 min, 200 g), pellets were resuspended in pre-warmed medium.

ES cell cultivation

The murine embryonic stem (ES) cell line Brachyury was routinely cultured and expanded feeder cell free as floating cell spheres. The suspended cell spheres were passaged every three to four days by dissociating them into single cells with 0.025% trypsin and reseeding with a cell density of 2×10^4 cells / ml.

Cryopreservation

CHO and Jurkat cells were frozen in culture medium containing 7.5% DMSO. The cells were gradually frozen at a rate of 1°C/min using a freezing container placed at -80°C overnight and finally stored at -196°C in liquid nitrogen.

MSCs were frozen in a cryo-medium containing 80% HS, 10% culture medium and 10 % DMSO. The cells were gradually frozen at a rate of 1°C·min^{-1} using a freezing container placed at -80°C overnight. The cryo-tubes were finally stored at -196°C in liquid nitrogen.

Cell thawing

The following procedure was applied for all cell types:
- Quickly submerge cryotube in a 42°C water bath (1-2 min),
- While still cool to the touch but completely thawed, remove the sample, spray with ethanol and place inside a flow hood.
- Add 1 mL of cold culture medium to the sample vial.
- Wait 2 minutes.
- Transfer the content to 15mL tube and add 2 mL of culture medium
- Wait 2 minutes.
- Top up to 10 mL with culture medium
- Centrifuge at 200 g for 5 min at 4°C.
- Aspirate supernatant.
- Flick pellet
- Resuspend in culture medium

6.2.2 Analytics

Cell concentration and viability

Cell concentration and viability were determined by trypan blue exclusion method using a Neubauer hemacytometer for counting.

L-Lactate and D-Glucose analysis

L-Lactate and D-Glucose concentrations were measured in supernatants using a YSI 2700 Select analyzer (YSI Incorporated Life Sciences, Yellow Springs, US).

L-Glutamin analysis

L-Glutamine concentrations were determined via HPLC using pre-column derivatization with o-phthalaldehyde as previously described[247].

SDS-PAGE

The electrophoretic separation of the proteins samples was performed using a 6 %- SDS-polyacrylamide (w/v) stacking gel and a 12 %- (w/v) separation gel. The PAGE occurred in a vertical electrophoretic chamber (Bio-Rad) using Tris-Glycin-SDS (TGS) as running buffer.

The protein samples were 1:1 mixed with SDS sample buffer, heated at 95 °C for 10 min, shortly centrifuged for 1 min, and loaded on the gel together with a protein marker. Gels were run first at 100 V for 30 min until the stacking gel was passed and subsequently run at 200 V for 1h.

For silver staining the following procedure was applied:

- Lay the gel in silver-destain-fix solution for at least 30 minutes.
- Wash gel shortly with ddH2O for 2 times.
- Lay the gel in Farmers Reducer for 2.5 minutes.
- Wash gel with ddH2O for 5 min. Repeat the wash step until the gel is colorless.
- Lay the gel in silver solution 0.1% (m/v) for 30 minutes then discard the solution.
- Wash gel with ddH2O for 2 times 30 seconds each.
- Rinse gel with Na2CO3 solution (2.5 %).
- Lay the gel in 100 ml Na2CO3 solution with 400 μL Formaldehyde. Wait until
- yellow-brown bands appear.
- Lay the gel in 5% acetic acid for 10 min to stop the stain.

For Coomassie staining the following procedure was applied:

- Wash the gel 3 times 5 min with ddH2O.
- Stain the gel in Coomacie stain solution for 1h.
- Wash the gel with ddH2O and lay the gel in destain solution until the background staining disappear.

Western Blot

For the transfer of fractioned protein samples from SDS gels to PVDF membranes, as well as for the specific immunodetection, the following protocol was used:

1) transfer:

- Wash the PVDF membrane with methanol for a few seconds.
- Soak the gel and the PVDF membrane in transfer buffer for a minimum of 15 min to
- remove salts and detergents.
- Saturate two fibered pads and two filter papers in transfer buffer.
- Assemble on the black side of a cassette in the following order:
  - fiber pad
  - filter paper
  - SDS gel
  - PVDF membrane
  - filter paper
  - fiber pad

- Insert the cassette into the electrode module. Be sure to check the direction so that the transfer is from the gel to the membrane.
- Place a stirrer and a Bio-Ice cooling unit (stored at -20 °C) in the buffer tank. Place the electrode module in the buffer tank.
- Fill the tank with transfer buffer. Place the buffer tank on a magnetic stir plate and stir at medium speed.
- Attach electrodes and electrophoresis at 100 V for 50 min.

2) Detection

- Block the membrane in block buffer for 1h with shaking.
- Remove the block buffer. Add the primary anti His-tag antibody to the block buffer (1:750) and incubate the blots for 1h with shaking.
- Wash 3 times each time 5 min with block buffer at room temperature.
- Add the secondary antibody to the TBST (1:3000) buffer and incubate for 1 h at room temperature with shaking.
- Wash 3 times each time 5 min with TBST buffer and then 2 times with TBS at room temperature.
- Wash the blot with AP buffer (AP conjugate substrate Kit) for 5 min.
- Shake the membrane with Color-Development-Reagent (AP conjugate substrate Kit), and wait about 5 minutes for bands to appear.

Bradford test

Bradford tests were performed in 96-well plates. For the calibration curve, BSA was used as a protein standard at the following concentrations: 10, 25, 50, 75, 100, 250, 400 and 500 μg/mL. The following protocol was used:

- Pipette 10 μl of each standard or unknown sample into the appropriate microplate wells.
- Add 300 μl of the Coomassie Plus Reagent to each well and mix with plate shaker for 30 seconds.
- Remove plate from shaker. For the most consistent results, incubate plate for 10 minutes at room temperature (RT).
- Measure the absorbance at or near 595 nm with a plate reader.
- Subtract the average 595 nm measurement for the Blank replicates from the 595 nm measurements of all other individual standard and unknown sample replicates.
- Prepare a standard curve by plotting the average Blank-corrected 595 nm measurement for each protein standard vs. its concentration in μg/ml. Use the standard curve to determine the protein concentration of each unknown sample.

Annexin-V test

Apoptosis was assayed using the Annexin V detection kit according to manufacturer's instructions. The volume of Annexin V and propidium iodide reagents were reduced to 2.5 μL for each assay.

Analysis of cellular senescence

The amount of senescent cells was determined using the Senescence β-Galactosidase Staining Kit and DAPI fluorescence counter stain in accordance to the manufacturers' instructions. The

different populations were cultured for 6 days after elutriation, passaged and seeded at a density of 6,000 cells/cm² for 48h before senescence β-galactosidase staining. After completion of the staining procedures, 4 representative images were taken from diverse areas of each cell culture using phase-contrast microscopy, fluorescence microscopy and CellB Imaging Software. For the calculation of the percentage of senescent cells the total number of cell nuclei and number of cell nuclei surrounded by cyan dye were enumerated.

6.2.3 Cell disruption

CHO cells in suspension were centrifuged 5 min at 200 g. Pellets of $5 \cdot 10^6$ cells were resuspended in 10 mL PBS in 50 mL tubes. Cell disruption was performed on ice using a Ultrasonic homogenizer with pulse of 1 s at 100 W for 3 min followed by 1 min intermission on ice. The procedure was repeated 3 times. After cell disruption, the samples were centrifuged 10 min at 1000 g and the supernatants were used for further analysis.

6.2.4 FPLC

The following protocol was used for the purification of His-tagged protein:

Step	Volume [mL]	Description	Parameters		Volume/Flow rate
1	0:00	Isocratic Flow	A: A-Buffer 1	100%	Volume: 10 mL
			B: Buffer B	0%	Flow: 1.00 mL/min
2	10:00	Isocratic Flow	A: A-Buffer 1	0%	Volume: 10 mL
			B: Buffer B	100%	Flow: 1.00 mL/min
3	20:00	Isocratic Flow	A: A-Buffer 1	100%	Volume: 20 mL
			B: Buffer B	0%	Flow: 1.00 mL/min
4	40:00	Isocratic Flow	A: A-Buffer 2	100%	Volume: 10 mL
			B: Buffer B	0%	Flow: 1.00 mL/min
5	50:00	Load/Inject Sample	Loade: Sample Direct Inject	Econo Pump Auto Inject Valve	Volume: 10 mL Flow: 1.00 mL/min
6	60:00	Isocratic Flow	A: A-Buffer 2	100%	Volume: 15 mL
			B: Buffer B	0%	Flow: 1.00 mL/min
7	75:00	Isocratic Flow	A: A-Buffer 3	100%	Volume: 10 mL
			B: Buffer B	0%	Flow: 1.00 mL/min
8	85:00	Isocratic Flow	A: A-Buffer 1	100%	Volume: 30 mL
			B: Buffer B	0%	Flow: 1.00 mL/min
	115:00	End of Protocol			

A-Buffer 1: Equilibration buffer; Buffer B: Co2+ solution; A-Buffer 2: Binding buffer;
A-Buffer 3: Elution buffer

6.2.5 Vivawell 8-strips Metal Chelate

8-*Strips* were used in combination with 96-well plates. The following protocol was used for the purification of His-tagged proteins:
- Wash the membranes with 300 μL Equilibration buffer and centrifuge for 3 min at 500 g
- Load the membranes twice with 300 μL Co^{2+} solution and centrifuge for 3 min at 500 g

- Wash the membranes twice with 300 µL Equilibration buffer and centrifuge for 3 min at 500 g
- Wash the membranes with 300 µL Binding buffer and centrifuge for 3 min at 500 g
- Load the membranes twice with 300 µL or adjusted volumes of the protein sample (filtrated, 0.2 µm) and centrifuge for 3 min at 500 g
- Wash the membranes twice with 300 µL Binding buffer and centrifuge for 3 min at 500 g
- Elute the protein by adding an appropriate volume of Elution buffer and centrifuge for 3 min at 500 g

6.2.6 Flow cytometric analysis of surface antigen expression

Analysis of SSEA-1 expression by ES cell Brachyury

Cells spheres were harvested, washed with PBS and trypsinated for 1 min at 37° C. Single cells were recovered by centrifugation at 200 x g for 5 min, washed twice in cold PBS supplemented with 2 % FCS and resuspended to a concentration of 10^5 cells / 100 µl for each test. For specific SSEA-1 staining, a titrated volume of a FITC-conjugated anti-mouse SSEA-1 IgM κ antibody was added in a volume of 20 µl to 100 µl cell suspension. Negative control staining was performed using matched FITC-conjugated isotype antibody. The dilution and the quantity of the antibodies used for the test are given in the following table:

	Antibody	Volume antibody [µL]	Blocking buffer [µL]	µg antibody/ Test
Test antibody	anti- SSEA-1-FITC	10	10	0.06
Isotype control	BD mouse IgM, k FITC	13,7*	6.3	0.06

* from a 1:50 pre-dilution

After storage for 20 minutes at room temperature in the dark, 400 µl of PBS supplemented with 2 % FCS as well as 1 µl propidium iodide was added. The cell suspension was then analyzed in an EPICS XL/MCL flow cytometer. Living cells were gated in a dot plot of forward versus side scatter signals and according to propidium iodide exclusion. At least, 10,000 gated events were acquired on a LOG fluorescence scale. Positive staining was defined as the emission of a fluorescence signal exceeding levels obtained by > 99 % of cells from the control population stained with matched isotype antibodies.

Monoparametric analysis for the immunophenotyping of UC-derived MSCs

Primary UC-derived cells were harvested by accutase treatment, washed twice in cold blocking puffer and resuspended to a concentration of 10^6 cells·ml^{-1}. Staining was performed by adding 20 µL of pre-diluted antibody solution to 100 µL of the cell suspension. Negative control staining was performed using matched isotype control antibodies. The optimal quantities of detection antibodies were determined for each assay in titration experiments to allow maximal fluorescence and low unspecific binding. The dilution and the quantity of antibody used for each test are given in the following table:

|	Antibody	Volume antibody [µL]	Blocking buffer [µL]	µg antibody/ Test
Test antibody	anti CD34-PE-Cy5	1.5	18.5	0.01
Test antibody	anti CD45PE-Cy5	6	14	0.01
Isotype control	BD mouse IgG1, k PE-Cy5	1.5	18.5	0.01
Test antibody	anti CD44-PE	2	18	0.03
Test antibody	anti CD73-PE	4	16	0.03
Isotype control	BD mouse IgG1, k PE	0.5	19.5	0.03
Test antibody	anti CD105-PE	0.5	19.5	0.05
Isotype control	Invitrogen mouse IgG1, (R-PE)	0.5	19.5	0.05
Test antibody	anti HLA-I-FITC	1	19	0.80
Test antibody	anti CD90-FITC	1	99	0.10
Test antibody	anti CD31-FITC	1.3	18.7	0.10
Isotype control	BD mouse IgG1, k FITC	2	18	0.10

After storage for 20 minutes at RT in the dark, 400 µL of blocking puffer was added and cells were analyzed in a EPICS XL/MCL flow cytometer. At least, 10,000 gated events were acquired on a LOG fluorescence scale. Living cells were gated in a dot plot of forward versus side scatter signals. Positive staining was defined as the emission of a fluorescence signal that exceeded levels obtained by >99 % of cells from the control population stained with matched isotype antibodies.

Three colors experiment
Cell staining was performed as described above. Three experiments were performed during which the cell samples were stained with different combinations of detection antibodies:

Experiment 1	Experiment 2	Experiment 3
anti HLA-I-FITC	anti HLA-I-FITC	anti HLA-I-FITC
anti CD73-PE	anti CD105-PE	anti CD44-PE
anti CD45PE-Cy5	anti CD45PE-Cy5	anti CD34-PE-Cy5

The fluorophores combination and filter settings used for the detection of fluorescence emission in the performed three color experiments are presented in the following figure:
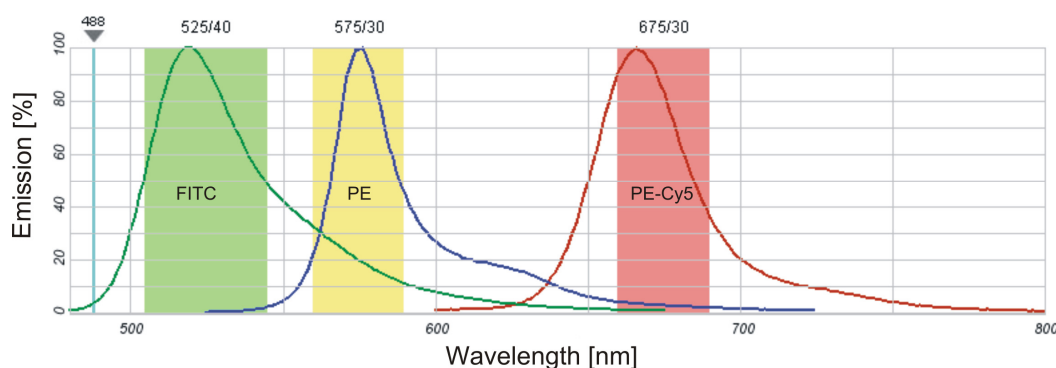
modified from: http://www.invitrogen.com

The compensation for every fluorescence channel was established by measuring samples that were individually stained with the detection antibody of the multi-color samples.

CD271, MSCA-1 and GD2 analysis

CD271 and MSCA-1 expression were analyzed using a PE-labeled antibodies according to manufacturer's instructions.

GD2 analysis was performed using a mouse primary antibody detected by a secondary goat anti-mouse PE-labeled antibody. Primary UC-derived cells were harvested by accutase treatment, washed twice in cold blocking puffer and resuspended to a concentration of 10^6 cells·ml^{-1}. One mL of the cell suspension (10^6 cells) was then centrifuged and the pellet was resuspended in 100 μL blocking buffer containing 2 μL anti GD2 antibody. After storage for 20 minutes at RT in the dark, the cells were washed twice with blocking buffer and resuspended in 100 μL containing 1 μL of the secondary antibody. After storage for 20 minutes at RT in the dark the cells were washed once in blocking buffer and resuspended in 1 mL for flow cytometric analysis. Negative control staining was performed in parallel omitting the primary antibody. For this analysis, more than $5·10^5$ living single cells were acquired according to propidium iodide exclusion and pulse high and area measurements.

6.2.7 Flow cytometric analysis of intra cellular protein expression

After harvest, the cells were washed once in blocking puffer and resuspended at a concentration of $1·10^6$ cells·mL^{-1}. A volume of 200 μL was transferred into a 1.5 mL eppi. 500 μl of fixation solution was added and the suspension was incubated for 20 minutes at room temperature at RT. The cells were washed once in 500 μL permeabilization solution and centrifuged for 5 minutes at 300 g. The cell pellet was then fully resuspended in 100 μl of permeabilization solution containing the primary mouse antibody (see table below). Cells were vortexed 1-2 seconds and incubate for 20 minutes at RT. Cells were washed twice in 500 μL permeabilization solution and resuspended in 100 μl permeabilization solution containing the goat anti-mouse PE-conjugated antibody. Cells were vortexed 1-2 seconds and incubate for 20 minutes at RT in the dark. Cells were washed twice and resuspended in 500 μL in permeabilization solution for immediate analysis.

Intracellular His-tagged protein staining

Antibody	Volume antibody μL/Test	Volume permeabilization solution μL/Test
Mouse anti His-tag	2	98
goat anti-mouse Ig-PE	1	99

Intracellular RUNX2 staining

Antibody	Volume antibody μL/Test	Volume permeabilization solution μL/Test
Mouse anti-human Runx2	1	99
goat anti-mouse Ig-PE	1	99

6.2.8 Total protein staining

Cells pellets (10^5 cells) were washed twice with PBS and then fixed with 500 μL fixation solution for 30 min at room temperature. The cells were washed twice with 500 μL permeabilization

solution (in PBS, without blocking buffer) and the pellets were resuspended in 100 μL of FITC staining solution (dilution from the stock solution to 5 μg·mL^{-1}). After 15 min at room temperature in the dark, the cells were washed twice with permeabilization solution and resuspended to a final volume of 500 μL for flow cytometric analysis.

For fluorescence microscopy, the adherent cultures cultivated in 6-well plates were washed twice with 1 mL PBS and then fixed with 1 mL fixation solution for 30 min at room temperature. The cells were washed twice with 1 mL permeabilization solution (without blocking buffer) and 1 mL of FITC staining solution (dilution from the stock solution to 5 μg·mL^{-1}) was added. After 15 min at room temperature in the dark, the cells were washed twice with PBS and 1 mL of DAPI solution was added to the wells. After 15 min at room temperature in the dark, the cells were washed twice with PBS and examined using a fluorescence microscope.

6.2.9 Counterflow Centrifugal Elutriation (CCE)

The CCE was performed using the Beckmann J6-MC with the JE-5.0 rotor and the appropriate 5ml-standard elutriation chamber (Beckman Coulter GmbH, Krefeld, Germany). Harvested cells were resuspended in PBS and applied to the standard chamber (rotation: 1600 rpm at 24°C) using a digital flow controller (Cole-Palmer Instruments Inc., Chicago, IL, USA). Subsequent fractions of 100 ml aliquots of the elutriated samples were collected upon progressive increase of the pump speed (see table).

Table 6.1: Elutriation Experiment

Fraction	Flow rate (ml/min)	Viable cells/ml x 10^6	Viability (%)	Avg. Diam. (μm)
1	8	0,60	82,0	11,1 ± 1,3
2	12	1,5	87,8	12,4 ± 1,1
3	15	0,19	32,4	14 ± 1,9
4	20	1,02	80,2	14,3 ± 1
5	28	0,63	73,0	15,4 ± 1,1
6	28 without centrifugation	0,63	64,6	19,1 ± 3,1
Control	Non elutriated cells	6,48	83,9	15 ± 1.8

6.2.10 Data analysis

Specific growth rate

Specific cell growth μ was estimated using the following equation:

$$\mu = \frac{\Delta x}{\Delta t} \cdot \frac{1}{x}$$

with:

x = living cell concentration [cell·mL^{-1}]

μ = specific cell growth [h^{-1}]

t = time [h]

Average population doubling time

For the calculation of the average population doubling time, it was assumed that the cells were dividing exponentially over the entire time frame:

$$T_d = \frac{\Delta t}{N_d}$$

And:

$$N_d = \frac{\ln\left(\dfrac{x}{x_0}\right)}{\ln 2}$$

With:

T_d = population doubling time

Δt = time difference

N_d = number of population doublings over Δt

x = number of living cells at the time t

x_0 = number of living cells at the time t = 0

6.2.11 Osteogenic differentiation

In vitro differentiation assay in post-confluent cultures

UC-MSCs (P0) were revitalized and cultivated for one passage in cultivation medium (α-MEM + 10% HS). The cells were harvested by accutase treatment and seeded in 6-well plates at a seeding density of 4000 cells/cm² in osteogenic medium. The cells were maintained under osteogenic condition for 28 days. Medium was replaced every second days.

In vitro differentiation assay in post-confluent cultures

UC-MSCs (P0) were revitalized and cultivated for one passage in cultivation medium (α-MEM + 10% HS). The cells were harvested by accutase treatment and seeded in 175 cm² culture flasks at a seeding density of 500 cells/cm² in osteogenic medium. The cells were maintained under osteogenic conditions and passaged when the cultures were judged 80-90% confluent by microscopic examinations. Osteogenic medium was replaced every second days.

6.2.12 In vitro staining procedures

AP staining

Staining was performed in 6-well plates. BCIP/NBT (5-Bromo-4-chloro-3-indolyl phosphate/Nitro blue tetrazolium) was used as a substrate for the detection of the AP activity. The following protocol was applied:

- Wash the cultures twice with cold PBS
- Fix cells with 1 mL 100 % EtOH, 30 min at 4°C
- Wash twice with ddH2O
- Add 1mL of BCIP/NBT solution
- Incubate 1 hour at 37 °C
- Wash once with ddH2O
- Microscopic examination

Alizarin red staining

Staining was performed in 6-well plates. The following protocol was applied:

- Wash the cultures twice with cold PBS
- Fix cells with 1 mL 100 % EtOH, 30 min at 4°C

- Wash twice with $_{dd}H_2O$
- Add 500 µL of Alizarin red S solution
- Incubate 15 min at RT
- Wash 5 times with $_{dd}H_2O$
- Microscopic examination

Von Kossa staining

Staining was performed in 6-well plates. The following protocol was applied:
- Wash the cultures twice with cold PBS
- Fix cells with 1 mL 100 % EtOH, 30 min at 4°C
- Wash twice with $_{dd}H_2O$
- Add 500 µL of AgNO$_3$ solution and incubate 30 min at RT in the dark
- Wash three times with $_{dd}H_2O$
- Add 500 µL of the formaldehyde solution
- Remove formaldehyde after 1-2 min reaction depending on the intensity of the staining
- Wash 3 times with $_{dd}H_2O$
- Microscopic examination

6.2.13 Alkaline phosphatase specific activity

The detection of the alkaline phosphatase activity was detected with p-Nitrophenyl phosphate as a substrate. The activity was measured for UC-MSCs in suspension following cell harvest.

The following protocol was used:
- Wash once the culture with pre-warmed PBS
- Treat with accutase for 5 min at 37°C
- Transfer to a 50 mL tube
- Centrifuge 5 min at 180g
- Resuspend in 5 mL PBS
- Determine the cell concentration
- Transfer 200 µL of the suspension in a reaction 1.5 mL tube
- Add 200 µL p-Nitrophenylphosphat solution (pre-warmed, in 2x AP buffer)
- Incubate at 37°C in thermoshaker (400 rpm) in the dark
- Document reaction time Δt
- Centrifuge the tubes 5 min at 200 g
- Transfer 50 µL of the supernatant in wells of a 96-Well plates (in triplicates)
- Measure absorption at 405 nm,
- Measure the absorption of the blank sample (200 µL PBS added to 200 µL p-Nitrophenylphosphat solution).
- Subtract the blank value from the measured absorption

The calibration curve was established using p-Nitrophenol as a standard using the following concentrations: 0, 10, 25, 50, 75 and 100 $\mu g \cdot mL^{-1}$. The concentration of p-NP (C_{pNP}) in the samples was calculated from the calibration curve. The specific activity was calculated using the following equation:

$$AP_{spec.} = \frac{C_{pNP}}{M_{pNP}} \cdot V \cdot \frac{1}{\Delta t} \cdot \frac{1}{x} \cdot 10^9$$

With:

$AP_{spec.}$ = AP specific activity [µmol p-NP·min^{-1}·10^{-9} cells]

C_{pNP} = p-NP concentration [µg·mL^{-1}]

M_{pNP} = Molecular weight p-NP [µg·µmol^{-1}]

V= Volume of the sample = 0.4 mL

Δt = reaction time [min]

x = number of cells in the sample

6.2.14 Flow cytometric cell sorting

Cells were sorted using a FACS Vantage SE cell sorter equipped with a 488 nm argon laser. The fluidic system was sterilized before sorting using 70% isopropanol and then washed with sterile PBS. Green FITC fluorescence was measured in the green channel (BP 530/30 nm) and PI in the red channel (BP: 630/22 nm). Living cells were gated on a dot plot of forward versus side scatter signals (FSC/SSC) as well as on the absence of PI fluorescence indicating cells with intact membranes. For bulk sorting procedure, the cells were sorted to collecting tubes containing fresh medium. For cloning, sorting was performed using the ACDU single cell sorting modus of the t FACS Vantage SE. Each cell was isolated in a well of a 96-well plate containing fresh medium.

6.2.15 RT-PCR

RNA isolation

RNA isolation was performed using the „RNeasy Plus Mini Kit". Cell pellet were first suspended in 0.5 ml RLT-Puffer (Lysispuffer) containing 1 % β-Mercaptoethanol. After 1 min incubation the suspension was several times homogenized with the pipette. The suspension was placed 10 min on ice and several times vortexed. The rest of the procedure was performed according manufacturer's instructions. RNA purity and concentration were determined using the spectrophotometer NanoDrops 1000.

Reverse transcription

For the reverse transcription the following protocol was used:
- Transfer 2 µg of isolated RNA into a reaction tube
- Add 3 µL of the oligo-dT-primers solution
- Adjust volume to 21 µL with RNAse free water
- Denaturate 5 min at 65°C
- Place the tube 1 min on ice
- Add 8µL 5x M-MLV-Puffer
- Add 4 µL dNTPs
- Add 6 µL RNAse free water
- Add 1 µL of reverse transcriptase (MLV RT)
- Incubate 1 h at 37°C

PCR

The polymerase chain reaction was performed with the following protocol:

- Prepare PCR mix :

10 µL	5x buffer (HotOls)
4 µL	dNTP's
1 µL	forward Primer
1 µL	reverse Primer
1 µL	cDNA
0.25 µL	HotOls DNA-Polymerase
32.75 µL	PCR water

- Denature 5 min at 95 °C

- Run the following PCR program in thermocycler:

Step	Time	Temperature
Denaturation	30 s	95°C
Primer annealing	30 s	See 6.1.4
Polymerization	30 s	72°C

Number of cycles: 30

Agarose gel for PCR products

Run a 2% agarose gel

Run the gel at 100 V

Agarose gel analysis

The intensity of the DNA bands was quantified using the AlphaEaseFC software. The background intensity was quantified automatically by the software for every detected band and subtracted to the measured signal. The intensity of every gene amplificate was then normalized on the detected intensity for the housekeeping gene GAPDH.

6.3 Complementary results

6.3.1 Transduction efficiency

The transduction efficiency was evaluated measuring the fraction of fluorescing cells within the CHO population following transduction with an expression construct coding for the reporter protein GFP. As a control, untransduced CHO^SFS cells were measured:
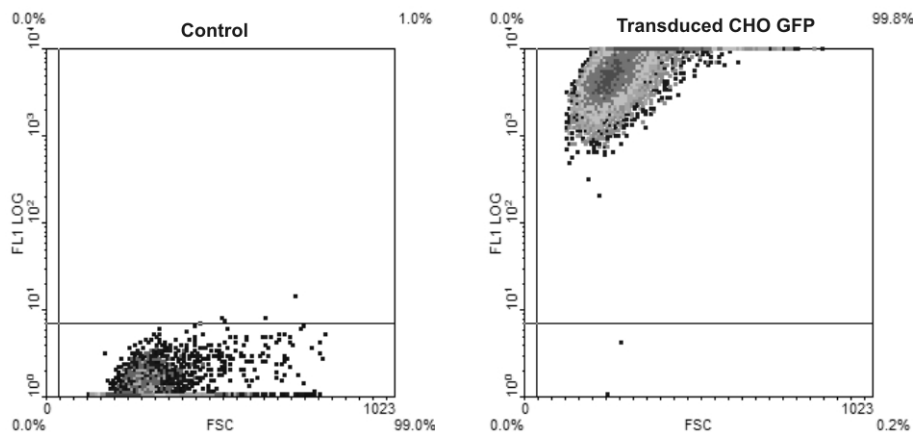
6.3.2 Intracellular hLIF staining

The specific staining of the hLIF was performed using a mouse antibody directed against the His-tag of the recombinant proteins. The primary antibody was detected by a secondary goat anti Ig mouse antibody labeled with the fluorochrome PE (Phycoerythrin):
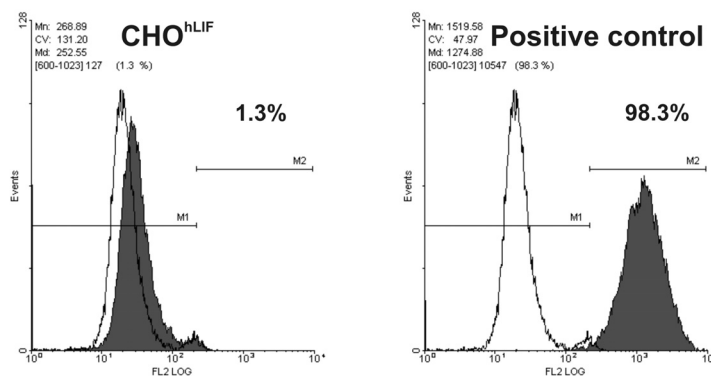
## 6.3.3 Optimization of flow cytometric assay for UC-derived cells

UC-derived cells were harvested using accutase, trypsin and a non enzymatic cell dissociation solution according to manufacturer's instructions. Incubation time of 3 and 8 minutes were tested for all solutions. The cells were subsequently stained for the surface antigen CD90 using a FITC-labeled antibody. The mean fluorescence the fluorescence distributions were determined. In addition, cell viability was assayed using the trypan blue exclusion method. Experiments were performed in triplicates. The results are presented in the following diagram:
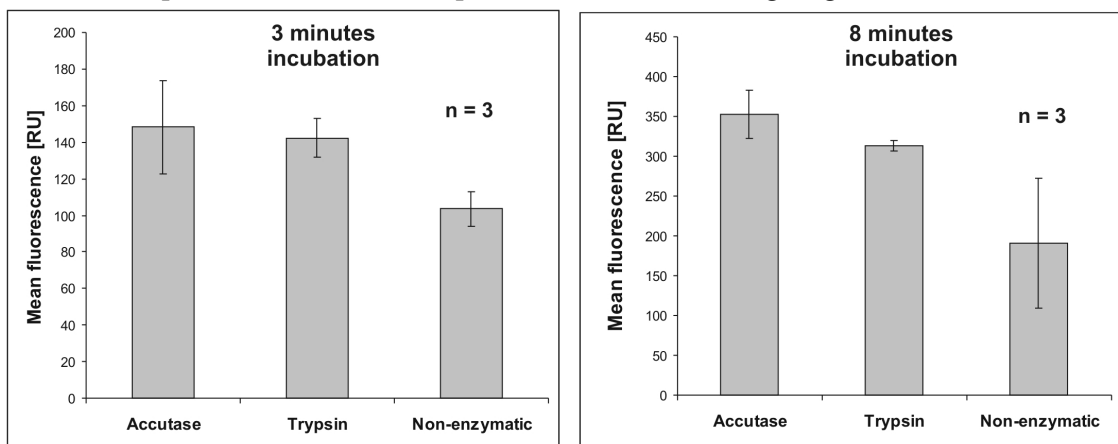
Cell treated with the non enzymatic solution displayed a reduced fluorescence and viability (>85 %). A good viability was observed for cells treated with accutase and trypsin (>95%), however a reduced fluorescence was measured in samples treated with trypsin, in particular after a prolonged treatment (8 minutes), suggesting that CD90 antigens have been damaged during the procedure. Accordingly, flow cytometric assays were performed on UC-MSC harvested using accutase.

6.3.4 Analysis of the CD proteins expression on the transcriptional level (RT-PCR)

The expression of typical MSC markers was analyzed on the transcriptional level using RT-PCR. UC-derived cells in P1 (UC) were used for this purpose. As control mRNA isolated from Jurkat (J)cells was same wise analyzed:
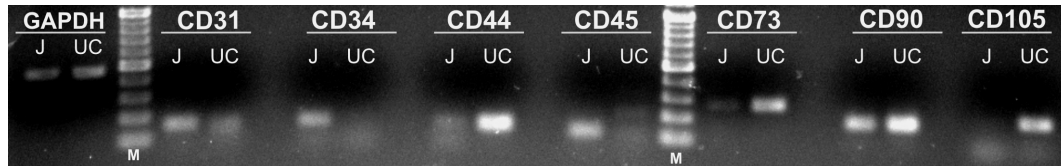

6.3.5 CD271 and MSCA-1 analysis

Analysis of CD271 and MSCA-1 expression of UC-MSCs (P1):
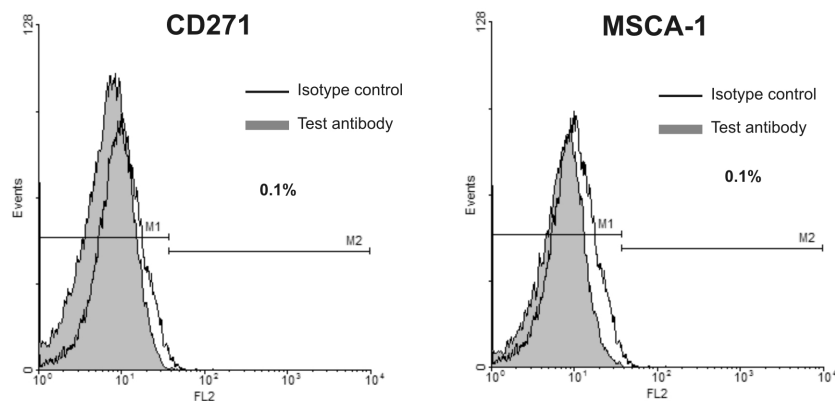
6.3.6 Elutriation experiment

Surface antigen expression of elutriated cells

The expression of the markers CD90, CD73, CD44 and CD105 were measured on logarithmic scale. The fluorescence distributions were compared using the Kolmogorov-Smirnov[248] test and both populations were found to be different at the 99,9 % confidence level.
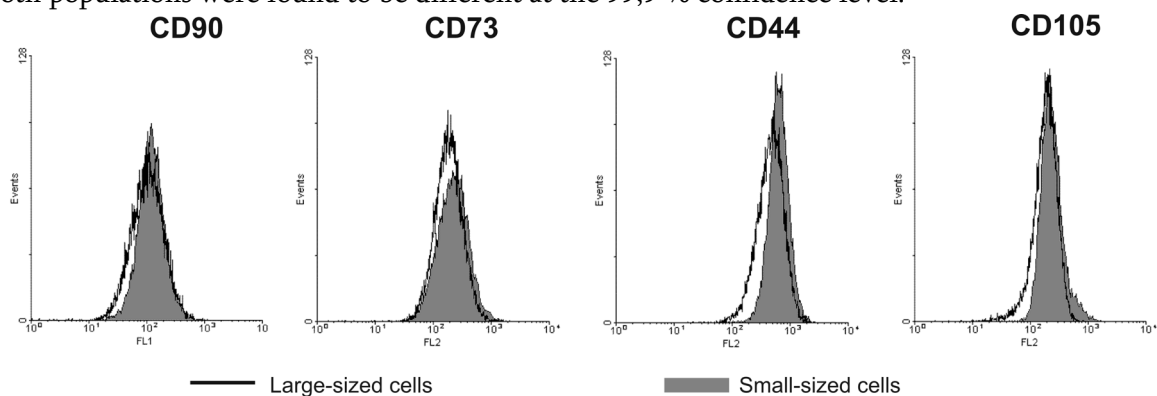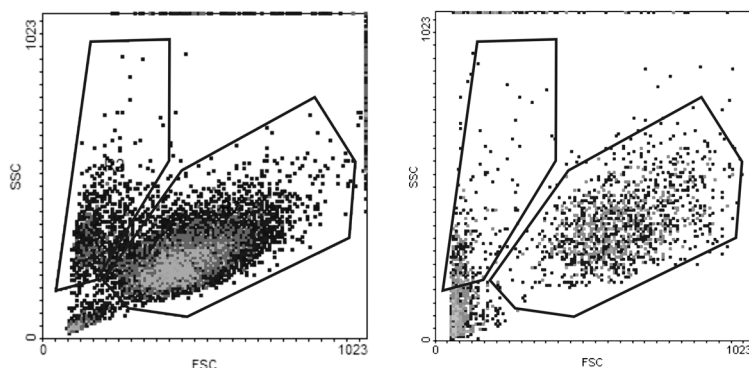

Correlation between total protein content (FITC staining) and side scatter signal

The cells were fixed using 4% paraformaldehyde in PBS for cell fixation, as this method demonstrated minimum impact on the scatter properties of cells:

The correlation between total protein content (FITC staining) and side scatter signal was demonstrated for cells at day 2, 3 and 4 after seeding in culture flasks, indicating that the linear relation between SSC signal and protein content remains true, regardless of the proliferation state, i.e. cell cycle status of the cells:
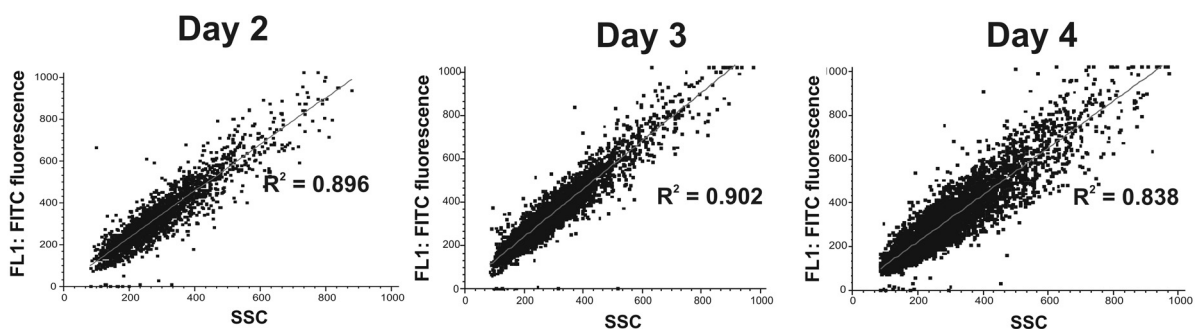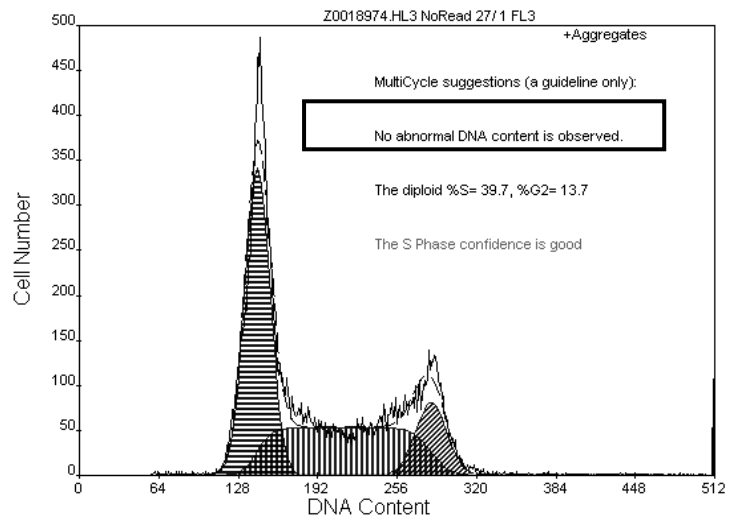

Ratio CD44/SSC and CD105/SSC

The expression of the CD44 and CD105 antigens normalized on total cell protein was evaluated using the ratio of fluorescence to SSC signals:
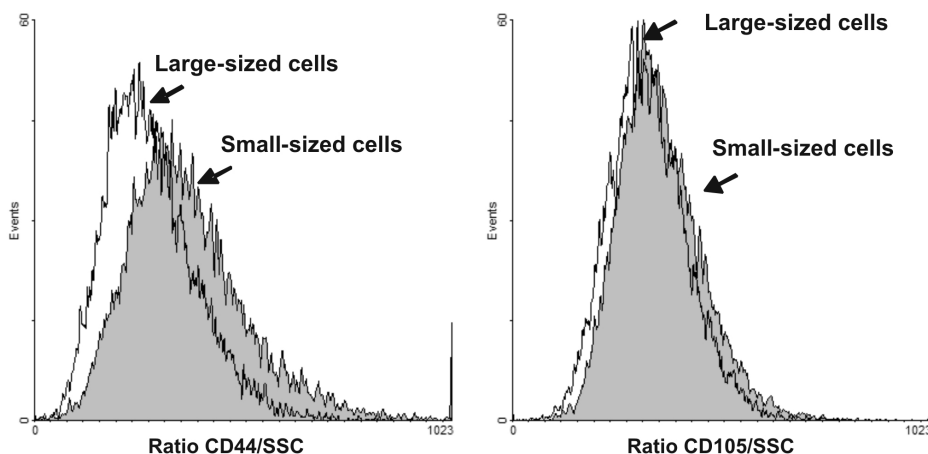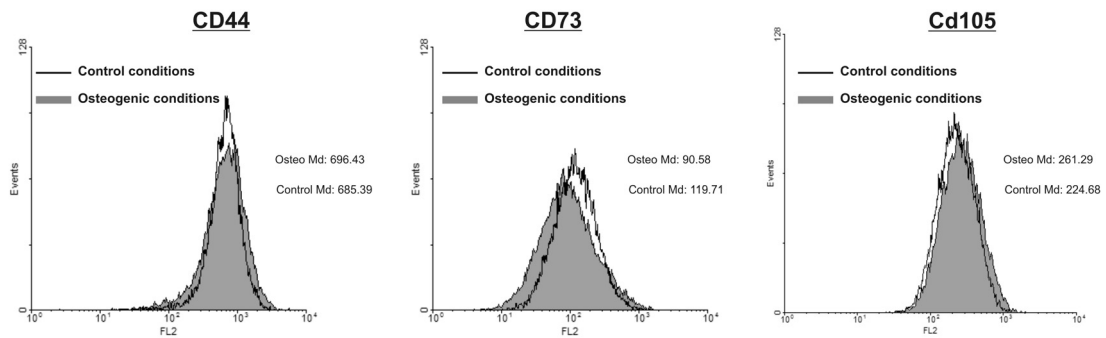

6.3.7 Cell cycle status of UC-derived cells

UC-derived MSCs exhibit a normal diploid DNA content in culture:

6.3.8 Monitoring of cell response to the osteogenic stimulation

Immunophenotype of cells cultivated under control (unfilled histogram) and osteogenic conditions (filled histogram) over 28 days:

List of publications

Articles

Moretti P., Behr L., Walter J., Kasper C., Stahl F., Scheper T.: Characterization and improvement of cell line performance via flow cytometry and cell sorting, *Eng. Life Sci.* 2010, 10, No. 2, 130–138

Moretti P., Majore I., Hass R., Kasper C.: Identification of subpopulations in mesenchymal stem cell-like cultures from human umbilical cord; Cell Commun Signal. 2009 Mar 20;7:6

Moretti P., Hatlapatka T., Marten D., Lavrentieva A., Majore I., Hass R., Kasper C.: Mesenchymal stromal cells derived from human umbilical cord tissues: Primitive cells with potential for clinical and tissue engineering applications, [Epub ahead of print], Adv Biochem Eng Biotechnol.; Volume: Bioreactor Systems for Tissue Engineering II: Strategies for stem cell expansion and differentiation; Springer Verlag

Tomala M., Lavrentieva A., Moretti P., Rinas U., Kasper C., Stahl F., Schambach A., Wahrlich E., Martin U., Cantz T., Scheper T.: A Novel Production and Purification Process for Soluble Human Leukemia Inhibitory Factor as Fusion Protein from Recombinant *Escherichia coli, Protein Expr. Purif.*, (2010), Artikel in Druck, doi:10.1016/j.pep.2010.04.002

Articles in conference proceedings

Zapp J., Moretti P.: Determination of Radical Scavenging Capacities in Phytoextracts using on-line HPLC-ABTS•+ Analysis. In GDCH (Edt.), Proceedings of the Euro Food Chem XIII conference, 2005, 668 – 691

Zapp J., Cassano M., Moretti P.: Determination of Radical Scavenging Capacities in Coffee Brews by Means of On-line Combination of HPLC with ABTS-Radical Bleaching Assay. In GDCH (Edt.), Proceedings of the Euro Food Chem XIII conference, 2005, 692 – 695

Oral presentations

Moretti P., Hatlapatka T., Majore I., Boehm S., Hass R., Scheper T., Kasper C.: Mesenchymal stromal cells from human umbilical cord tissue: identification of sub-populations, DGfZ Meeting, 15 October 2009, Leipzig, Germany

Moretti P., Hatlapatka T., Majore I., Boehm S., Scheper T.: Characterization of mesenchymal stem cells isolated from human umbilical cord. DGfZ/ESCCA Meeting, 17 September 2008, Bremen, Germany

Posters

P. Moretti, I. Majore, S. Boehm, T. Hatlapatka, M. Tomala, R. Hass, T. Scheper, C. Kasper: Monitoring of long-term cultivation and osteogenic differentiation of Human Umbilical Cord-derived mesenchymal stem cell-like cultures. ESACT Meeting, Dublin 2009

P. Moretti, T. Hatlapatka, M. Tomala, I. Majore, F. Stahl, T. Scheper, C. Kasper: Characterisation of human mesenchymal stem cells and monitoring of long term cultivation via multicolour flow cytometry. Bioperspectives, Hannover 2008

P. Moretti, M. Reck, C. Repenning, F. Stahl, K. Friehs, T. Scheper: Flow cytometric monitoring of protein secretion via the Tat-pathway in *E.coli.* Analysis of microbial cells at the single cell level, Bad Schandau 2008

Curriculum vitae

Persönliche Daten

Name   Pierre Moretti
Geburtsdatum   27. März 1981
Geburtsort   Algrange, Frankreich
Staatsangehörigkeit   französisch

Schulbildung

1988-1992   Grundschule „Ecole Paul Verlaine", Hagondange, Frankreich
1992-1999   Collège et Lycée, Collège Lycée Charlemagne, Thionville, Frankreich
              Abschluss : Abitur (Baccalauréat scientifique)

Studium

1999-2001   „Diplôme Universitaire de Technologie" (DUT) Lebensmittel- und
              Bioindustrie, Institut für Technologie (IUT) der Universität Nancy
              Henri Poincaré, Nancy, Frankreich

2001-2004   Diplom Ingenieur (FH), Lebensmitteltechnologie mit Schwerpunkt
              Biotechnologie, Fachhochschule Lippe-Höxter, Lemgo, Deutschland

2004-2006   Master of Science "Life Science", Gottfried Wilhelm Leibniz
              Universität Hannover, Hannover, Deutschland

2007-2010   Promotion am Institut für Technische Chemie, Gottfried Wilhelm
              Leibniz Universität Hannover, Hannover, Deutschland